

CCM-79-8

# Center for Composite Materials

DISTRIBUTION STATEMENT A

Approved for public release;  
Distribution Unlimited

ANALYSIS OF THE "JOGGLE-LAP" JOINT  
FOR  
AUTOMOTIVE APPLICATIONS

19951228 077

DTIC QUALITY INSPECTED 2

RICHARD C. GIVLER

DEPARTMENT OF DEFENSE  
PLASTICS TECHNICAL EVALUATION CENTER  
ARRADCOM, DOVER, N.J. 07801



College of Engineering  
University of Delaware  
Newark, Delaware

PLASTIC 35253

-- 1 OF 1

\*\*\*DTIC DOES NOT HAVE THIS ITEM\*\*\*

-- 1 - AD NUMBER: D429745

-- 5 - CORPORATE AUTHOR: DELAWARE UNIV NEWARK CENTER FOR COMPOSITE MATERIALS

-- 6 - UNCLASSIFIED TITLE: ANALYSIS OF THE 'JOGGLE-LAP' JOINT FOR AUTOMOTIVE APPLICATIONS,

--10 - PERSONAL AUTHORS: GIVLER, R. C. ;

--11 - REPORT DATE: MAY 01, 1979

--12 - PAGINATION: 136P

--14 - REPORT NUMBER: CCM-79-8

--20 - REPORT CLASSIFICATION: UNCLASSIFIED

--21 - SUPPLEMENTARY NOTE: SUBMITTED AS A SENIOR THESIS IN PARTIAL FULFILLMENT FOR A DEGREE WITH DISTINCTION.

--22 - LIMITATIONS (ALPHA): APPROVED FOR PUBLIC RELEASE; DISTRIBUTION UNLIMITED. AVAILABILITY: CENTER FOR COMPOSITE MATERIALS, COLLEGE OF ENGINEERING, UNIVERSITY OF DELAWARE, NEWARK, DELAWARE 19711.

--33 - LIMITATION CODES: 1 24

-----\*\*\*\*\*

END OF DISPLAY LIST

<<ENTER NEXT COMMAND>>

Alt-Z FOR HELP3 ANSI

3 HDX 3

3 LOG CLOSED 3 PRINT OFF 3 PARITY

Analysis of the "Joggle-Lap" Joint  
for  
Automotive Applications

Richard C. Givler  
R. Byron Pipes, Thesis Advisor

submitted as a Senior Thesis in partial  
fulfillment for a Degree with Distinction

Center for Composite Materials  
University of Delaware  
Newark, Delaware 19711

May 1, 1979

## Abstract

An analytical model is developed to describe the response of the "joggle-lap" joint to both tensile and bending loads. The model consists of a non-linear beam analysis which calculates stress profiles through the adherent thickness. A plane stress finite-element model was incorporated into the analysis to correctly determine the stress field in the adhesive zone where it was shown that beam analysis was less accurate. Elastic response of the "joggle-lap" joint due to tensile loads was verified through experimental testing and ultimate loads were accurately predicted within experimental error. Maximum adherent flexural stress was found to determine joint failure. A parametric study was undertaken by using the verified analytical model and the results were recorded as a series of design curves.

## Table of Contents

	<u>Page</u>
I. Introduction	1
II. Background	4
A. Adherent Materials	
B. Adhesive Materials	
III. Methods of Analysis	16
A. Tensile Loading	
a. Beam Model	
b. Finite Element Model	
B. Flexure Loading	
a. Beam Model	
b. Finite Element Model	
IV. Experimental Results	48
A. Tension	
B. Bending	
V. Failure Analysis	61
VI. Conclusions	65
VII. Acknowledgements	72
VIII. References	73
IX. Bibliography	74
X. Appendices	75
A. Derivation of the Governing Equations for a Curved Beam	
B. Beam Bending Model of the Joggle Lap Joint	
C. Computer Routines	
a. JOGGLE	
b. CONVERT	
D. SMC Material Property Data	
XI. Plates 1-7	120

## List of Figures

<u>Figure</u>	<u>Title</u>	<u>Page</u>
1	The Joggle Lap Joint Subject to Tensile and Bending Loads	2
2	SMC-R Machine	5
3	Typical Cure Cycle of SMC	7
4	Pressure Variation of a Typical Cure	9
5	Effect of Glue Line Thickness on Bond Joint Strength	15
6	Piecewise Representation of the Joggle Lap Joint	17
7	Deflection of Neutral Surface at Failure Load	20
8	Slope of the Neutral Axis at the Failure Load	21
9	Moment Along Neutral Surface at the Failure Load	22
10	Shear Along the Neutral Surface at the Failure Load	23
11	Response of the Joggle-lap Joint at $S_3 = 0$ (Deflection)	25
12	Response of the Joggle-lap Joint at $S_3 = 0$ (Moment)	25
13	Finite Element Mesh of the Adhesive Zone	27
14	Deformed Mesh at the Failure Load	28
15	The Adhesive Zone in Tension - Contours of $\sigma_1$ Stress	29
16	The Adhesive Zone in Tension - Contours of $\sigma_2$ Stress	30

# List of Figures (Cont'd)

<u>Figure</u>	<u>Title</u>	<u>Page</u>
17	The Adhesive Zone in Tension - Contours of $\tau_{12}$ Stress	31
18-19	Shear Stress Variation Through the Thickness of the Adhesive Zone	34-35
20	Distribution of Stress on Left Side of Finite Element Model	37
21	Sign Convention for Left Hand Side of Finite Element Model	37
22	Illustration of the Corrective Moment	40
23	Method of Equivalent Sections	43
24	The Adhesive Zone in Bending - Contours of $\sigma_1$ Stress	45
25	The Adhesive Zone in Bending - Contours of $\sigma_2$ Stress	46
26	The Adhesive Zone in Bending - Contours of $\tau_{12}$ Stress	47
27-28	Elastic Response Due to Tension - Top Fiber Stresses	51-52
29-30	Elastic Response Due to Tension - Bottom Fiber Stresses	53-54
31-32	Top Fiber Stresses Due to Bending	56-57
33-34	Bottom Fiber Stresses Due to Bending	58-59
35	Bottom Fiber Stresses at the Failure Load	63
36	Top Fiber Stresses at the Failure Load	64
37	Effects of Adherent Thickness on Joint Strength	66
38	Effects of Inside Radius of Joint Strength	67

List of Figures (Cont'd)

<u>Figure</u>	<u>Title</u>	<u>Page</u>
39	Effects of Contact Area on Joint Strength	68
40	Effect of Load on Joint Strength	69
41	Curved Beam Element	75
42	Equilibrium of Curved Beam Section	77
43	Curved Beam Element Subject to Deflection	79
44	Differential Element in the Local Coordinate System	80
45	Deriving the General Deflection Equation for a Curved Beam	80
46	SEG1 Modeled as a Straight Beam	83
47	SEG2 Modeled as a Curved Beam	85
48	SEG3 Modeled as a Curved Beam	89
49	SEG4 Modeled as a Layered Beam	91
50	SEG5 Modeled as a Straight Beam	91
51	Iterative Process for Determining $u_o$	94
52-54	Modulus Determination of SMC	117-119



## Nomenclature

$a$	cross-sectional area
$b$	adhesive bond thickness
$C_0, C_1, C_2$	constants
DEFLA	deflection
DUDSA	angular rotation
$e$	eccentricity
$e_l$	elongation
$E$	modulus of elasticity for an isotropic material
$E_f$	modulus of elasticity of fibers
$E_m$	modulus of elasticity of matrix
$E_n$	modulus of elasticity normal to the fiber plane
$E_x, E_y, E_z$	modulus of elasticity of a general anisotropic body
$F$	applied force
$F_i \ i=1-5$	force components
$h_i \ i=1-5$	nodal points
$H_i \ i=1-5$	axial force of SEGi
$I$	moment of inertia about neutral surface
$I_{eq.}$	equivalent moment of inertia
$l_1$	length of SEG1
$M_i \ i=1-5$	applied moment at SEGi
$M_{corr}$	correcting moment
$M(S)$	moment distribution

# Nomenclature (Cont'd)

$R$	radius of curvature
$SEGi_{i=1-5}$	beam elements of the "joggle-lap" joint
$S$	specific gravity
$S_i \ i=4-6$	ultimate shear strength
$t$	adherent thickness
$\bar{u}$	distance between neutral axis and centroidal axis
$u_o$	deflection at the end of SEGi
$u_i, \ s_i \ i=1-5$	local coordinate system corresponding to individual beam element
$v_f$	volume fraction of fiber
$v_m$	volume fraction of matrix
$V_i \ i=1-5$	shear force on SEGi
$W$	weight fraction
$X, Y$	global coordinate system
$Y$	radial coordinate in curved beam members
$X_i^T$	ultimate tensile strength
$X_i^C$	ultimate compressive strength
$\alpha$	angle measure
$\Delta$	infinitesimal difference
$\epsilon_x, \epsilon_y, \epsilon_z$	strain components
$\epsilon_{ult}$	ultimate strain
$\theta$	angle measure
$\lambda$	linear measure

Nomenclature (Cont'd)

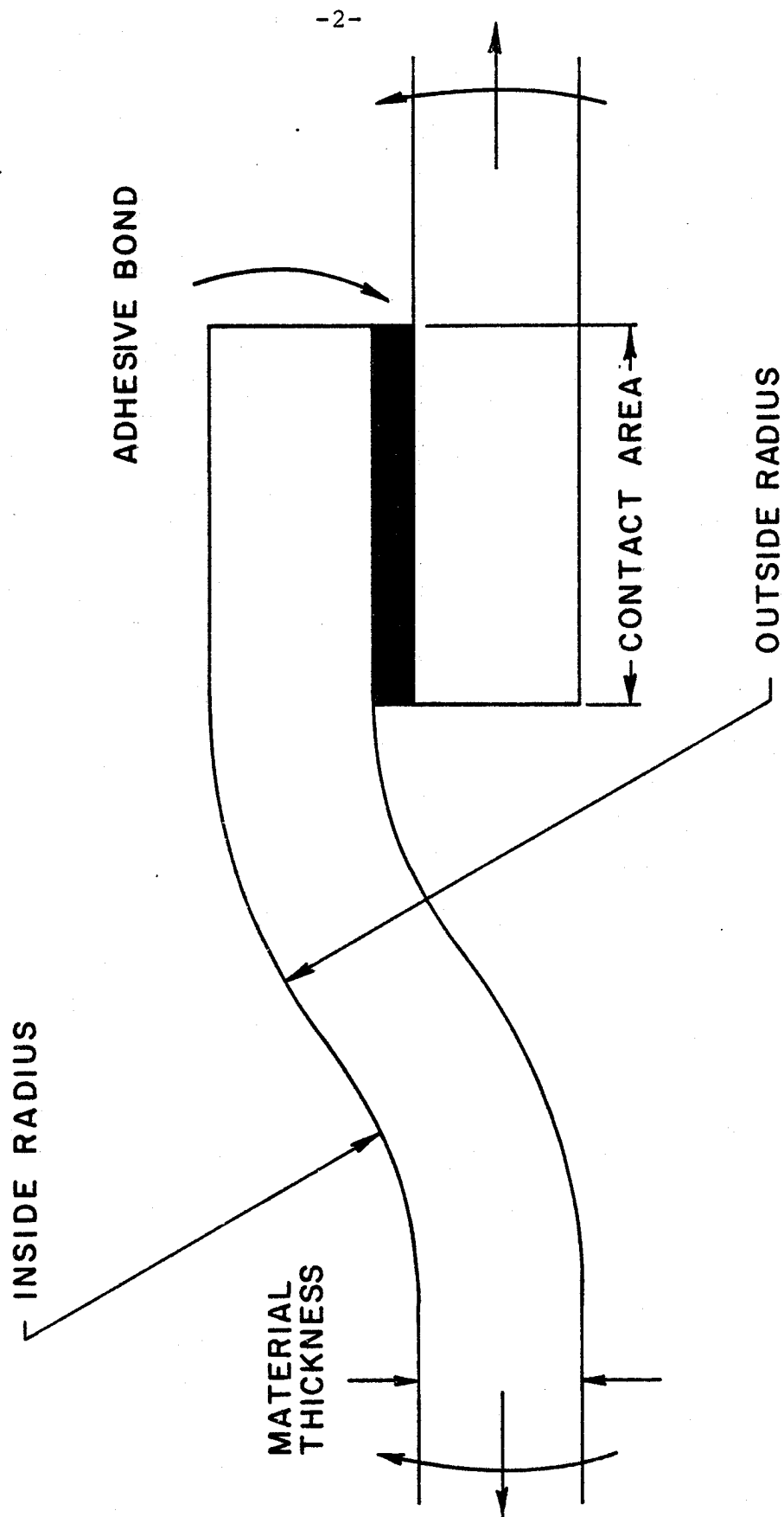
$\nu_{ij}$	Poisson's ratio
$\pi$	3.14159...
$\sigma_1, \sigma_2, \tau_{12}$	plane stress components
$\sigma_x, \sigma_y, \sigma_{xy}$	
$\sigma_{ult}$	ultimate strength
$\phi$	angle measure

## I. Introduction

Recent government regulations for increased gasoline mileage requirements have induced automobile manufacturers to seek light weight replacement material systems for existing metal parts. Since the automotive industry is a high volume operation, sheet molding compound (SMC) parts offer a feasible answer to the problem. The SMC molding time of from 1 to 3 min/piece depending on the size and thickness of the part is compatible with automotive assembly line production.

International Harvester et al are currently employing SMC molded body components on their vehicles to replace former sheet metal parts. This new direction has brought with it several problems, one of which is the design of adhesive joints. The joint must accommodate high rate fabrication techniques and provide optimum strength and durability. In addition, the joint must satisfy certain cosmetic requirements such as adjacent flush edges. With these criteria in mind, the "joggle-lap" joint has been chosen for detailed study and analysis. This joint configuration is shown in Figure 1. Since a joint of this type experiences a variety of loading conditions in practice, it was decided to model the joint

FIGURE 1: THE JOGGLE LAP JOINT SUBJECT TO TENSILE AND BENDING LOADS



in pure tension and pure bending. By superposition, it is apparent that any combination of these two loading conditions may then be constructed.

This work focuses on the development of an analytical model to describe the behavior of the "joggle-lap" joint due to both tensile and bending loading conditions. The first section utilizes small deflection beam theory for both straight and curved beam elements to obtain a solution for the displacement and stress fields of the joint. Included in this analysis is the derivation of the governing differential equations for the deflection of the curved beam.

The second section utilizes a finite-element model to reveal localized stress concentrations in the adhesive zone. Boundary conditions for the finite element model are obtained from a transformation of stresses in the deformed geometry to equivalent stresses in the undeformed geometry. This transformation of stresses is performed via a computer routine for ease of calculation.

Finally, experimental verification of the analytical predictions is reported along with a description of testing procedures. The maximum flexural stress is shown to correlate strength data and failure analysis. Also, the microstructure of the joint was examined as a possible explanation of the failure mode.

## II. Background

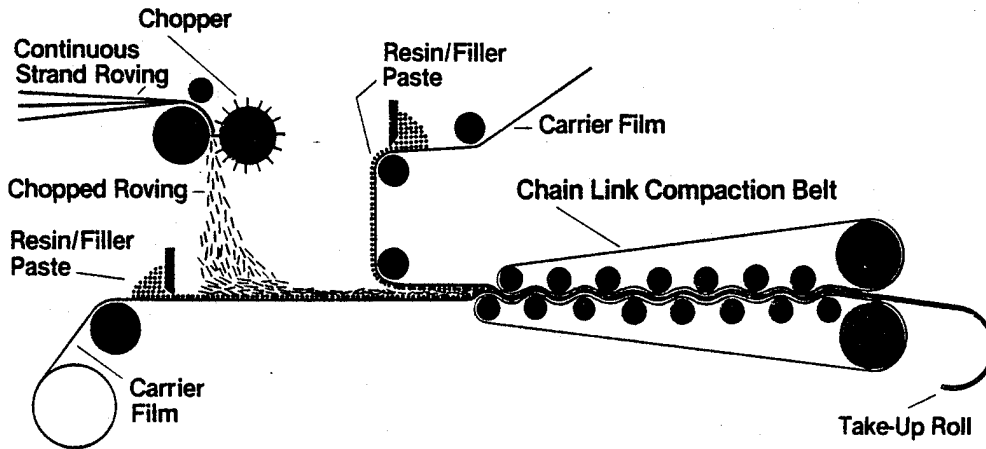
### A. Adherent Materials

The adherents of the proposed "joggle-lap" joint were composed of a random-fiber composite known as SMC-25. SMC is defined as a sheet molding compound that contains reinforcements with an average fiber length of approximately 1 inch (2.54 cm) with random orientation in the plane. The number 25 indicates that the composite is 25 percent glass fibers by weight. The major constituents of SMC are E-glass fibers and a styrenated polyester resin in the form of a paste. It is quite common to use mineral fillers during the manufacture of the paste to facilitate flow when molding or to obtain certain characteristics from the molded part such as a high resistance to flame or increased stiffness. Another prime reason for using fillers is the fact that they are much cheaper than the polyester resin itself and thus reduce the cost of materials. At times, chemical additives may also be introduced into the paste to serve as catalysts during the molding cycle.

The process of SMC manufacturing is a highly innovative one which is completely automated. Figure 2 (taken from Owens/Corning Fiberglass SMC Review) depicts

### SMC-R Machine

FIGURE 2: SMC-R MACHINE



a typical process currently in use by a competitive supplier of SMC. The first step of the procedure is to distribute the resin onto a polyethylene carrier film as shown. Continuous glass fibers are then chopped into lengths of less than three inches and distributed in a random fashion on the wetted film. A second layer of resin-coated polyethylene film serves as a top layer to the sandwich-like sheet. Several rows of rollers act to insure that the glass fibers are fully impregnated with the polyester resin thus yielding consistency in moldability of the SMC. Finally the product is directed to a take-up roll for ease of handling during shipping and storage.

SMC is usually placed in a constant temperature room while storing to allow maturation to take place. Maturation is nothing more than allowing the SMC to increase



in viscosity to enhance relative ease of handling of the sheet. Maturing the SMC sheet for extended periods of time greatly reduces the flow characteristics of the product while molding. Recommended shelf-life for SMC stored at 10-15° C is about 2 weeks, however in general it may often be used up to 2 months after the date of its manufacture.

Once the SMC sheet has reached maturity, it is ready for molding. Upon removing the protective polyethylene film, the molding compound is cut to size and strategically placed in the mold. This procedure is known as charging the mold. The so-called strategic locations of the mold are those positions that allow the SMC to flow to all parts of the mold and maintain uniform part thickness. To date these locations have been determined by trial and error coupled with experience.

Compression molding combines both temperature and pressure to induce an exothermic reaction which serves to cure the part in the mold. Figure 3 (taken from ref [3]) is an example of a typical curing cycle showing the temperature of the part as a function of time. It should be noted that platen temperatures of 200° C are usually sufficient for SMC molding and may be achieved with superheated steam. Another important fact seen from the figure is the overall cure time. Average cure times are generally

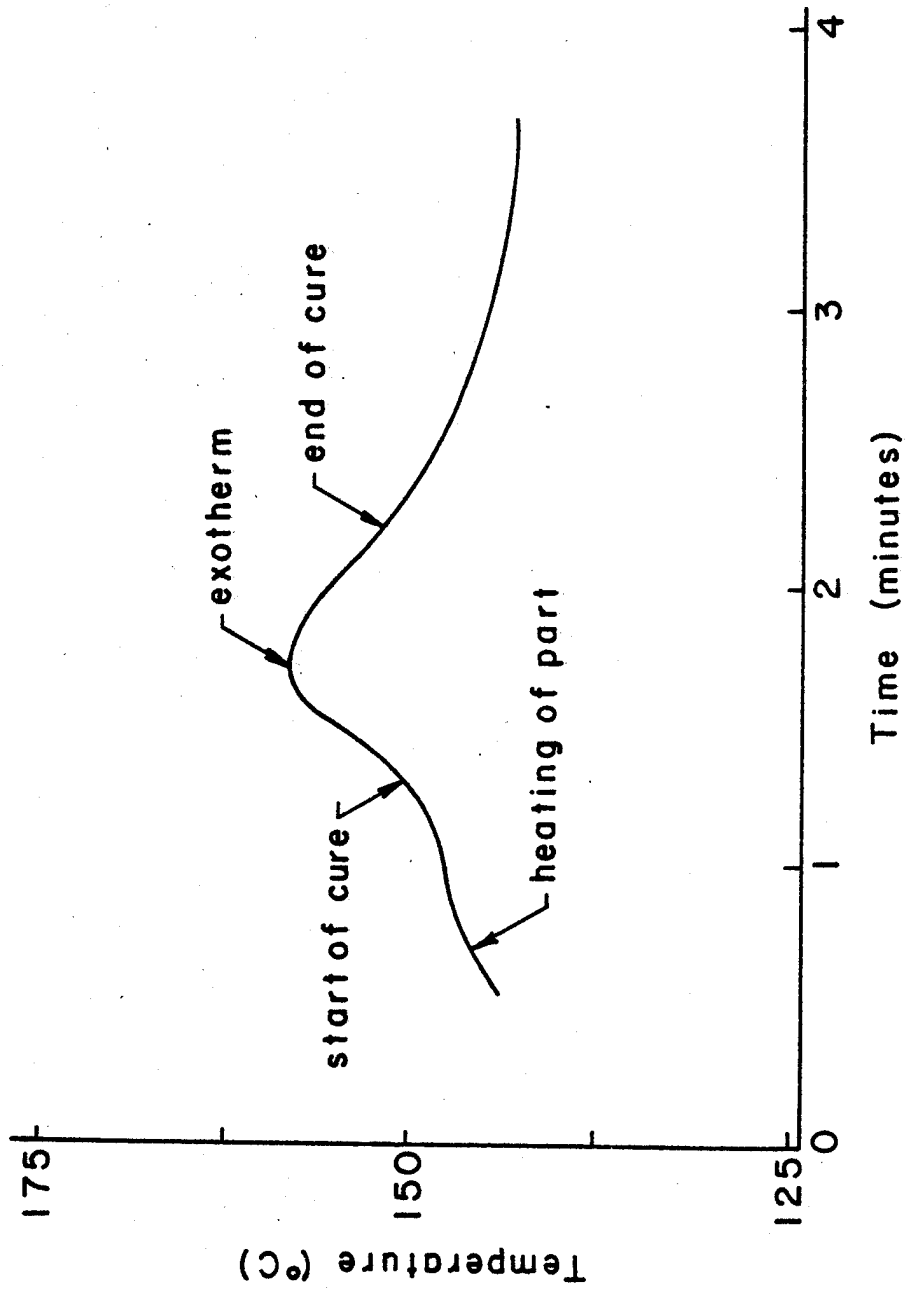


FIGURE 3: TYPICAL CURE CYCLE OF SMC

1-3 minutes (depending upon the thickness of the part) which lends itself to production line applications inherent in the automotive industry. Figure 4 (taken from ref [3]) shows the effect of pressure upon a typical cure cycle. Note that the peak pressure and maximum temperature correspond to the initiation of the exothermic reaction. The key to successful molding is to acquire fine control of the application of pressure to the cure cycle.

The main feature of SMC is the ability of the glass fibers to flow with the paste during the molding process. Since the fibers are transported to all parts of the mold, it is possible to produce a geometrically complicated part with quasi-constant mechanical properties. It has been shown by Pipes and Taggart [ref 5], that in areas of intensified flow, the fibers tend to align themselves with the direction of flow and thus produce areas of varying mechanical properties. It is therefore beneficial to understand the flow characteristics within the mold to produce a part with controlled and/or uniform mechanical properties. Taggart et al have determined the properties of SMC-25 to be those found in Table 1. Some scattering in the data was reported due to the inherent local variations in the material. To determine the normal modulus (modulus normal to the plane of the fibers), the relationship shown may be

FIGURE 4: PRESSURE VARIATION OF A TYPICAL CURE

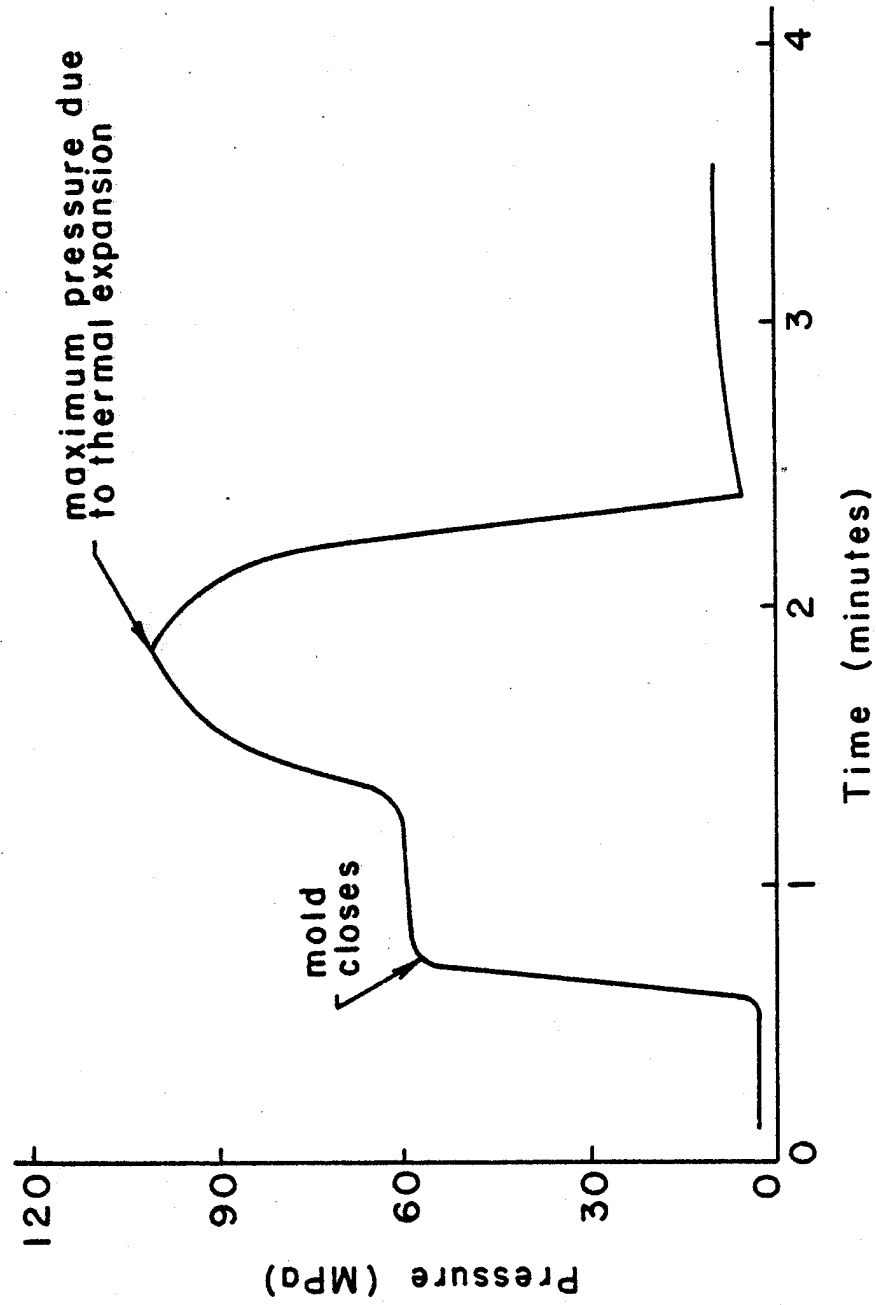


Table 1  
Properties of SMC-25

Tension

$E_{\text{tension}}$ $L$	GPa (Msi)	14.48	(2.1)
$\nu_{\text{tension}}$			.3
$\sigma_{\text{ult}}^{\text{tension}}$	MPa (ksi)	90	(13.1)
$\epsilon_{\text{ult}}^{\text{tension}}$	( $\mu$ in/in)		11,400

Compression

$E_{\text{compression}}$ $L$	GPa (Msi)	12.41	(1.8)
$\nu_{\text{compression}}$			.28
$\sigma_{\text{ult}}^{\text{compression}}$	MPa (ksi)	204	(29.6)
$\epsilon_{\text{ult}}^{\text{compression}}$	( $\mu$ in/in)		20,600

used. This relationship resembles the well-known rule of mixtures for continuous fibrous composites.

$$\frac{1}{E_n} = \frac{v_f}{E_f} + \frac{v_m}{E_m} \quad (1)$$

where  $E_n$  = normal modulus of elasticity of the composite

$v_f$  = volume fraction of fiber

$v_m$  = volume fraction of matrix

$E_f$  = modulus of glass fiber

$E_m$  = modulus of matrix

Table 2 provides the needed data for determining the normal modulus of elasticity. By definition, SMC is composed

Table 2<sup>1</sup>

	polyester resin	E-glass fiber
Modulus of Elasticity (10 <sup>6</sup> psi)	.5	10
Specific gravity	1.28	2.54

of 25% fiber by weight. Utilizing the equation written below

$$v_f + v_m = 1 \quad (2)$$

allows one to solve for  $v_f$  where  $v_m$  may be rewritten as

$$v_m = v_f \left[ \frac{S_f}{S_m} \right] \cdot \left[ \frac{W_m}{W_f} \right]$$

$S_f$  = specific gravity of fiber

$S_m$  = specific gravity of matrix

$W_m$  = weight fraction of matrix

$W_f$  = weight fraction of fiber

Making the appropriate substitutions, Eq. (2) becomes

$$\frac{.75}{.25} \left[ \frac{2.54}{1.28} \right] v_f + v_f = 1$$

Thus the corresponding volume fraction of fiber and matrix are .14 and .86 respectively. From Eq. (1) the value of  $E_n$  is now calculated to be  $0.58 \times 10^6$  psi.

---

<sup>1</sup>Vinson and Chou

## B. Adhesive Materials

The adhesive system chosen for the "joggle-lap" joint was developed by the Adhesives Division of Goodyear Chemicals. The Pliogrip 6000 series is a general purpose structural adhesive with a polyurethane base. Currently available as a two-part system, Pliogrip 6000 exhibits both high flexibility and resilience. With the proper selection of curatives, the working time of the adhesive may be accurately controlled between 1-6 minutes.

In order to utilize this adhesive system only minimal surface preparation is necessary. The two surfaces to be bonded are prepared with a plastic wash primer (Pliogrip 6033/6034 Wash Primer) that is applied with a cloth. No sand blasting or surface stripping is necessary. To maintain reliably bonded parts, Pliogrip 6000 must be mixed at a precise ratio of 4 parts resin to 1 part curative by weight or volume. Deviations from this standard will yield resin-rich areas of uncured adhesive. The actual mixing of the two components must be carried out without the introduction of air into the system, thus the need for specialized equipment. Without this precaution, entrapped air bubbles in the cured adhesive would yield voids and greatly affect the performance of the bond. Curing this adhesive system can be accomplished at room temperature, however the use of heated fixtures will reduce cure times.

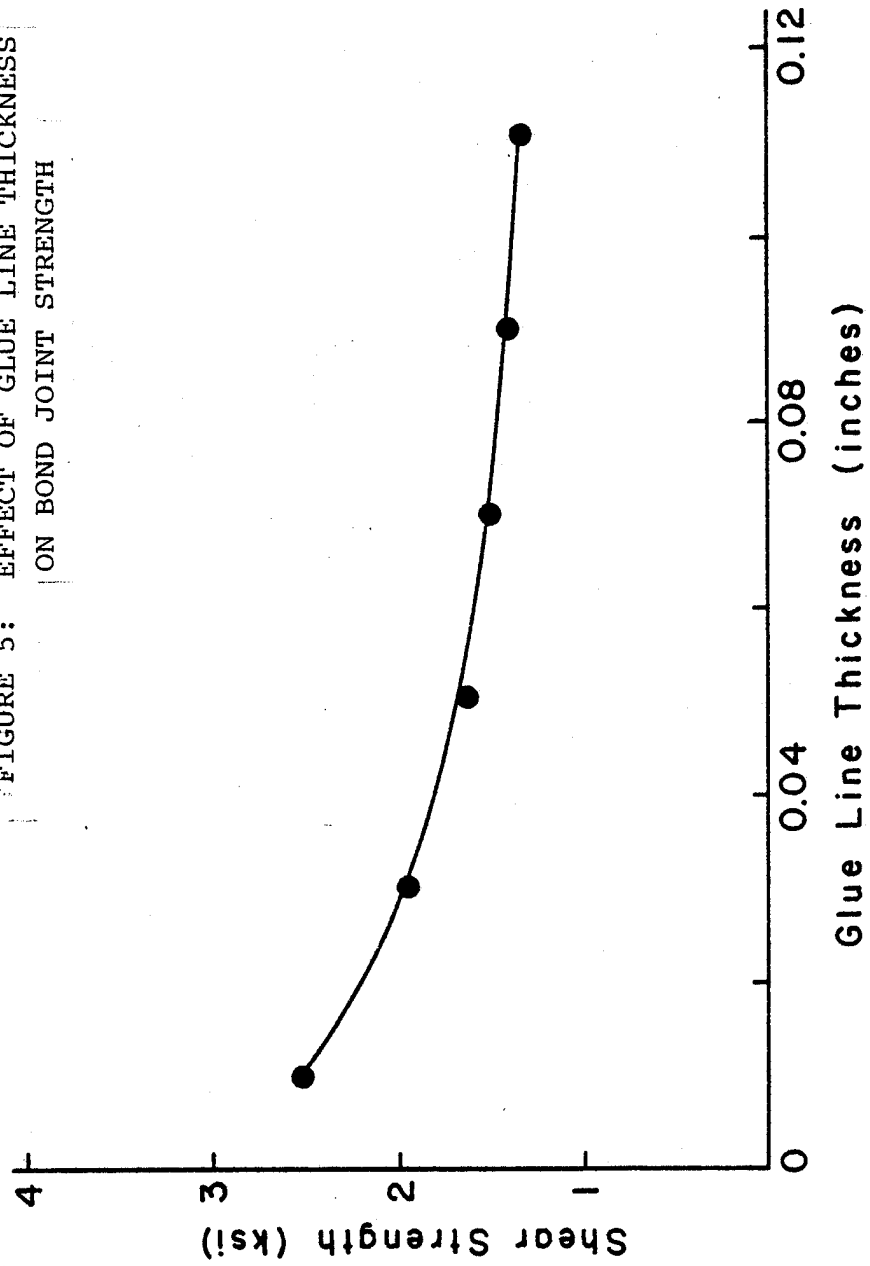


Recommended clamping pressures of heated fixtures range from 20 to 40 psi.

An important criterion in the design of bonded joints is that of the adhesive thickness. It has been shown that adhesive properties vary inversely with adhesive thickness. Thus the bulk properties of the adhesive are distinctly different from those in the film state. So the question is posed as to the optimum bond thickness as a function of shear strength. Figure 5 (taken from Pliogrip technical data, Goodyear Adhesives) shows the effect of glue line thickness on bond joint strength. A bond line thickness of 0.030 inches was chosen as optimal even though thicknesses less than 0.030 inches yield greater bond strengths. It was felt that bonding thicknesses less than 0.030 inches are not capable of being fabricated with consistency under production operations. (i.e. molded FRP parts will inherently not fit together with reliable precision).

To achieve uniform bond lines, one of two procedures is generally used. Adherents may have a small raised button of 0.030 inches in thickness which acts as a spacer for the joint to insure a uniform bond. Another procedure is to introduce small glass spheres (0.030 inches dia.) directly into the adhesive to achieve similar spacing. The effect of these spheres on joint strength has not been determined but it is argued that the variation from the norm is negligible.

FIGURE 5: EFFECT OF GLUE LINE THICKNESS  
ON BOND JOINT STRENGTH



### III. Methods of Analysis

#### A. Tensile Loading

##### a. Beam Model

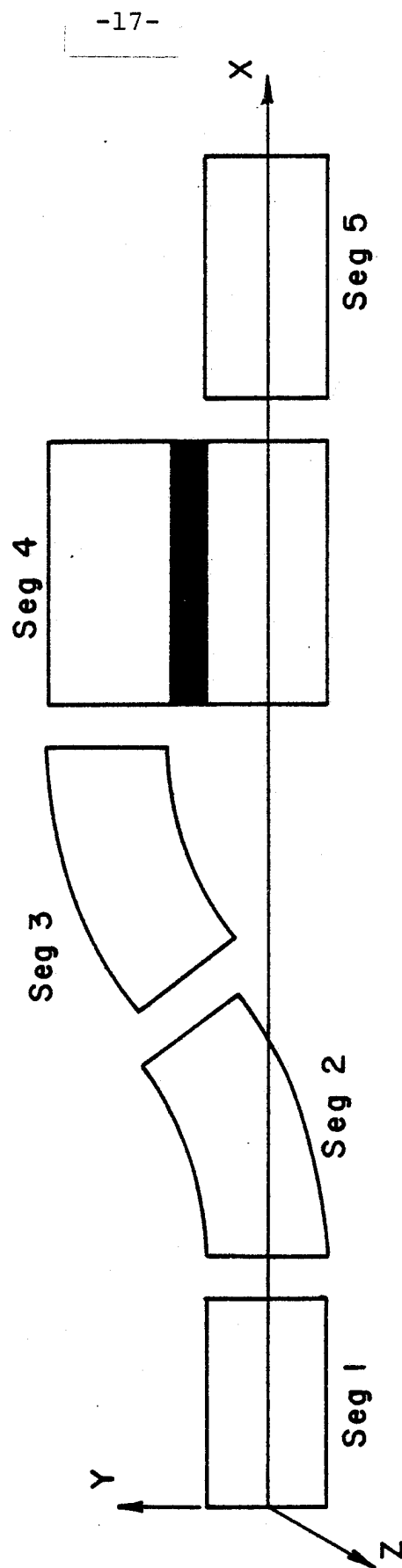
Recently, Adkins [ref 2] investigated the response of a scarf joint to simple tensile loadings. It was found that the scarf joint exhibits flexural deformation under tensile loading due to the misalignment between the neutral surface and the loading axis. This eccentricity induces a moment distribution along the joint (see Figure 9) which acts to align the neutral surface with the loading axis.

The analysis of the "joggle-lap" joint, shown previously in Figure 1, is an extension of the concept discussed above. Again it is clear that under tension the joint will experience a lateral deflection as the neutral axis attempts to align with the applied force. To analyze the joint behavior under tensile loading conditions, it was decided to divide the joint into five segments. The obvious places to divide the joint are illustrated in Figure 6 along with the corresponding identifying labels and global coordinate system. Reference to beam segments via their identifying numbers will be utilized throughout the remainder of this analysis.

In general, the goal of the analysis will be to determine the displacements of the neutral axis as measured perpendicularly from the undeformed neutral surface. Once

FIGURE 6: PIECEWISE REPRESENTATION  
OF THE JOGGLE LAP JOINT

global  
coordinate  
system



the deflections are known, one may calculate a moment distribution along the joint and thus determine the stress distribution at any given cross-section.

The initial intention of such an investigation was to develop a closed form solution for the stresses within the joint. This effort was soon thwarted by the non-linearities encountered in the governing equations for the beam elements. These non-linearities result from a coupling between the moment and deflection solutions, as will be evident later. As an alternative solution, the displacement field was obtained via numerical integration routines.

Linear elastic beam theory states that for a beam under general loading conditions, the local radius of curvature is given by

$$R = \frac{EI}{M} \quad (3)$$

where       $R$  = radius of curvature  
             $E$  = modulus of elasticity  
             $I$  = moment of inertia about the neutral surface  
             $M$  = applied moment

The radius of curvature may be written in terms of the lateral deflection as given by Eq. (4)

$$\frac{1}{R} = \frac{\frac{d^2y}{dx^2}}{[1 + (\frac{dy}{dx})^2]^{3/2}} \quad (4)$$

Realizing that under the assumptions made with regard to small deflection theory, the term  $(\frac{dy}{dx})^2$  will be negligible when compared to unity. Thus one arrives at the governing equation for straight beam elements.

$$\frac{d^2y}{dx^2} = \frac{M}{EI} \quad (5)$$

Since the material system is relatively stiff, it is assumed that small deflection beam theory will yield sufficiently accurate results. Thus, one may write a governing differential equation for each segment of the joint. By matching boundary conditions of deflection and slope at each interface, the deflection of the entire joint may be obtained as a function of distance along the neutral axis. Details of the analysis may be referenced in Appendix B.

To enhance one's understanding of the joint behavior under applied tensile loadings, Figures 7 through 10 show deflection, slope, moment, and shear diagrams respectively at a load of 200 lbs. Many of the discontinuities found in the plots arise from a shift in the neutral axis which is a common occurrence among lap joints.

It was stated previously that analyzing the "joggle-lap" joint under tension was a non-linear problem. This was seen by the fact that the moment was a function of the deflection. Another way to view the non-linearities of the

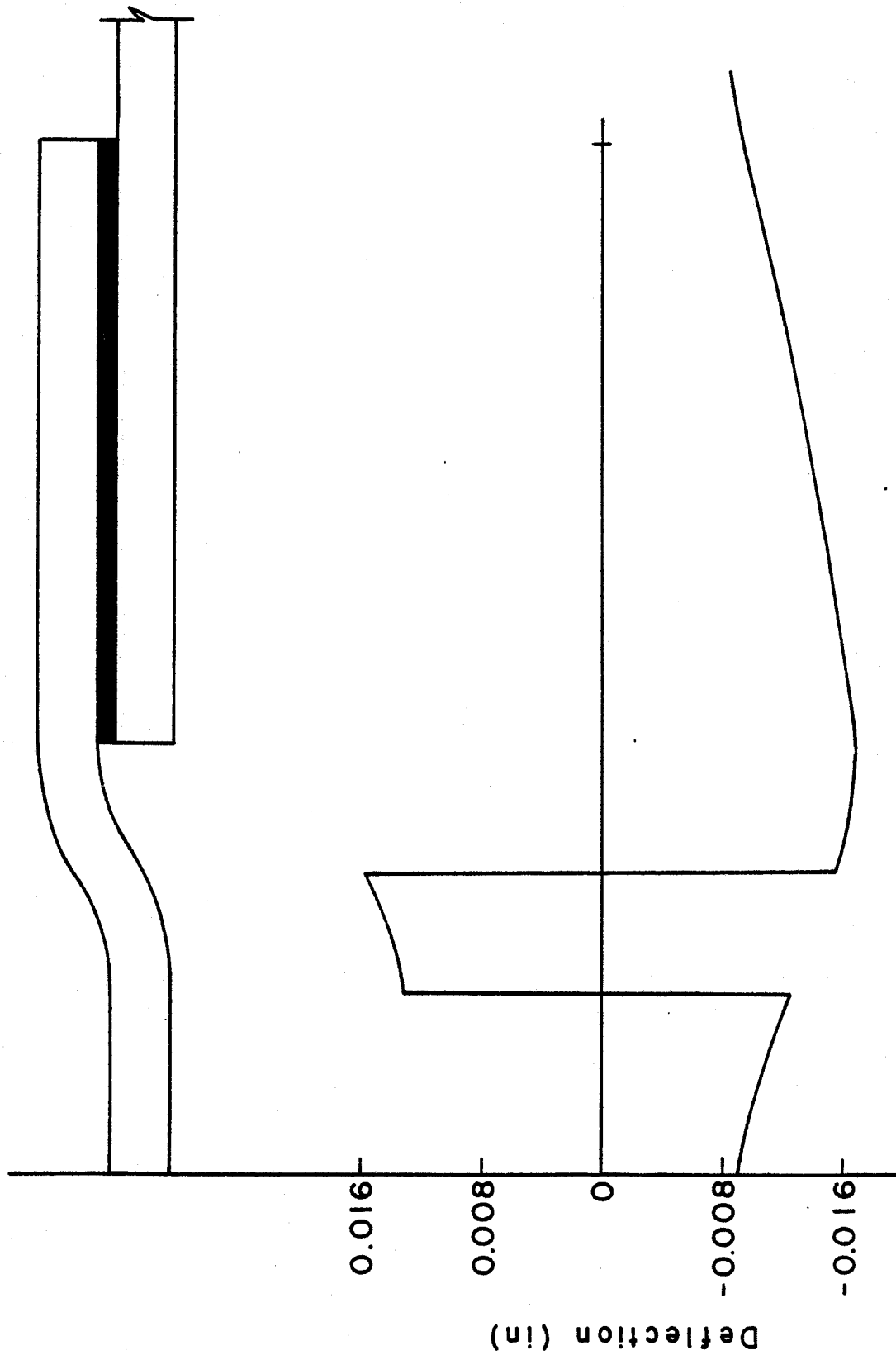


FIGURE 7: DEFLECTION OF NEUTRAL SURFACE AT FAILURE LOAD

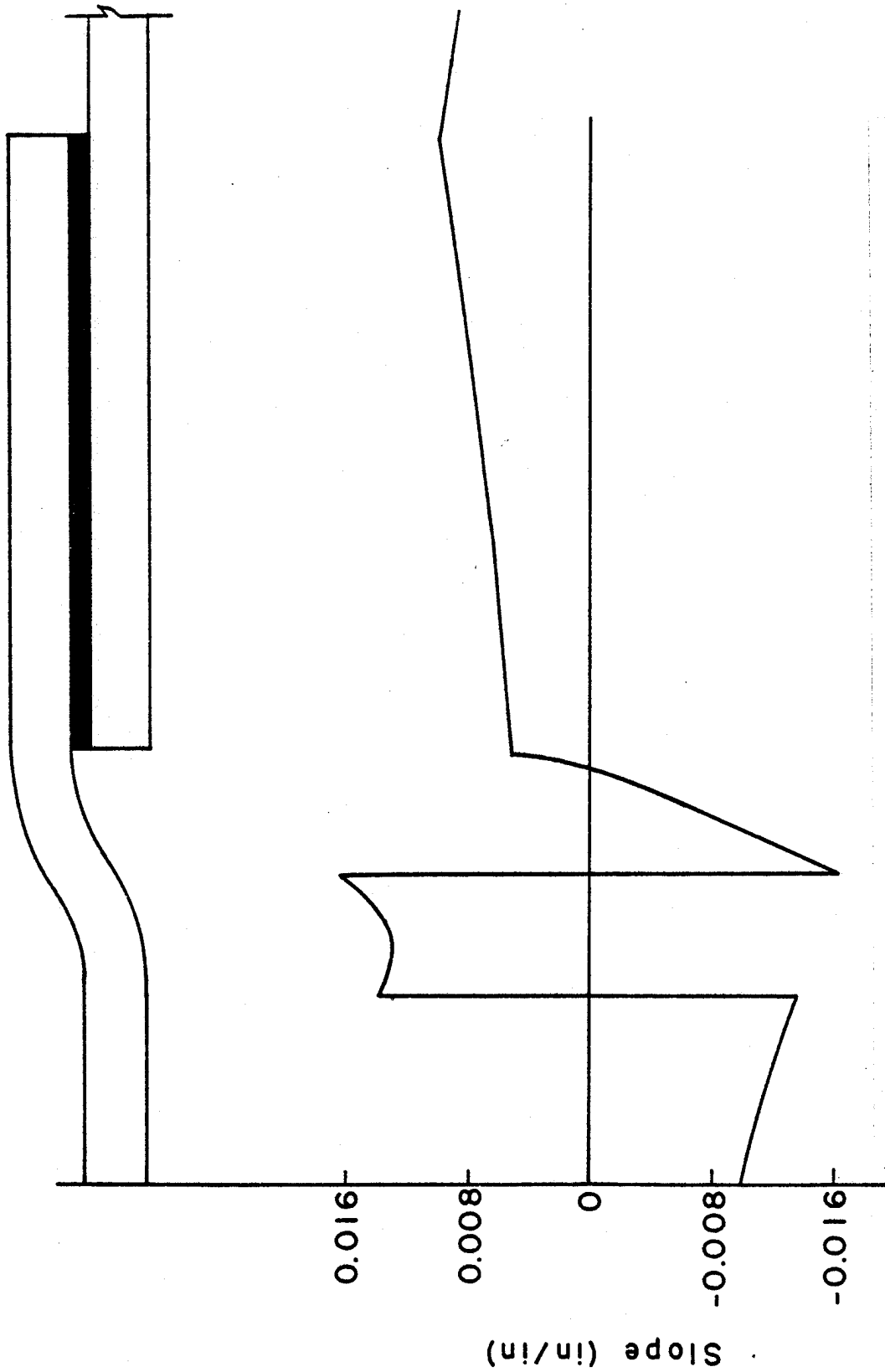


FIGURE 8: SLOPE OF THE NEUTRAL AXIS AT THE FAILURE LOAD



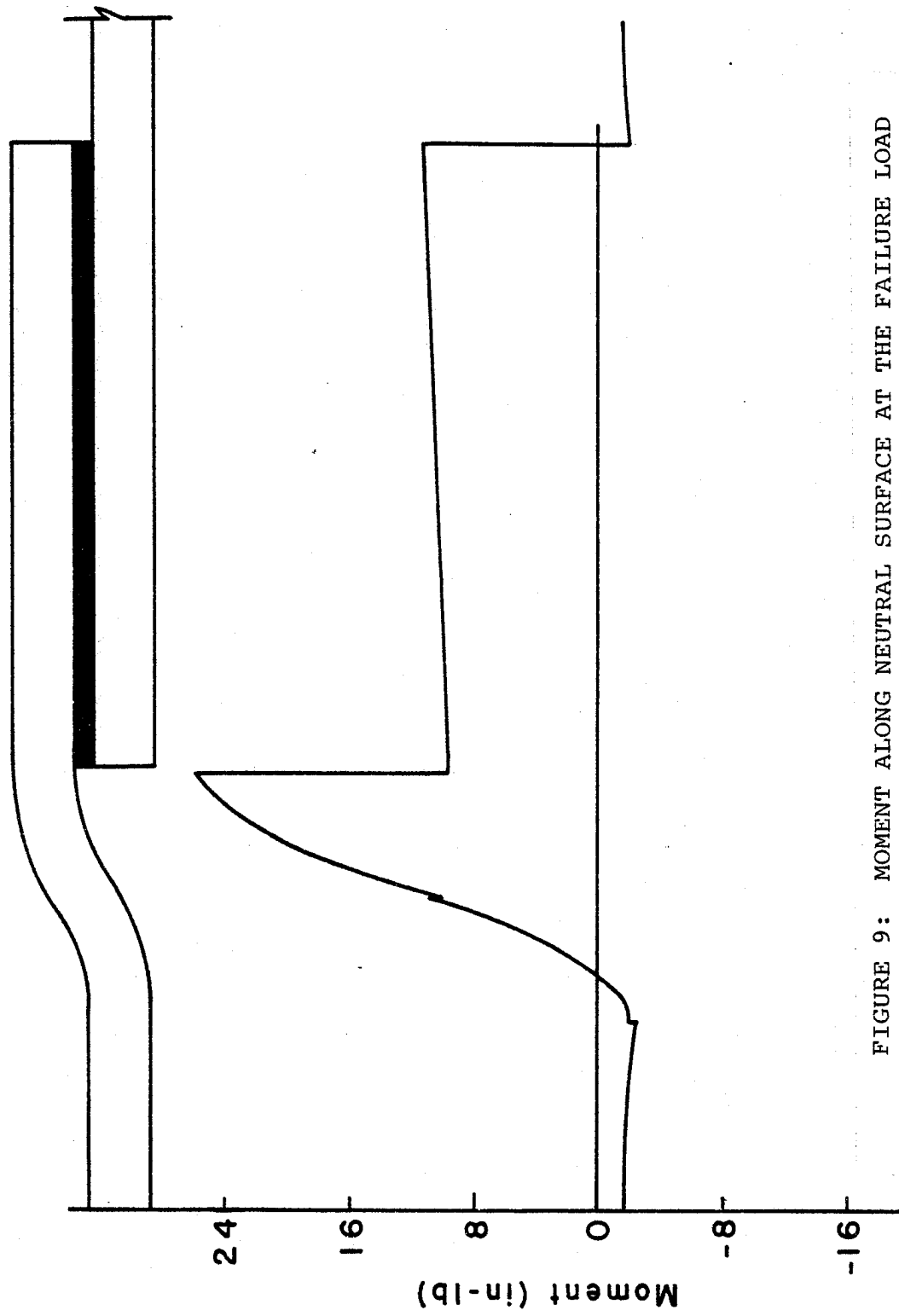


FIGURE 9: MOMENT ALONG NEUTRAL SURFACE AT THE FAILURE LOAD

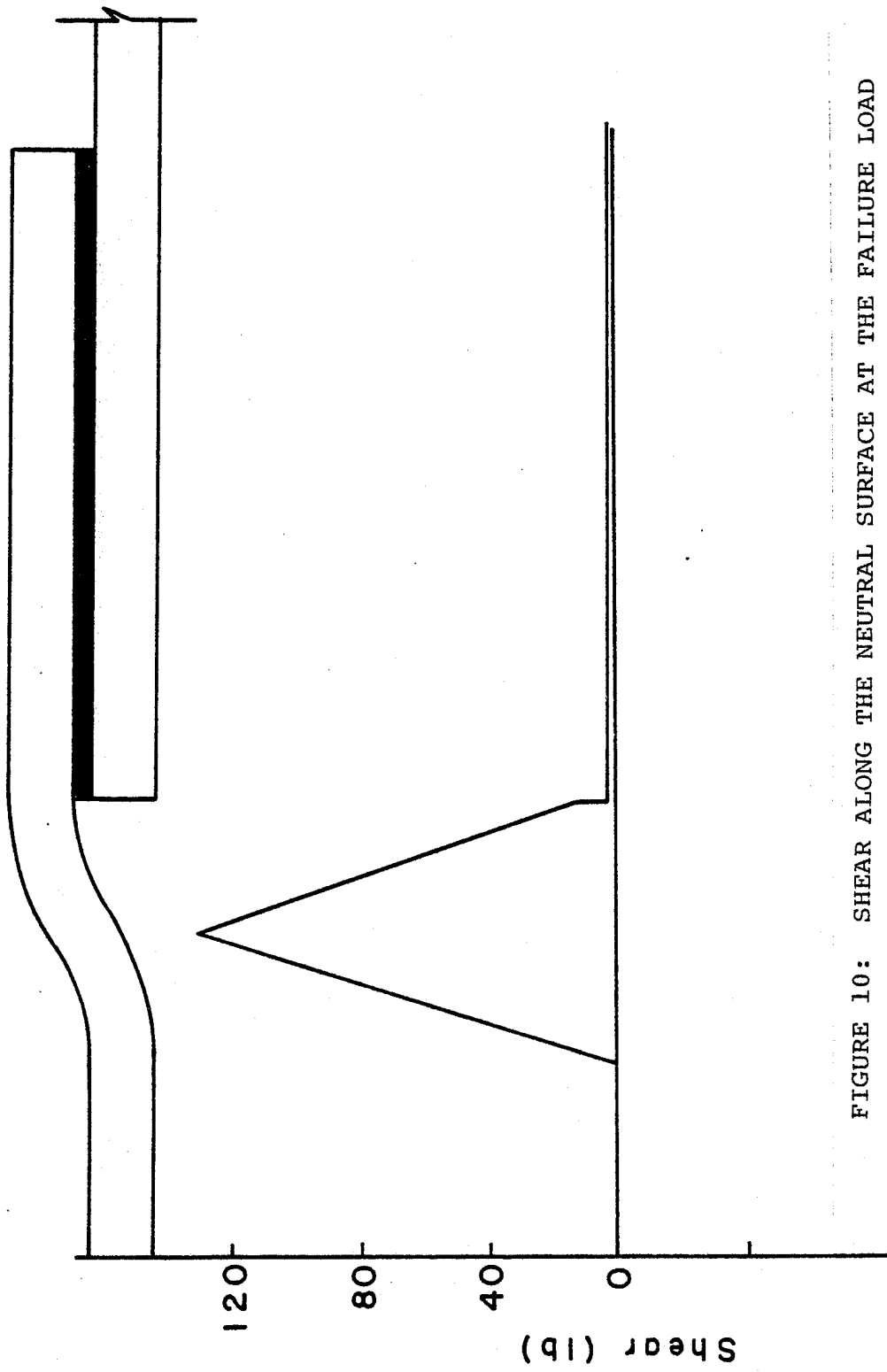
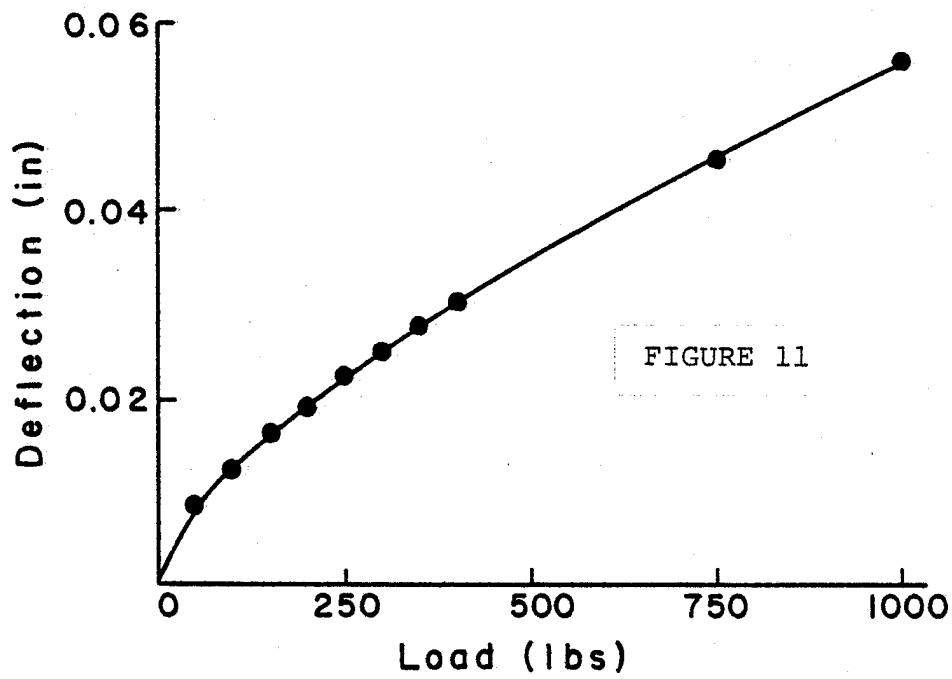
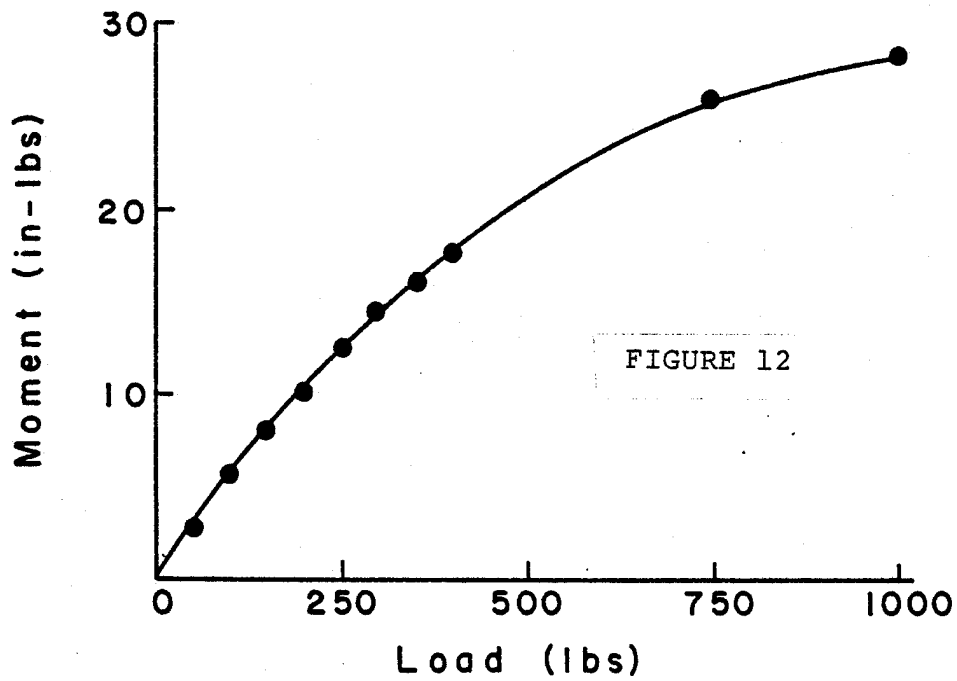


FIGURE 10: SHEAR ALONG THE NEUTRAL SURFACE AT THE FAILURE LOAD

joint behavior is to investigate the response of the joint to varying tensile loads. Figures 11 and 12 provide a clear indication of the deviation from linearity even for small values of load. Both the deflection (Figure 11) and moment (Figure 12) were recorded at the beginning of SEG3. (i.e.  $S_3 = 0$ )



RESPONSE OF THE JOGGLE-LAP JOINT AT  $S_3 = 0$



#### b. Finite Element Model (tension)

Anticipating the shortcomings of a beam bending model in the adhesive zone, defined to be the area of actual bonding, it was decided to model this area using finite-element methods. One of the underlying assumptions of small deflection beam theory is that plane sections remain plane during pure bending action. Clearly the validity of this assumption is questionable in the bonded area. Another reason for employing the finite element technique was to uncover any local stress concentrations that may not be revealed in a beam analysis. The finite-element mesh, consisting of 7 material types, is shown in Figure 13. Boundary conditions in the form of concentrated loads were applied to each of the finely meshed ends. Loading conditions were applied away from the adhesive layer at a distance of 1.5 times the thickness in an effort to minimize the effects of the end loads upon the stress solution. An explanation of how these boundary conditions were determined will follow shortly. A plane stress analysis was utilized to calculate the displacement and stress fields. Figures 15 through 17 are the result of a plotting routine which displays lines of constant stress. The figures should be interpreted in the same manner as that of a topographical map. Adjacent lines spaced closely together indicate areas of high stress gradients and possible sites for structural failure. The

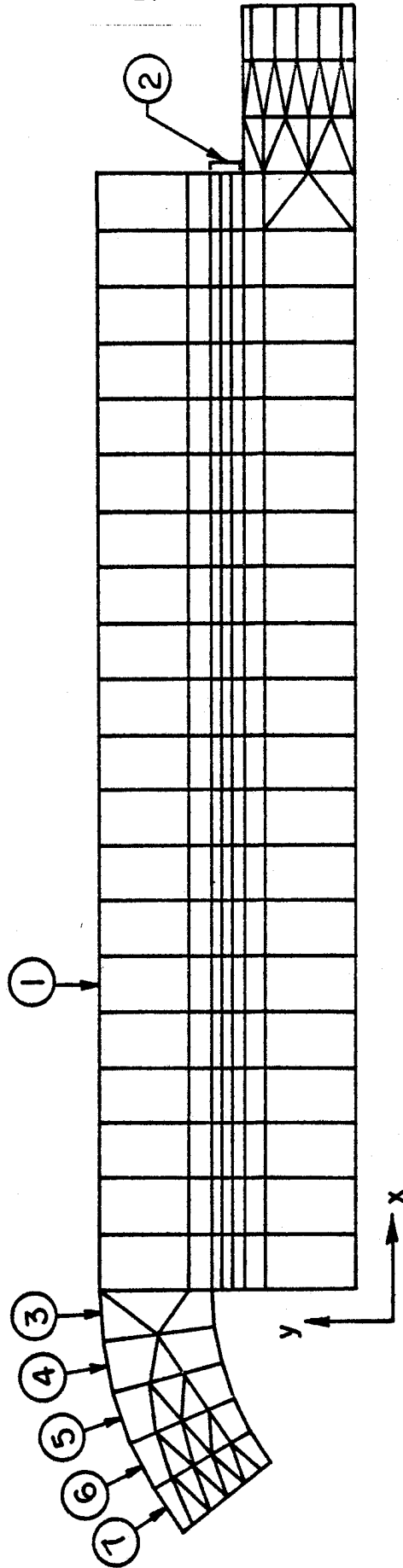


FIGURE 13: FINITE ELEMENT MESH OF THE ADHESIVE ZONE

7 Material Types

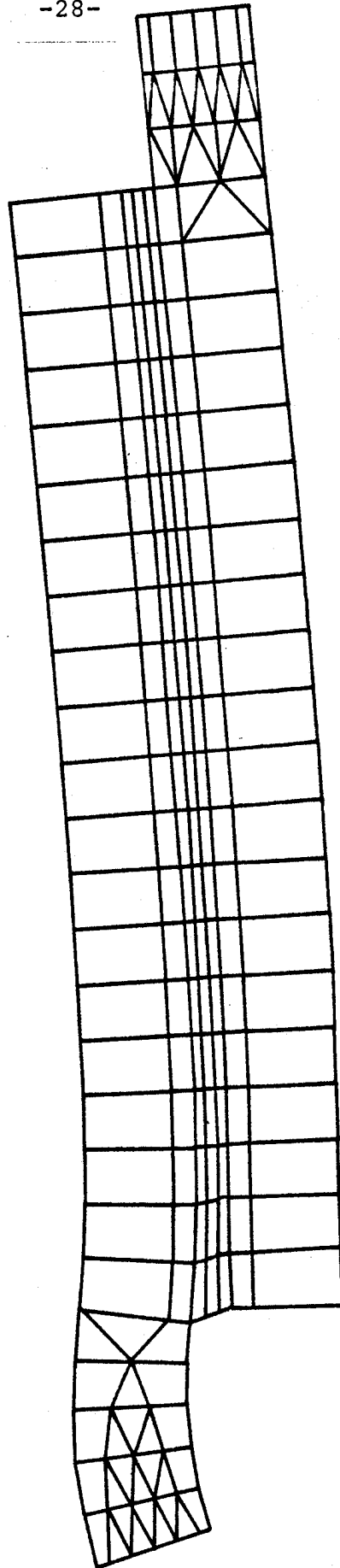


FIGURE 14: DEFORMED MESH AT THE FAILURE LOAD

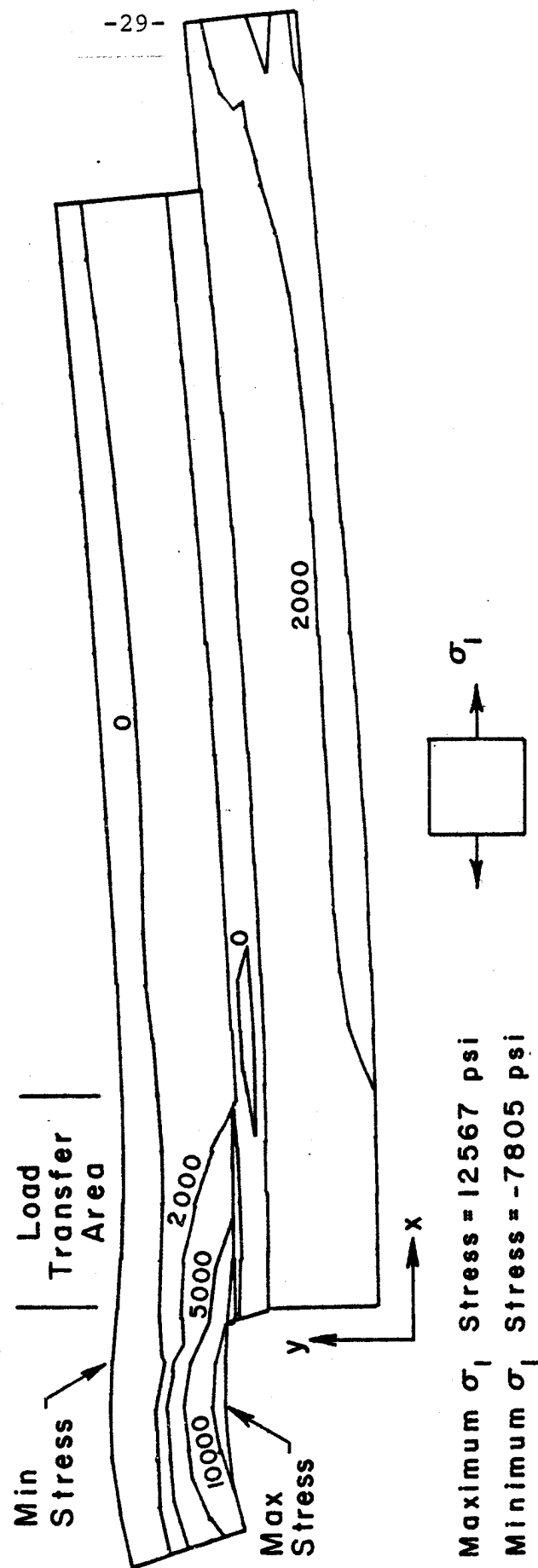


FIGURE 15: THE ADHESIVE ZONE IN TENSION - CONTOURS OF  $\sigma_1$  STRESS



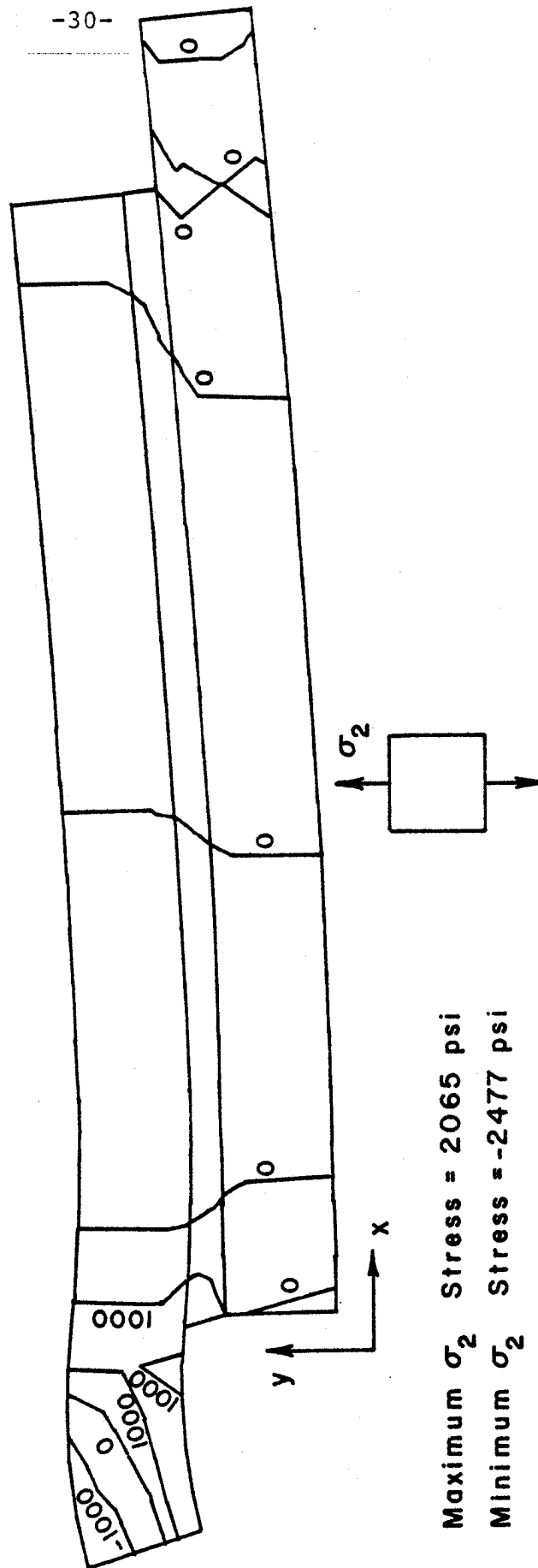


FIGURE 16: THE ADHESIVE ZONE IN TENSION - CONTOURS OF  $\sigma_2$  STRESS

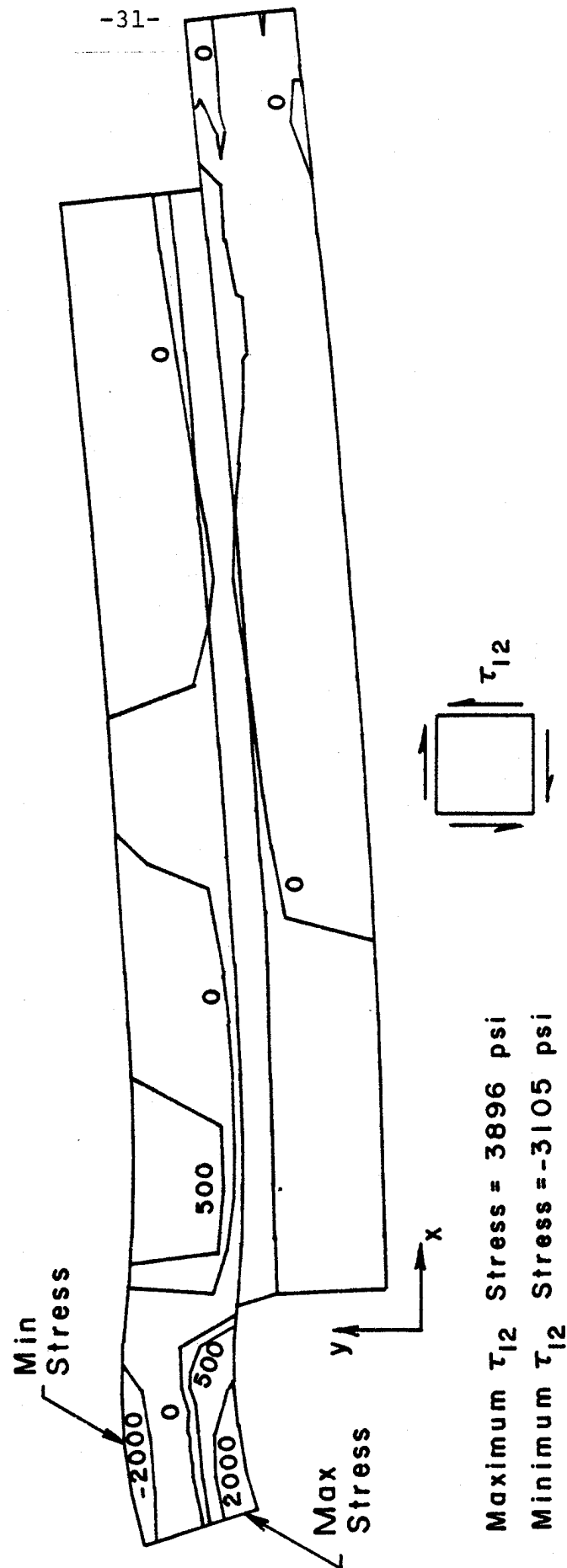


FIGURE 17: THE ADHESIVE ZONE IN TENSION - CONTOURS OF  $\tau_{12}$  STRESS

figures are labeled according to the component of stress being displayed. All three plots are the result of loading the specimen at the tensile failure load and are representative of the deformed geometry.

The limitations of the beam bending model are clearly displayed in Figure 15 and reveal the justification for the finite-element model. Shown in the figure is a smooth transition of stress across a change in cross-sectional area, (i.e. shift of the neutral axis) as calculated by the finite-element method. Experimental results have shown this to be a correct representation of the stresses. Beam analysis would have shown a sharp discontinuity in the stress profile where such a shift in the neutral axis occurs. Since the moment is nearly constant throughout SEG4 (see Figure 9) beam analysis would calculate  $\sigma_1$  stress contours parallel to the adhesive layer. The  $\sigma_1$ ,  $\sigma_2$ , and  $\tau_{12}$  stress components are global oriented stresses as opposed to those that can vary according to element orientation. Marked on each figure are those areas where the assumptions made via beam analysis quite appreciably affect the accuracy of a correct solution.

Many analyses of lap joints assume a condition of constant shear stress in the adhesive layer itself. This would indeed be the case if the adherents were infinitely stiff as compared to the adhesive and also if the existence of a load transfer area was prohibited. Shear stress data

from the finite element model is plotted in Figures 18 and 19 and the indication is clear that the shear stress is not a constant in the load transfer area. The case of constant shear stress found toward the center of the adhesive zone, however, reveals the linear nature of the displacement function through the adhesive thickness in this area.

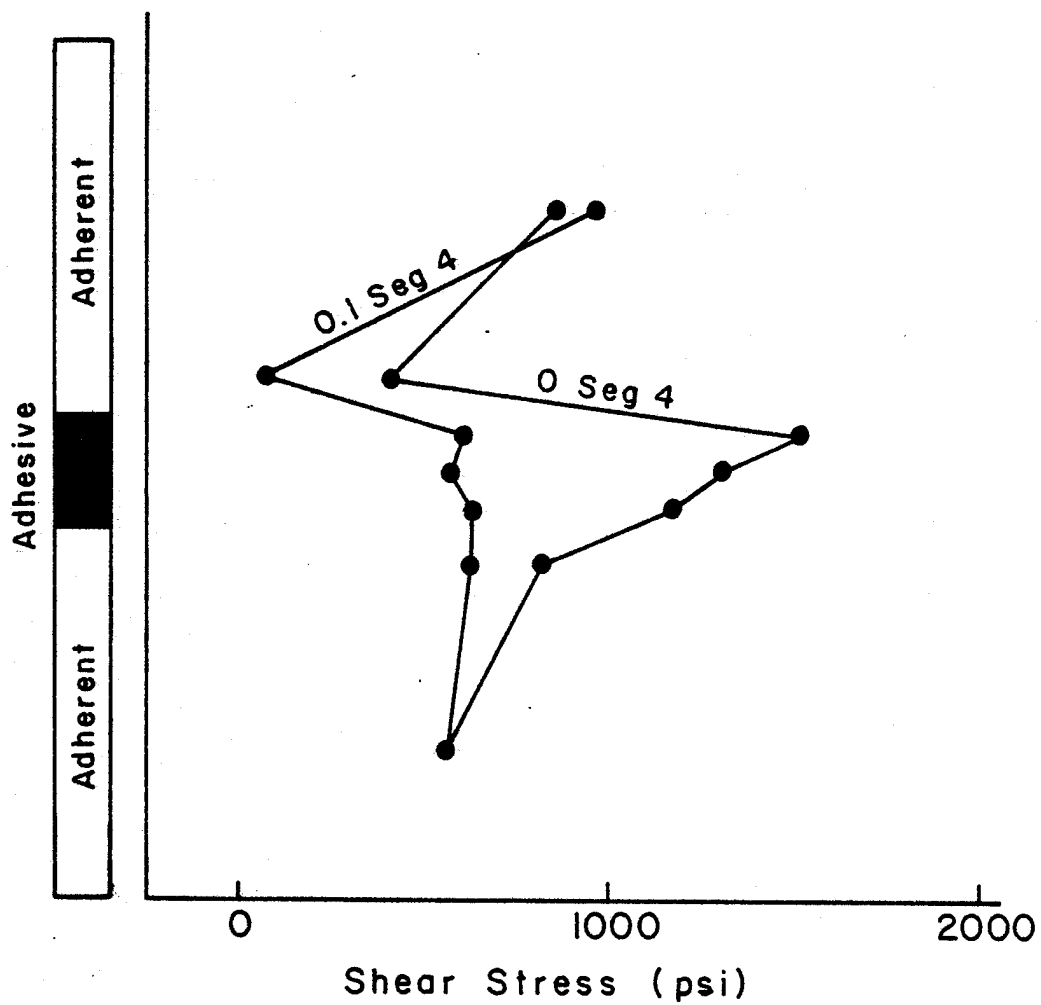


FIGURE 18: SHEAR STRESS VARIATION THROUGH THE THICKNESS OF THE ADHESIVE ZONE

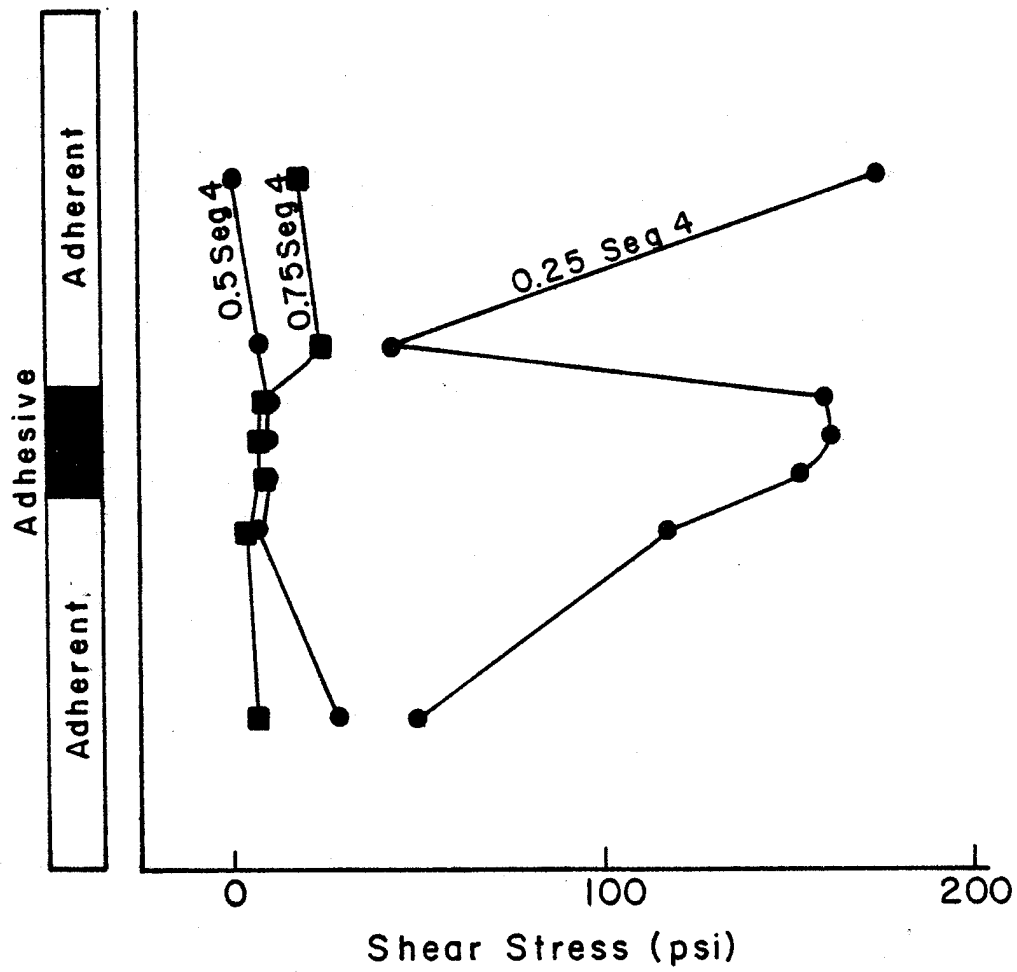


FIGURE 19: SHEAR STRESS VARIATION THROUGH THE THICKNESS OF THE ADHESIVE ZONE

## Boundary Conditions for the Finite-Element Model

The boundary conditions for the finite-element model are determined by applying the stress distribution as directed by the beam bending model to the finely meshed ends of the undeformed geometry of the finite element model. In other words, the stresses in the deformed geometry (beam model) must be moved through a distance to their equivalent point of application in the undeformed geometry (finite-element model). The reason for this difficulty with boundary conditions is that we are currently utilizing a linearized finite element routine, SAP V<sup>2</sup>, to solve a non-linear problem. Justification of such a procedure will hopefully become lucid with time.

To facilitate the derivation of a transformation routine, Figures 20 and 21 illustrate the following sign conventions. Figure 20 depicts a stress distribution for the left hand face of the finite element model with tension being taken as positive and compression being negative. Note that the neutral axis is not coincident with the centroidal axis inherent in the analysis of a curved beam. As mentioned previously, this fact yields a hyperbolic stress distribution which slightly complicates the computations. (SEE derivations of governing equation for stresses in a curved beam, Appendix A)

---

<sup>2</sup>Structural Analysis Program V; University of Southern California, Department of Civil Engineering, Oct. 77.





Figure 21 reveals a planar view of the deformed and undeformed sections. It is assumed in this derivation that the section of the beam can at most undergo a translation and a rotation. Translations are measured via the parameter DEFLA and are positive radially outward as shown. Small deflection theory also allows the rotations to be written as a change in slope. This parameter is DUDSA and is positive counter-clockwise.

With these sign conventions clearly in mind the stress distribution of the deformed geometry may now be resolved into concentrated force components. Representing the hyperbolic stress distribution as equivalent point forces and point couples acting at nodal points labeled 1 through 5 on Figure 21 corresponds mathematically to an integration of the stress distribution between fixed limits.

$$F_{ni} = \frac{M}{\bar{u} a} \int_{h_{i-1}}^{h_i} \frac{u}{R-u} du + \int_{h_{i-1}}^{h_i} F \cos (\theta + \text{DUDSA}) du \quad (6)$$

where  $i = 1-5$

$F_{ni}$  = nodal force component

$M$  = moment

$\bar{u}$  = distance between neutral and centroidal axes

$a$  = cross-sectional area

$R$  = radius of curvature

$F$  = load

$\theta$  = angle subtended by SEG3

DUDSA = local slope of deformed neutral axis

The first term of Eq. (6) represents the contribution from the hyperbolic stress distribution. The second term acts to superimpose the component of force due to longitudinal loading.

A correcting moment is calculated for each node to equilibrate the two representations of stress on the section.

$$M_{\text{corr}} = \int_{h_{i-1}}^{h_i} \sigma(u)u \, du - F_{ni}u \quad (7)$$

The need for the correcting moment is due to the fact that a distributed force is now represented by a point force as shown in Figure 22.

The next step follows from a translation of the point forces. Elementary statics dictates that a point force may be equivalently represented by the same point force and an added moment to account for the translation from the original line of action.

After carrying out a similar procedure for the stresses at the right hand side of the finite element model, the entire system is set in equilibrium by accounting for the shear acting on each face of the model. The values of shear are obtained directly from the beam bending model. Thus a correct set of boundary conditions has been determined for the finite-element model of the adhesive zone. A computer routine designated by CONVERT was written to calculate appropriate boundary conditions and may be found

in Appendix C.

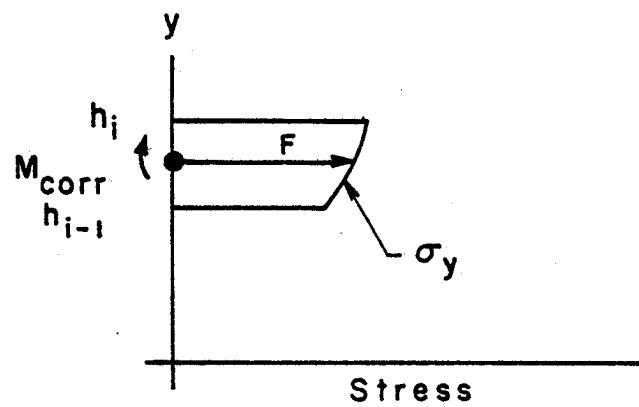


FIGURE 22: ILLUSTRATION OF THE CORRECTIVE MOMENT

## Methods of Analysis

### B. Flexure Loading

#### a. Beam Model

The bending behavior of the "joggle-lap" joint was also studied. It was found that the theoretical analysis was far simpler than that encountered for tensile loading. Each segment of the joint (see Figure 6) was modeled as if it were in pure bending. Stresses in the straight beam numbers were calculated via the flexure formula while for the curved beams the formula

$$\sigma_y = \frac{My}{(R-y)\bar{y}a} \quad (8)$$

where M = moment

y = coordinate from the neutral surface  
(positive radially inward)

R = radius of curvature

$\bar{y}$  = distance between centroidal and neutral axes

a = crosssectional area

was used.

In order to compute bending stresses in SEG4 (layered beam) it is necessary to introduce the notion of equivalent sections. In this method we assume all materials to have the same modulus of elasticity. By replacing the actual section with a mechanically equivalent one allows

the flexure formula to be used as a means of computing stresses. The width of the sections are varied so that the new width equals the ratio of the old modulus of the material to the new modulus of the material times the old width as shown in Figure 23. Computing  $I_{eq}$  for the specimen geometry,

$$I_{eq} = \sum_{i=1}^3 \left( \frac{1}{12} b_i h_i^3 + a_i d_i^2 \right)$$

b = length of base

h = length of side

a = area

d = distance between element neutral axis and overall section neutral axis

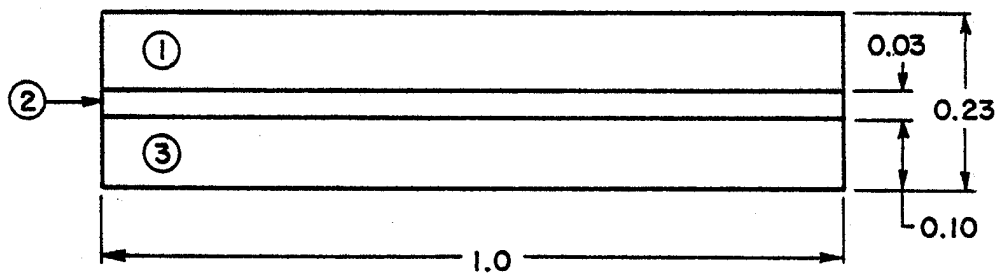
it is apparent that the effect of the adhesive layer on overall section stiffness is negligible. Using the flexure formula and the relation

$$(\sigma_x)_{actual} = \frac{E_{old}}{E_{new}} (\sigma_x)_{equiv.}$$

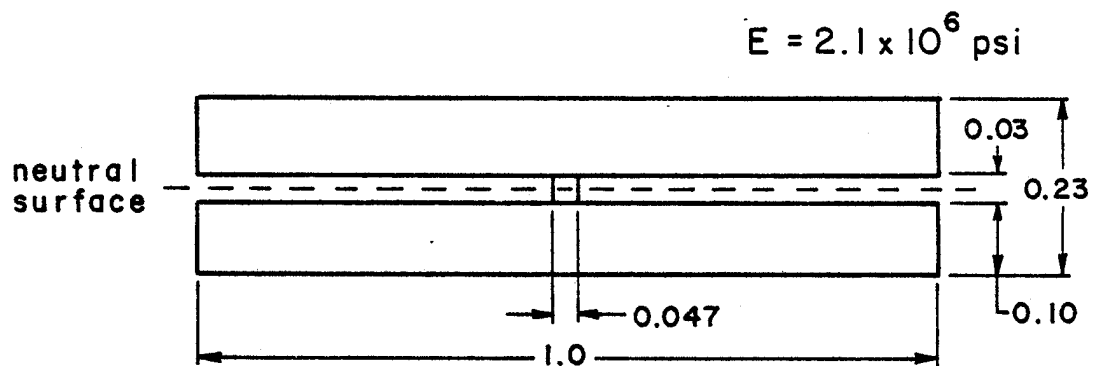
the stresses in SEG4 may easily be calculated.

$$E_{1,3} = 2.1 \times 10^6 \text{ psi}$$

$$E_2 = 1.0 \times 10^5 \text{ psi}$$



Actual End Section View



Equivalent Section

FIGURE 23: METHOD OF EQUIVALENT SECTIONS

b. Finite Element Model (flexure)

The boundary conditions of the finite-element model may be changed to accommodate pure bending. By utilizing couples at the finely meshed ends of the model, stresses in the adhesive zone may be monitored where it has been shown that the results from beam theory are less accurate. Figures 24 through 26 display  $\sigma_1$ ,  $\sigma_2$ , and  $\tau_{12}$  stress contours respectively within the "joggle-lap" joint in pure bending.

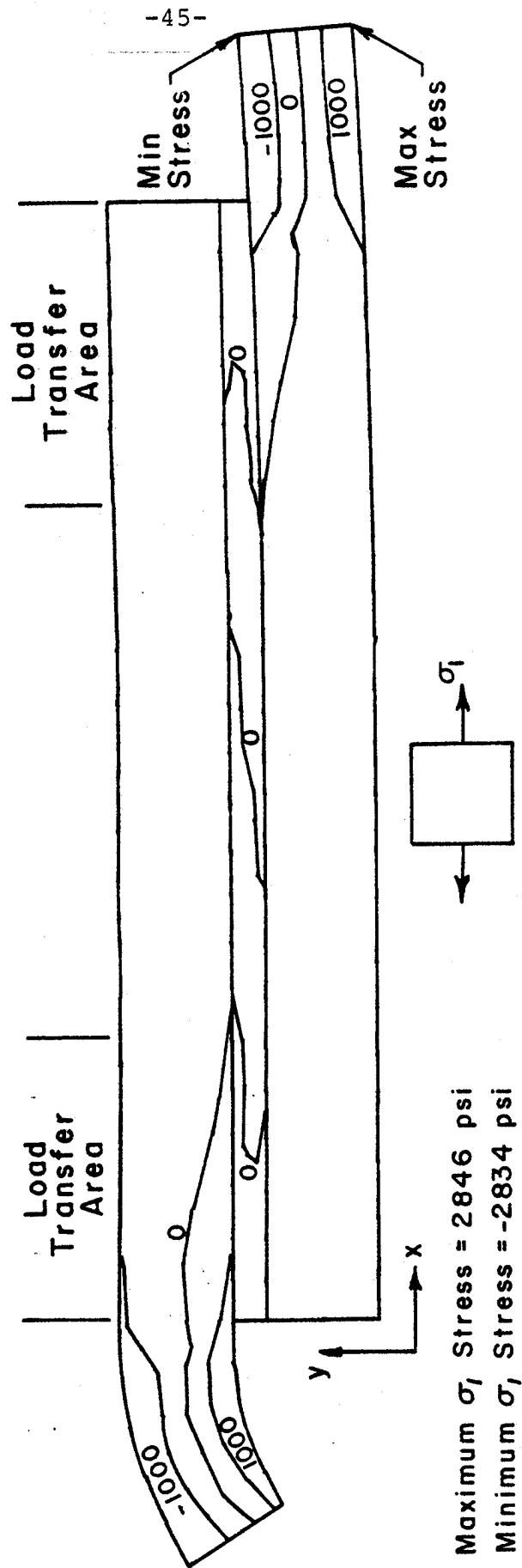


FIGURE 24: THE ADHESIVE ZONE IN BENDING - CONTOURS OF  $\sigma_1$  STRESS



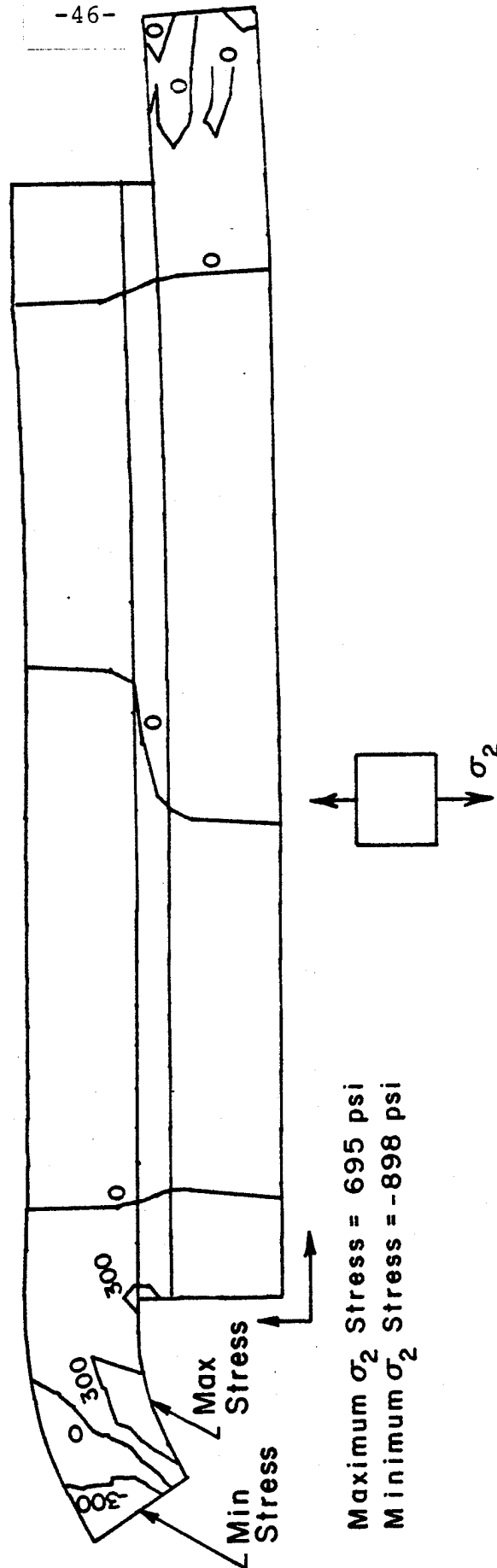


FIGURE 25: THE ADHESIVE ZONE IN BENDING - CONTOURS OF  $\sigma_2$  STRESS

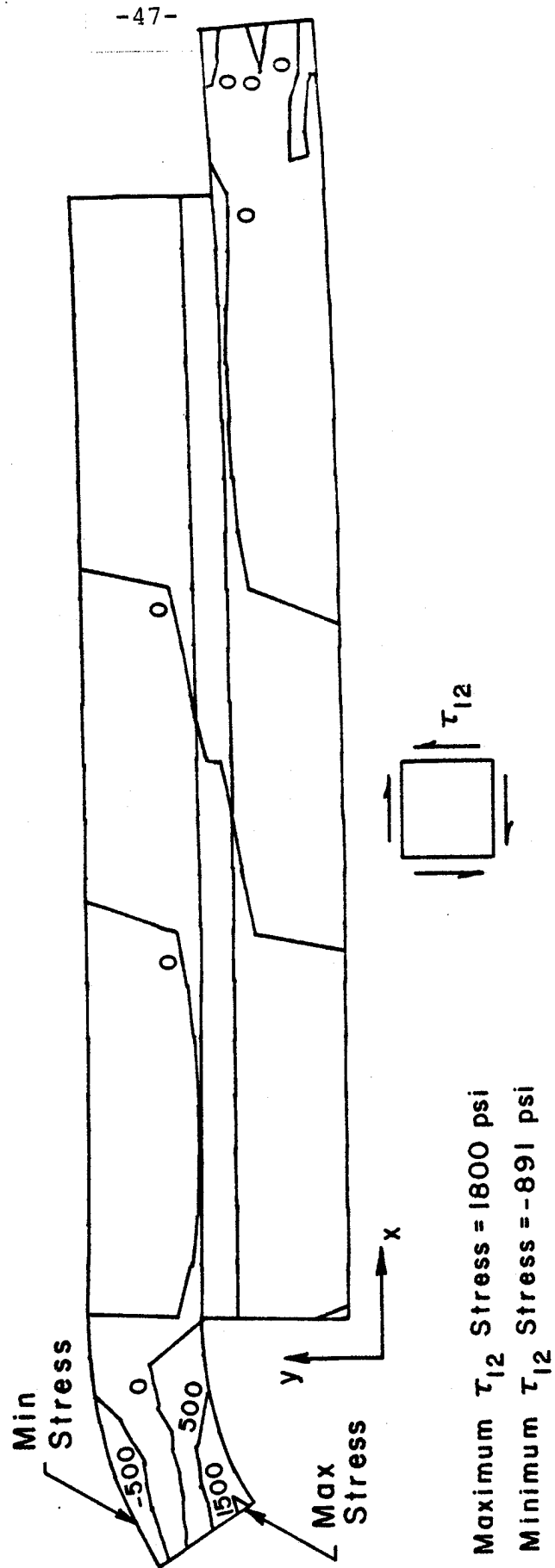


FIGURE 26: THE ADHESIVE ZONE IN BENDING - CONTOURS OF  $\tau_{12}$  STRESS

#### IV. Experimental Results

##### A. Tension

As set forth in the objectives of such a study, an emphasis was to be placed upon developing joint geometries which will accommodate high rate fabrication techniques. In an effort to meet this criterion experimentally, it was necessary to utilize a joint configuration currently being molded in industry. The time and expense of developing in-house molding capabilities proved to be beyond the scope of the research at hand. Thus, test sections were cut from premolded panels of SMC which were later bonded together to form the joint.

The bonding operation was also directed toward high fabrication procedures. All test specimens were adhesively joined at Goodyear Adhesives Division, Ashland, Ohio, via production adhesives application techniques. It was felt that by using these sophisticated application procedures optimum adhesive properties could be obtained.

In general, SMC is defined to be an anisotropic material because of the substantial difference between in-plane and out-of-plane properties. Referring to the coordinate system of Figure 1, the constitutive relations

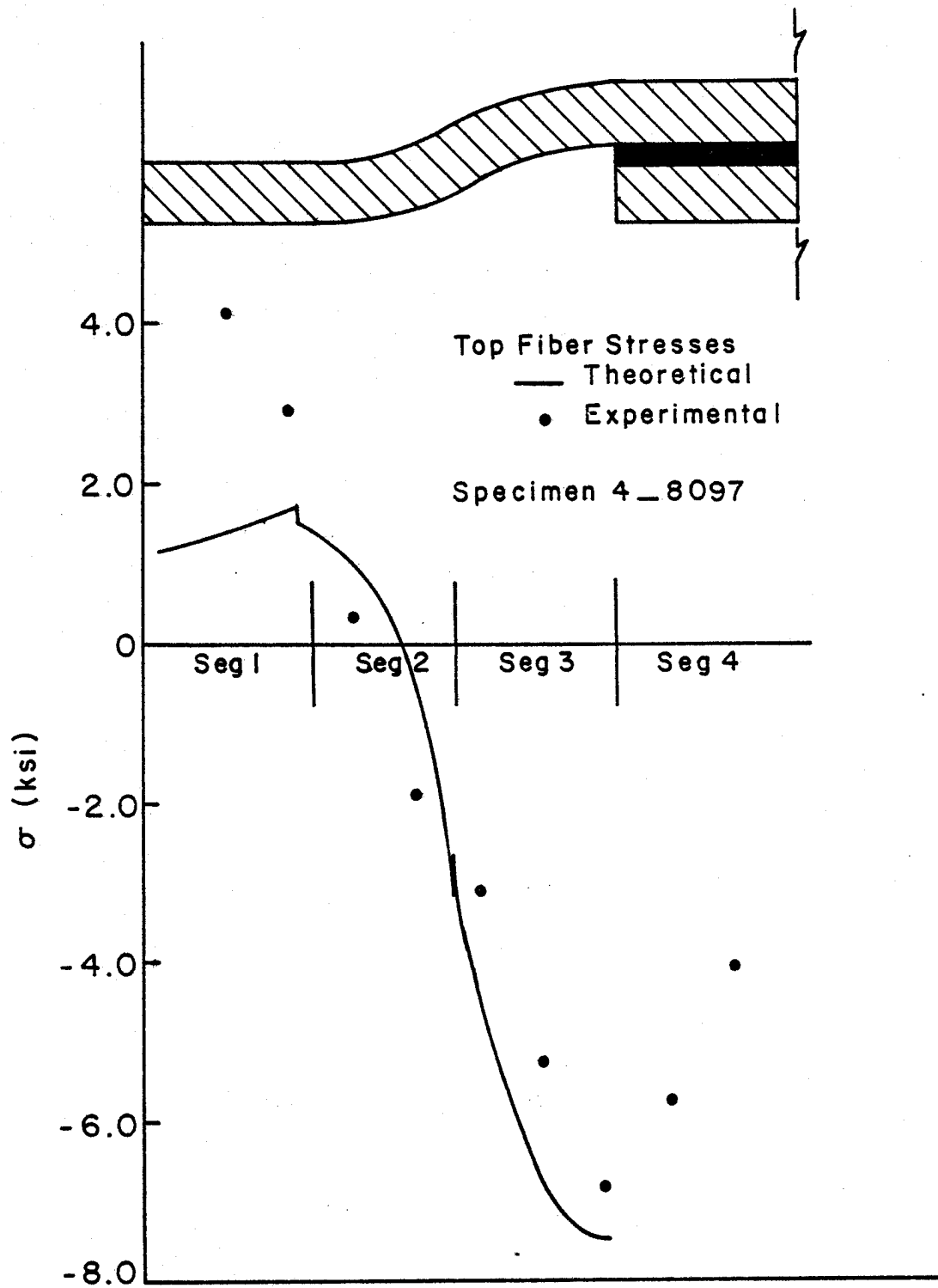


FIGURE 27: ELASTIC RESPONSE DUE TO TENSION - TOP FIBER STRESSES

THIS  
PAGE  
IS  
MISSING  
IN  
ORIGINAL  
DOCUMENT

49/50

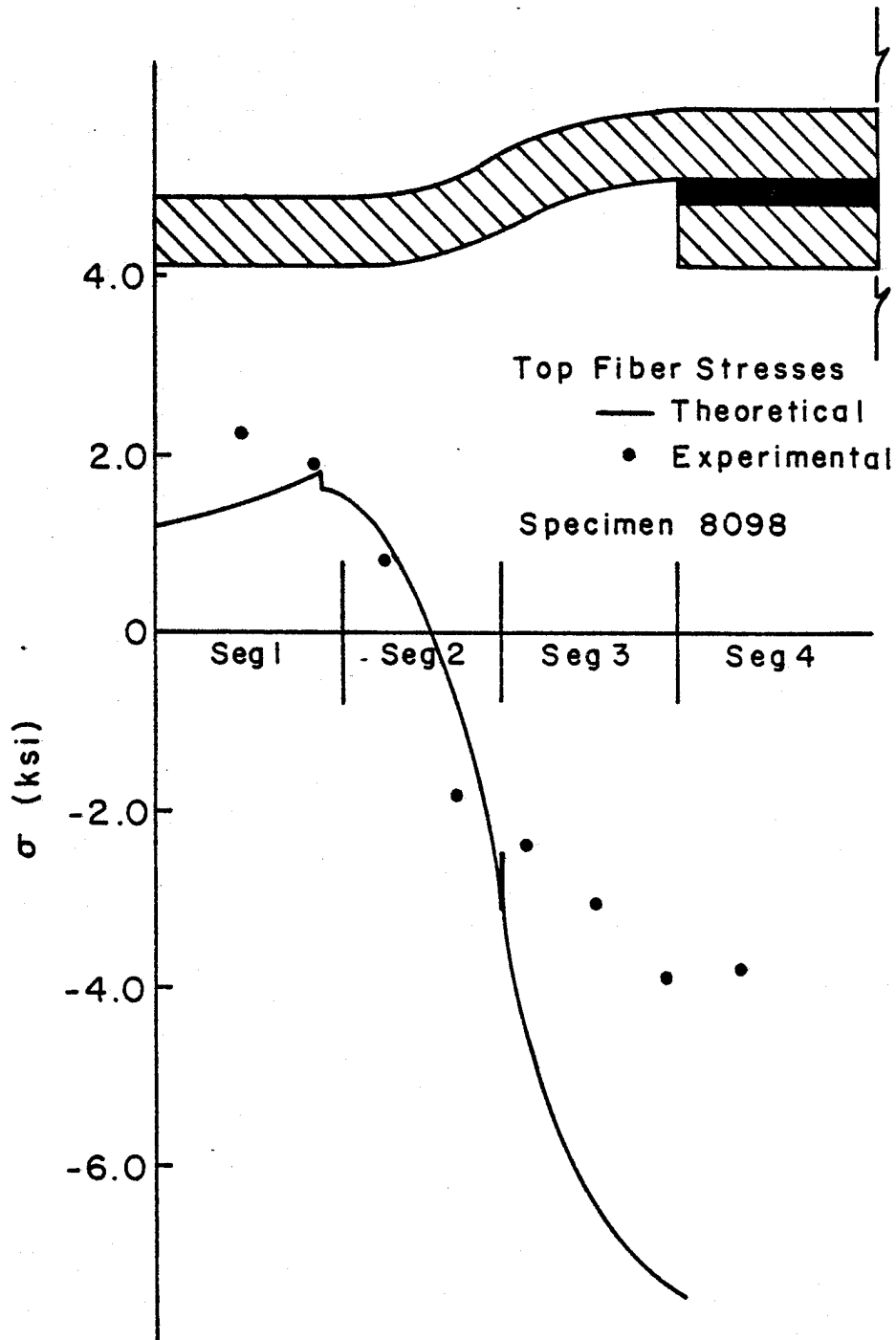


FIGURE 28: ELASTIC RESPONSE DUE TO TENSION - TOP FIBER STRESSES

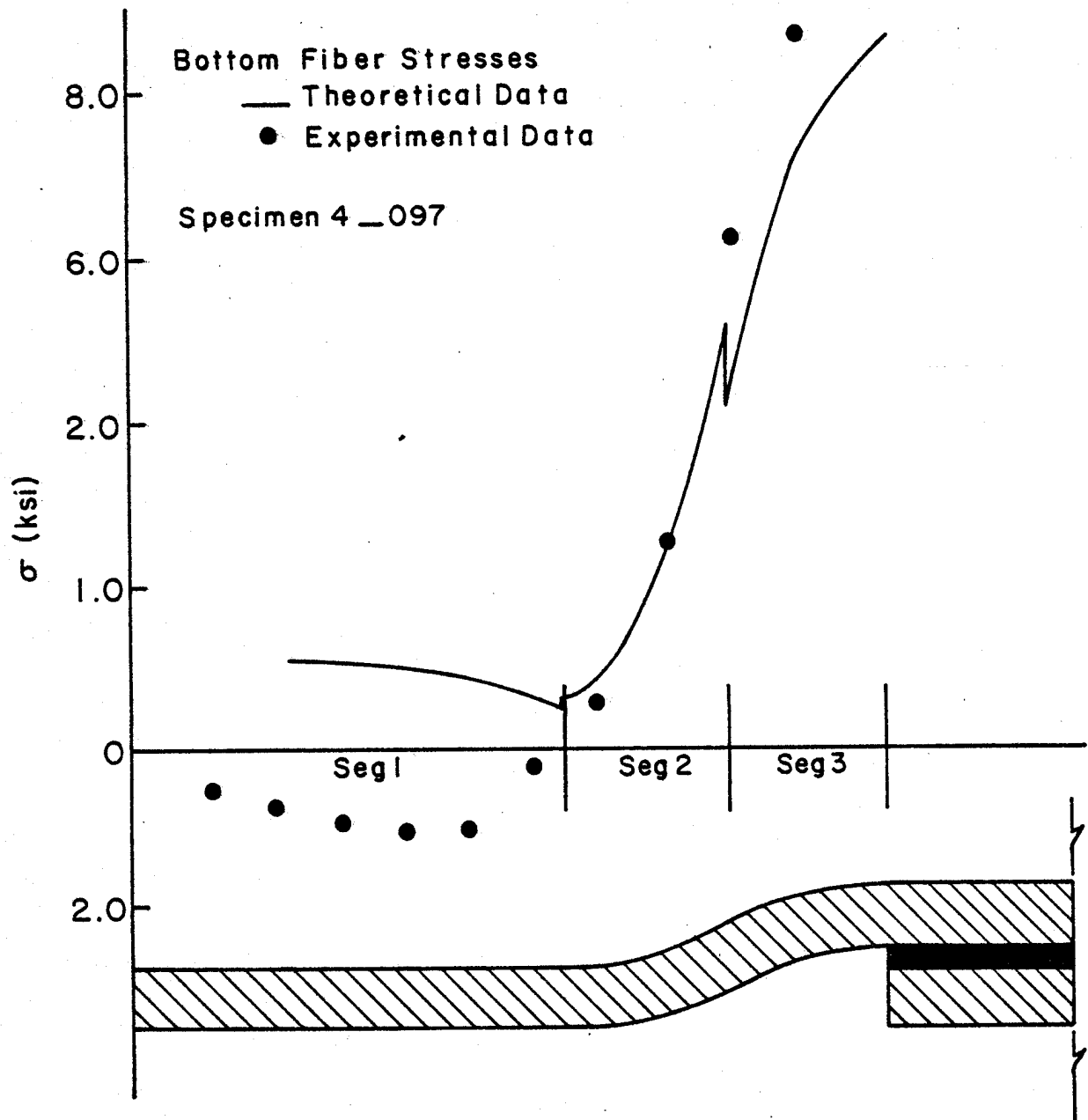


FIGURE 29: ELASTIC RESPONSE DUE TO TENSION - BOTTOM FIBER STRESSES

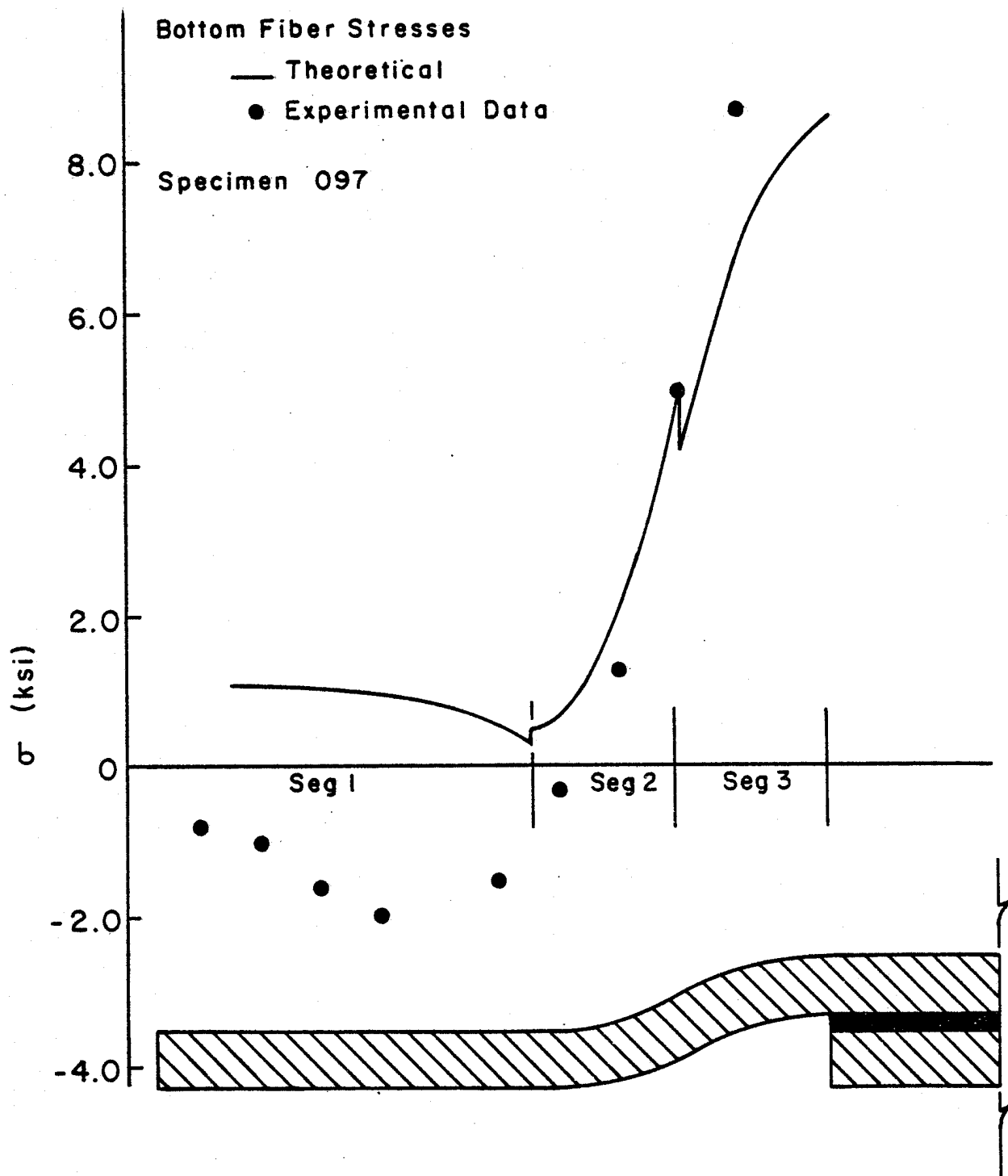


FIGURE 30: ELASTIC RESPONSE DUE TO TENSION - BOTTOM FIBER STRESSES



that the joint invariably strained beyond the small-deflection range at considerably small loadings. It was therefore a rather arduous task to approximately determine the experimentally applied moment to the joint. The correlation between the theoretical and experimental data may be referenced in Figures 31-34. As in the case of tensile loading, it should be noted that the stresses in SEG1 are again considerably higher than those predicted by theory, which is attributable to the molded geometry.

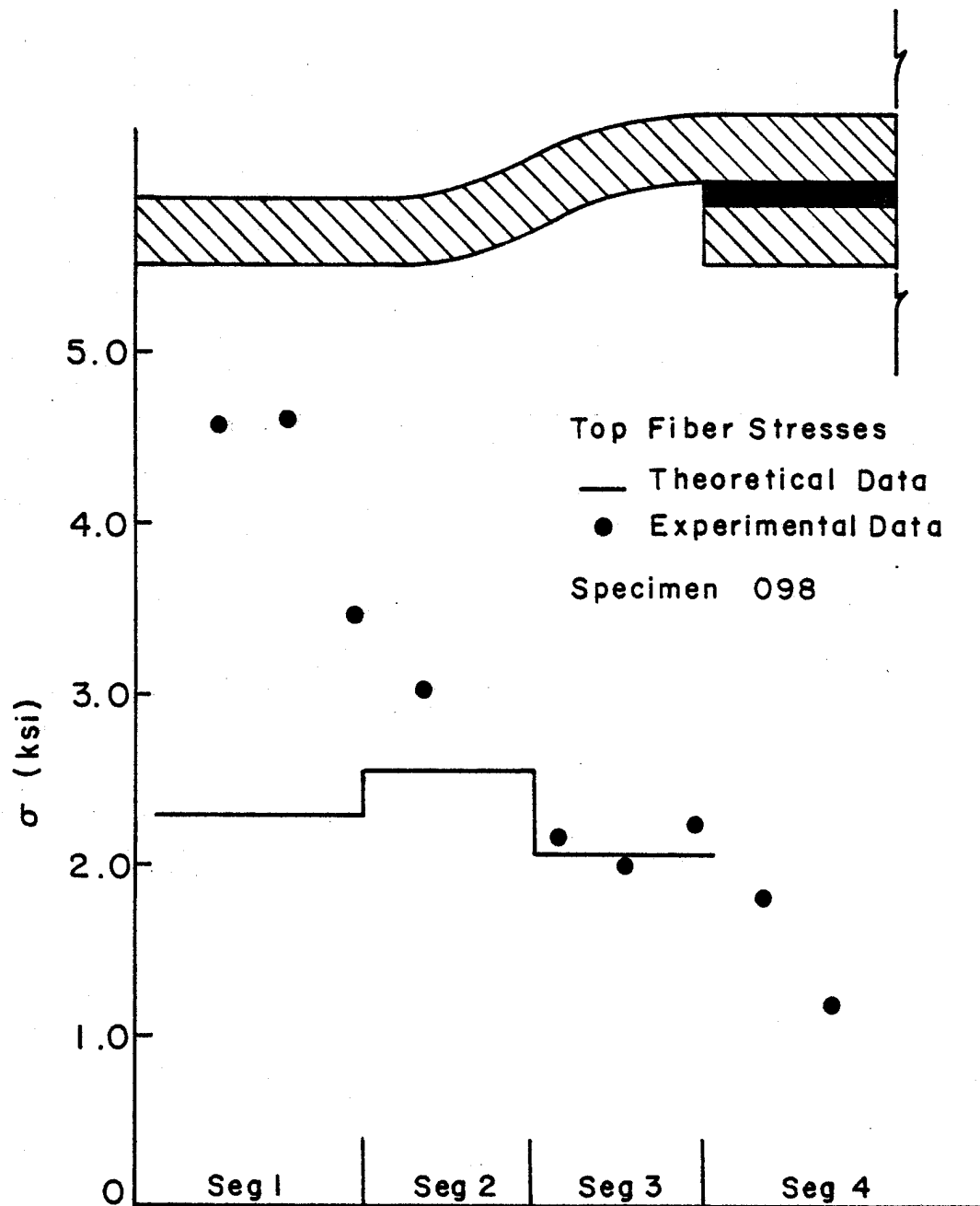


FIGURE 31: TOP FIBER STRESSES DUE TO BENDING

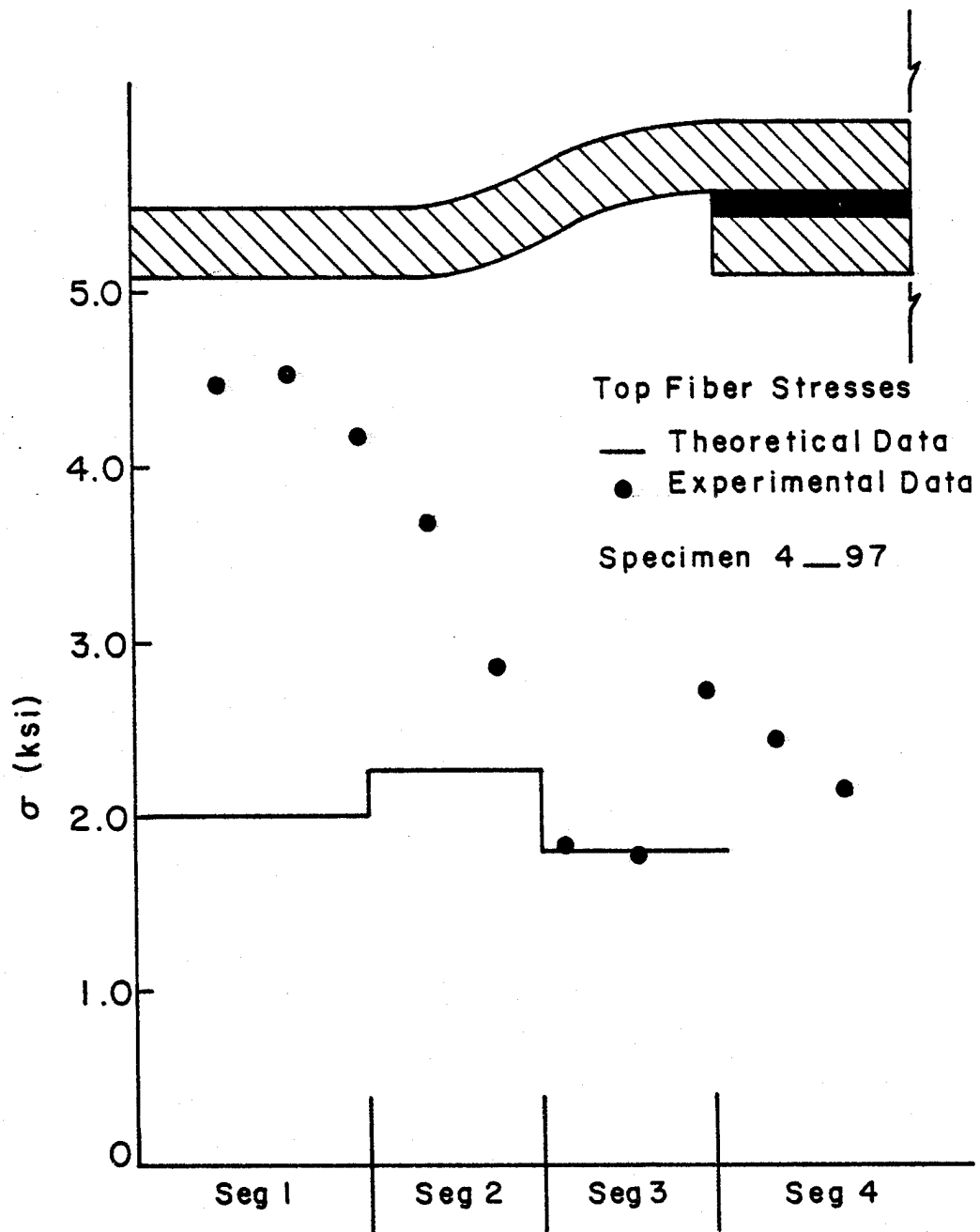


FIGURE 32: TOP FIBER STRESSES DUE TO BENDING

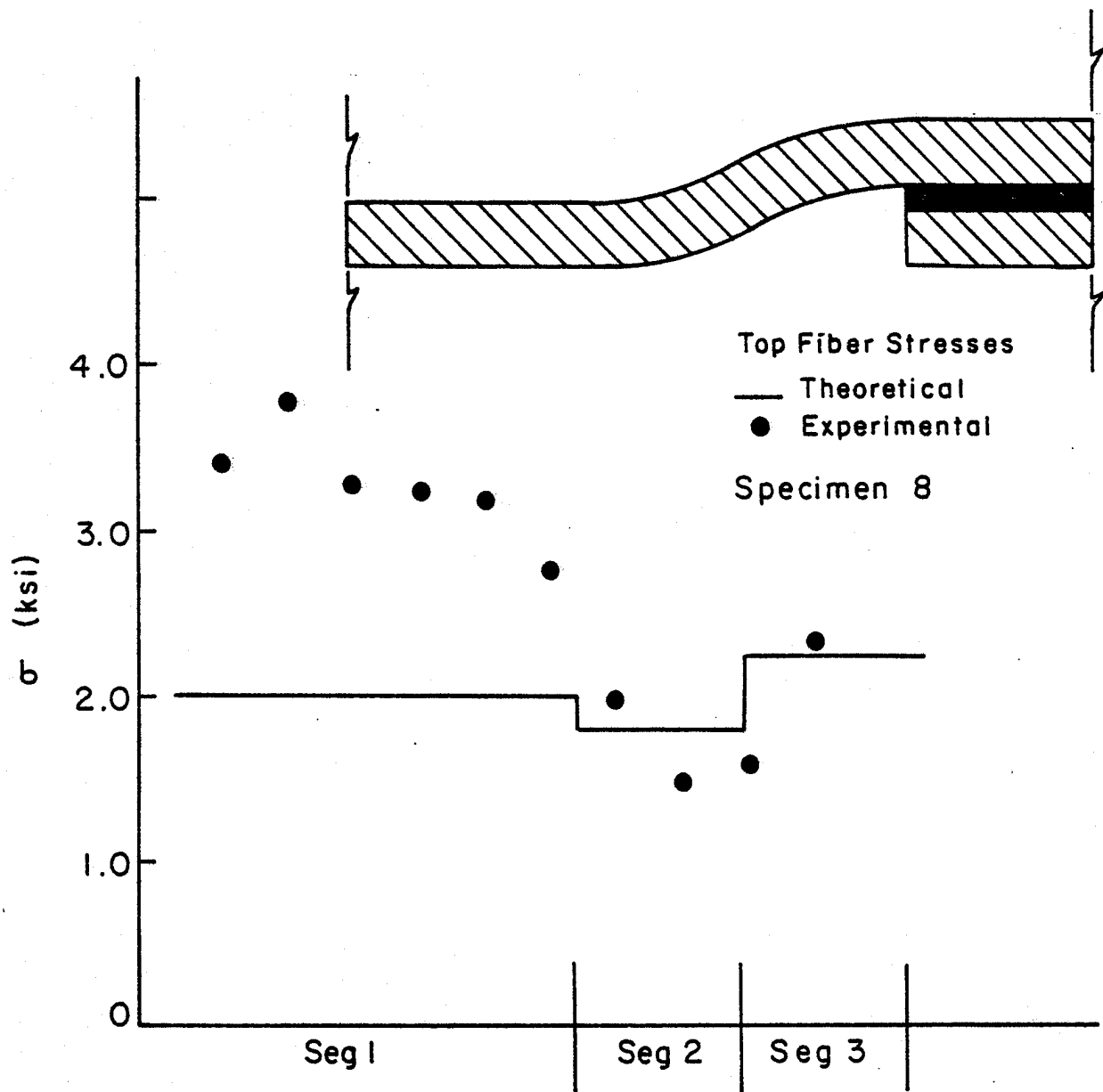


FIGURE 33: BOTTOM FIBER STRESSES DUE TO BENDING

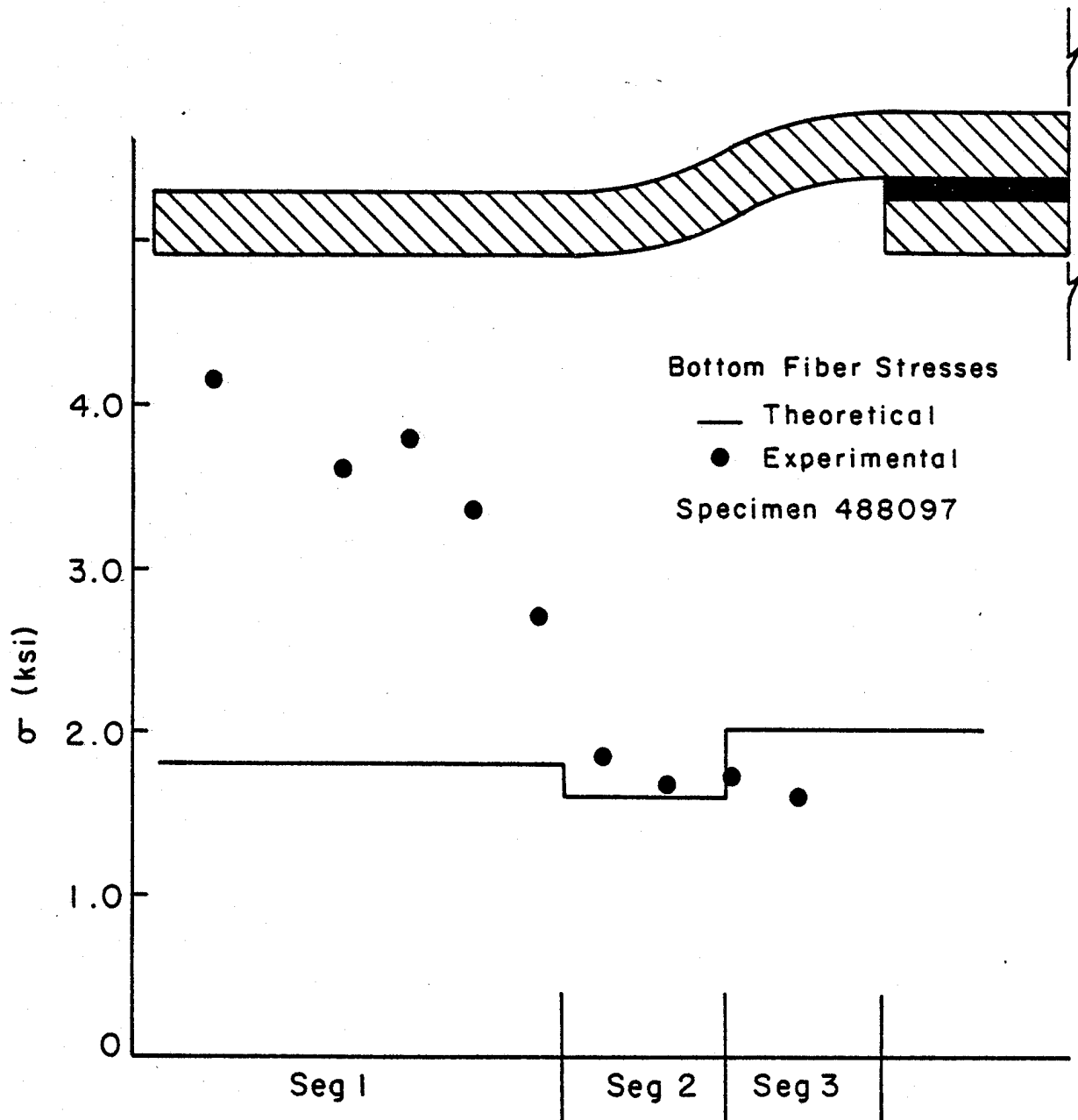


FIGURE 34: BOTTOM FIBER STRESSES DUE TO BENDING

Table 3

Experimental Results from Tension Tests

Specimen #	Contact Area (in <sup>2</sup> )	Loading Condition	Failure Load (LBS)	Failure Mode*
4__097	1	tension	191	flexure
4_8097	1	tension	206	flexure
4___98	1	tension	209	flexure
4__098	1	tension	171	flexure
___97	1.75	tension	169	flexure
___98	1.75	tension	242	flexure
__097	1.75	tension	151	flexure
_8098	1.75	tension	200	flexure

\*after failure initiation, it was observed that the crack was propagated via interlaminar shear

## V. Failure Analysis

One of the most important parameters to predict in a study of this type is the ultimate loading conditions. This in essence dictates the choice of a failure criterion. The maximum stress theory will be employed in this report because of its simplicity in application and execution. Other popular failure criteria, such as the Tsai-Wu criterion were deemed inappropriate due to the limiting assumptions made in accordance with beam theory.

Maximum stress criterion states that the material will fail when any component of stress exceeds the corresponding material strength. In general, the above statement may be written in equation form as

$$\sigma_i \geq X_i^T \quad (\sigma_i > 0) \quad i = 1-3 \quad (14)$$

$$|\sigma_i| \geq X_i^C \quad (\sigma_i < 0) \quad i = 1-3 \quad (15)$$

$$|\sigma_i| \geq S_i \quad i = 4-6 \quad (16)$$

where  $X_i^T$  = ultimate tensile strength  
 $X_i^C$  = ultimate compressive strength  
 $S_i$  = ultimate shear strength

These equations simplify to those listed below after employing the local coordinate nomenclature for the

"joggle-lap" joint.

$$\sigma_u \geq x^T \quad (\sigma_u > 0) \quad (17)$$

$$|\sigma_u| \geq x^C \quad (\sigma_u < 0) \quad (18)$$

$$|\sigma_{us}| \geq s_i \quad (19)$$

Applying this failure criterion to the model, it was found that the bottom fiber tensile stresses (see Figure 35) predicted the ultimate loading of the joint within experimental error. Thus the maximum flexural stress was utilized to predict failure.

All failures occurring as a result of tensile loading were initiated along the bottom surface of SEG3. Crack initiation was observed to be of the net tension mode, while propagation appeared to be due to "interlaminar shear". There was a general consistency among the initiation and propagation of the crack for all tension tests.

It was thought at one time that the curved sections of the joint (SEG2, SEG3) were either fiber deficient or highly anisotropic yielding a potential low strength area. However, a photomicrograph of this cross-sectional area clearly shows no such tendencies. (See Plate 7)



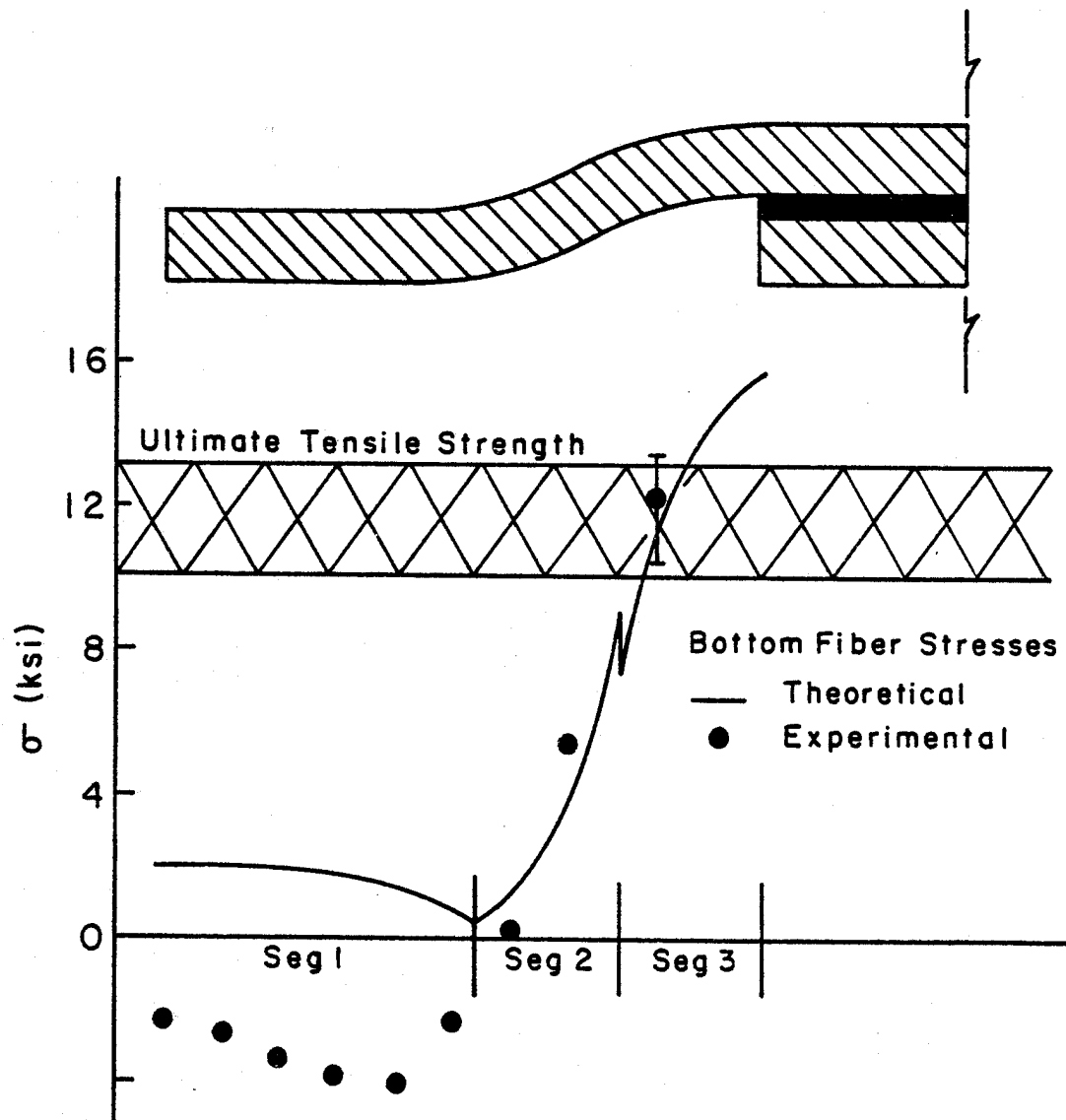


FIGURE 35: BOTTOM FIBER STRESSES AT THE FAILURE LOAD

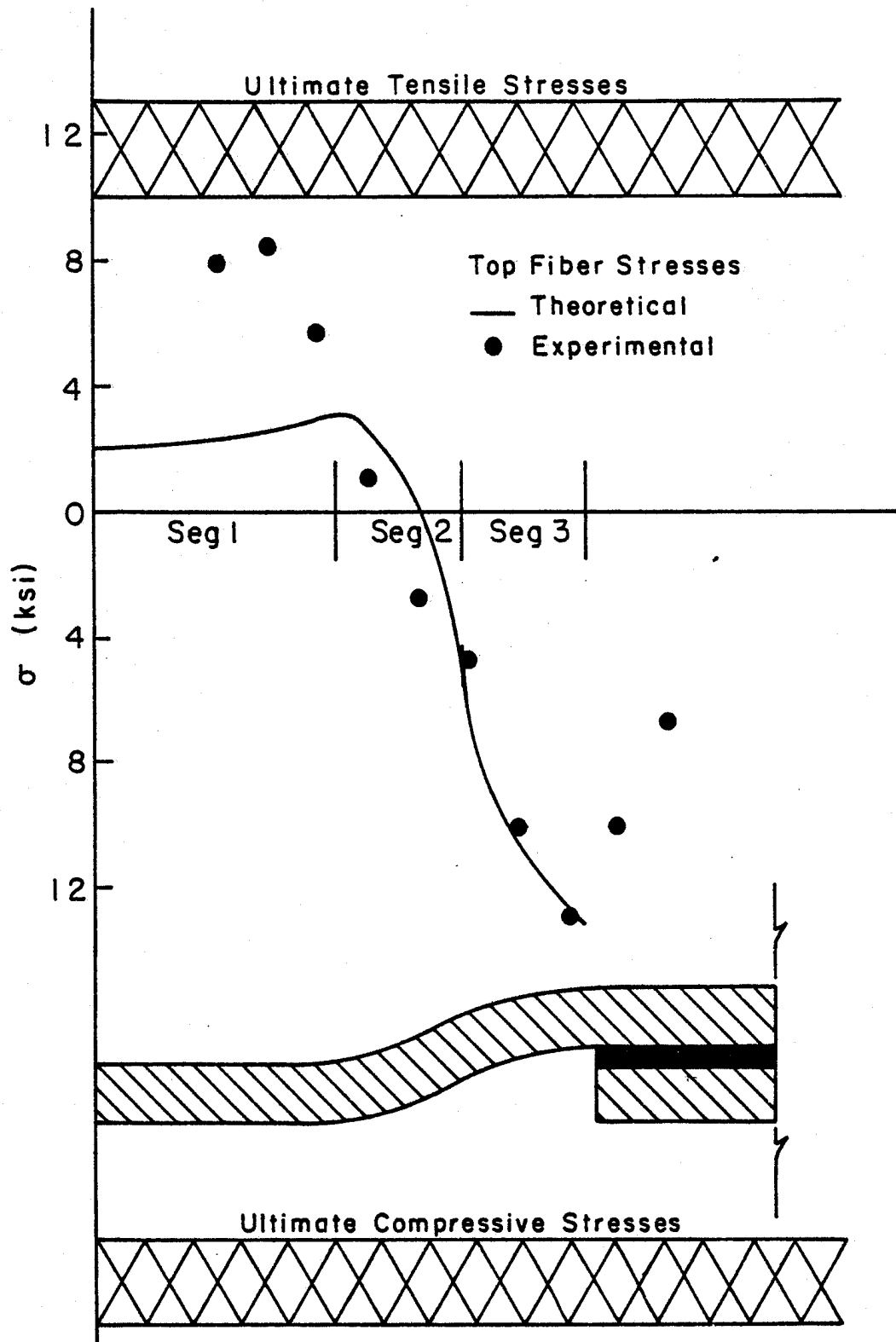


FIGURE 36: TOP FIBER STRESSES AT THE FAILURE LOAD

## VI. Conclusions

The response of the "joggle-lap" joint was investigated for both tensile and bending loads in this report. It was found that experimental data correlated rather well to the values of stress predicted by the analytical model. The results of the bending study were not as favorable, in that experimental verification proved to be more difficult.

A parametric study was undertaken for the "joggle-lap" joint subject to tensile loads in an effort to isolate the crucial design parameters. In Figures 37 through 40 a normalized stress value is plotted against one of four parameters - adherent thickness, inside radius, contact area, and load. From these design curves the following conclusions are inferred.

- If weight saving requirements are not stringent, the effect of increasing adherent thickness drastically reduces maximum flexural adherent stress.
- Increasing the radius of curvature has a negligible effect on reducing maximum adherent stress due to a trade-off between mechanisms.

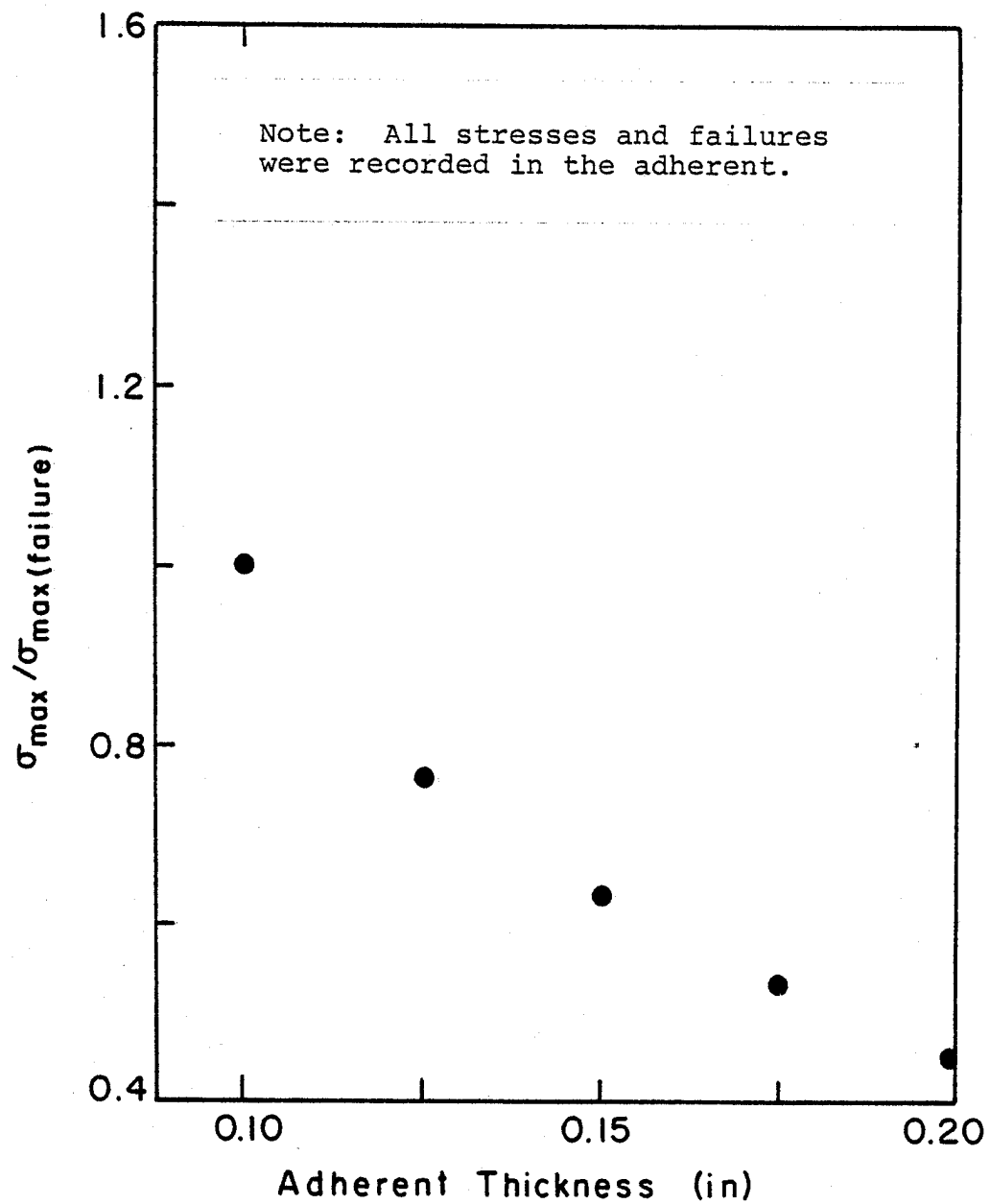


FIGURE 37: EFFECTS OF ADHERENT THICKNESS ON JOINT STRENGTH

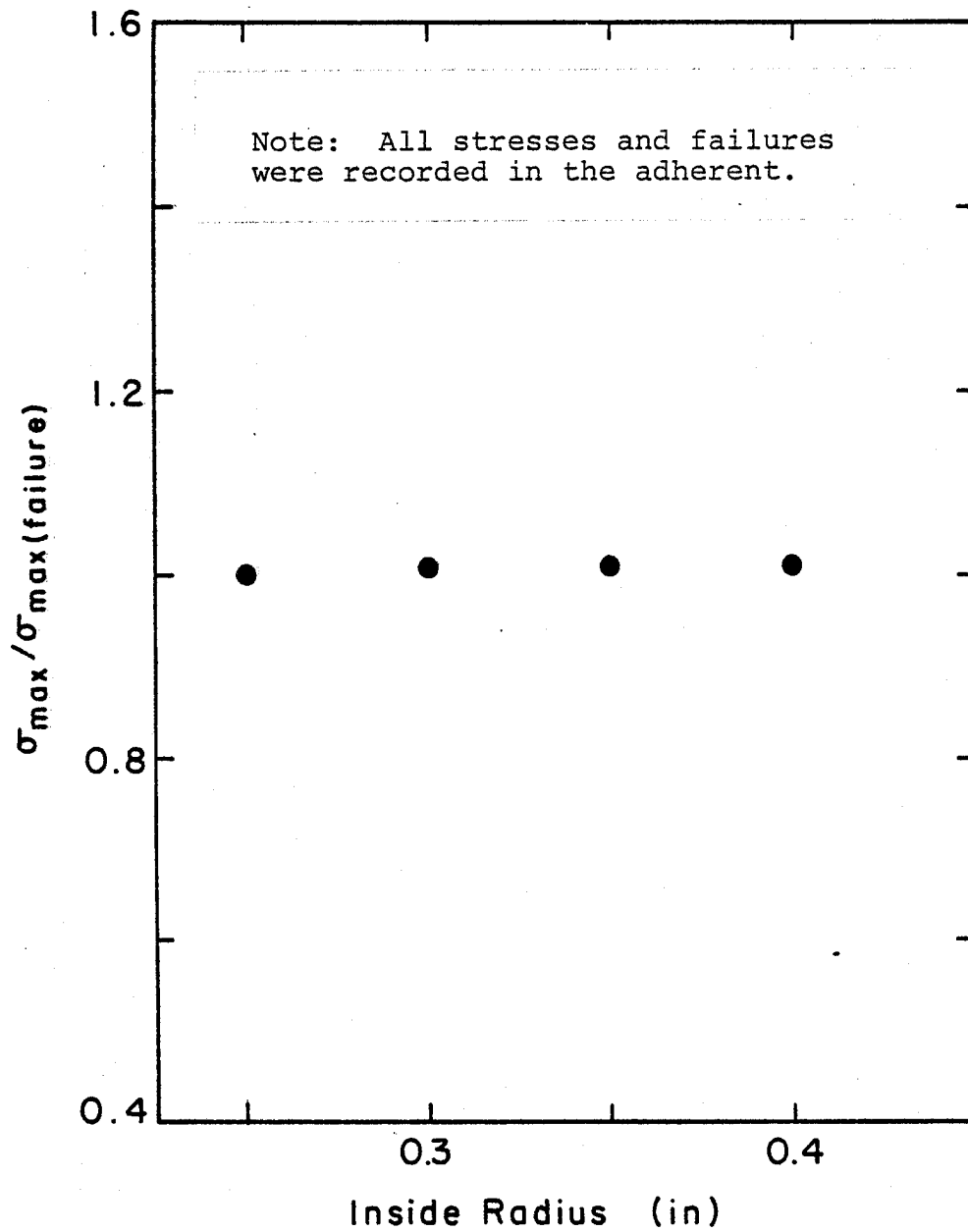


FIGURE 38: EFFECTS OF INSIDE RADIUS OF JOINT STRENGTH

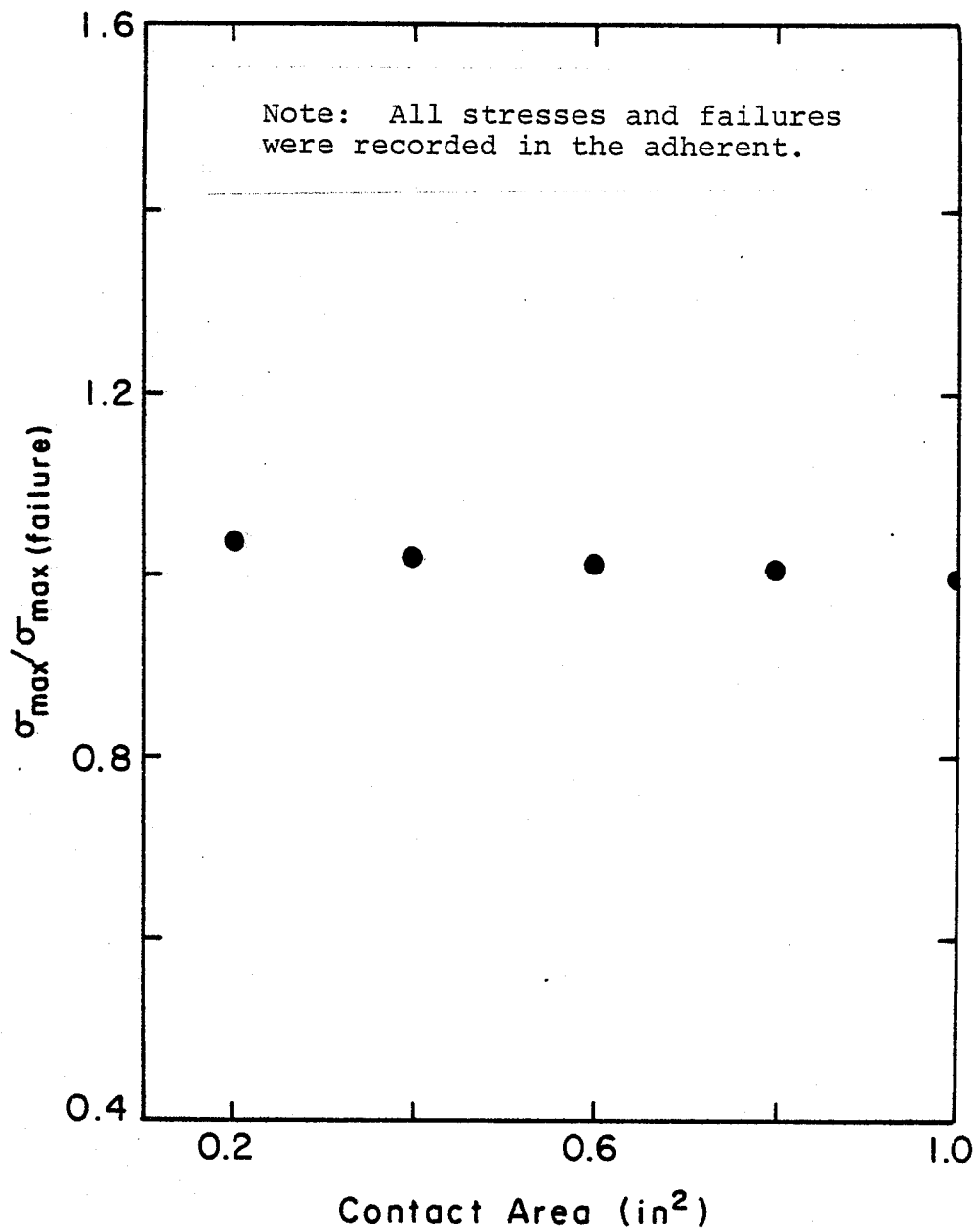


FIGURE 39: EFFECTS OF CONTACT AREA ON JOINT STRENGTH

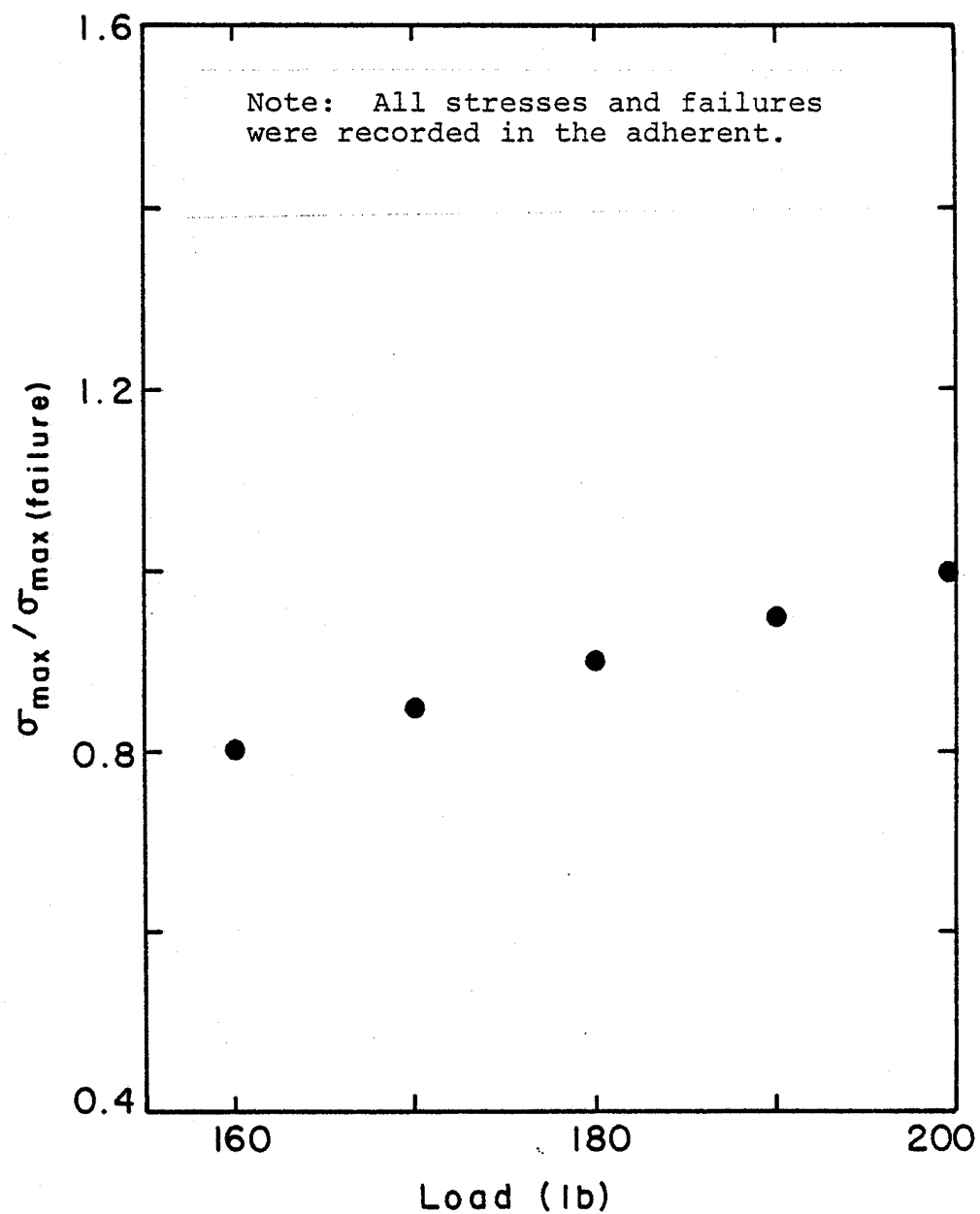


FIGURE 40: EFFECT OF LOAD ON JOINT STRENGTH

- Neglecting local stress concentrations, the effect of reducing the overlap length does not increase adherent stress significantly.
- In the region of the failure load, the maximum adherent stress increases linearly with load.

An important parameter in joint design is that of joint efficiency. This parameter is defined to be the ratio of ultimate joint load divided by the ultimate load carried by the material if the joint were not present. The joint efficiency of the "joggle-lap" joint in tension is calculated to be 0.153.

The adhesive system employed in this report proved to be quite adequate from a structural point of view. For the given overlap length of 1 in (2.54 cm) there were no recorded failures in the adhesive layer. Failure loads were predicted using the maximum flexural stress as the limiting criterion.

This report would be incomplete if it did not offer several suggestions for future work as an outgrowth of this study. An obvious limitation to the work reported herein is the inability to extensively verify the analytical model by experimental testing of various joint geometries.



Further development in this area would greatly increase the reliability of the computer model.

More detailed work needs to be completed in the response of the "joggle-lap" joint to bending loads. This report included only a cursory investigation of bending behavior as a means of identifying the underlying problems associated with the experimental verification of theory.

It is felt that this report will provide a fundamental basis for future research concerning the "joggle-lap" joint.

## VII. Acknowledgements

The authors wish to thank David W. Adkins and Joseph J. Quigley, graduate students at the University of Delaware, for their expertise and guidance throughout this research effort. Also, we wish to express our appreciation to Dr. Terry V. Baughn and Bill Englehart of International Harvester for their vested interest in the program and for supplying all of the test specimens. Special thanks are also directed to Larry Carapellotti and his staff at Goodyear Adhesives for their assistance in bonding the experimental specimens.

VIII. List of References

- [1] R. Byron Pipes, "Damage Repair Technology for Composite Materials", NASA Grant No. 1304; Semi-annual Progress Report, April 1977
- [2] David W. Adkins, "Damage Repair Technology for Composite Materials", NASA Grant No. 1304; Semi-annual Progress Report, May 1978
- [3] L. Marker and B. Ford, "Rheology and Molding Characteristics of Glass Fiber Reinforced Sheet Molding Compounds", 32nd Annual Technical Conference, SPI, Inc., 1977
- [4] J. W. Gillespie, Jr., "Evaluation of the Embedded Spar Composite Design Concept", Master's Thesis, University of Delaware, 1978
- [5] R. B. Pipes and D. Taggart, "Influence of Fiber Orientation on the Properties of Short Fiber Composites", Center for Composite Materials, Delaware, 1978

## IX. Bibliography

Byars, E. F. and Snyder, R. D., Engineering Mechanics of Deformable Bodies. Intext Educational Publishers, 1975.

Lubin, George, Handbook of Fiberglass and Advanced Plastics Composites. Krieger Publishing Co., 1975.

Seely, Fred B., M.S., Advanced Mechanics of Materials. John Wiley & Sons, Inc., 1952.

Shames, Irving H., Introduction to Solid Mechanics. Prentice Hall Inc., 1975.

Timoshenko, S., Strength of Materials. D. Van Nostrand Co., Inc., 1935.

Vinson, J. R. and Chou, T. W., Composite Materials and Their Use in Structures. New York, John Wiley & Sons, Inc., 1975.

X. Appendices

Appendix A

Derivation of the Governing Equations  
for a Curved Beam

Consider the curved beam element shown in  
Figure 41.

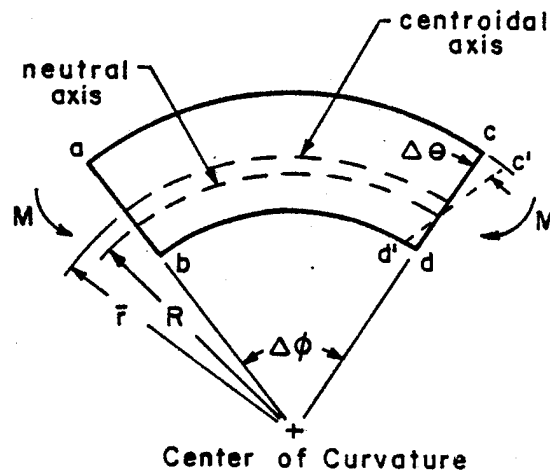


FIGURE 41: CURVED BEAM ELEMENT

The analysis begins by seeking an expression for the strain distribution perpendicular to the neutral axis. Assume that the curved beam, with an initial radius of curvature  $R$ , undergoes a small elastic deformation due to the applied moment. (It is important to note that the neutral axis of bending for a curved beam does not necessarily coincide with the centroidal axis of the beam.) Under the action of this moment it becomes apparent that segment  $cd$  rotates about the neutral axis

to a new position c'd'. It is assumed here, as in classical beam analysis, that plane sections remain plane. It is readily seen that while the deformation of the beam varies linearly with the distance from the neutral axis, the strains do not. The reason is that the original length of all the fibers prior to the application of the moment are not constant.

Thus the following relation for the strain distribution is written below.

$$\epsilon = \frac{e_{\ell}}{\Delta L} = \frac{-y\Delta\theta}{(R-y)\Delta\phi} \quad (20)$$

where  $e_{\ell}$  = elongation  
 $y$  = radial coordinate (positive radially inward)  
 $\Delta\theta$  = angle of deformation  
 $\Delta\phi$  = angle subtended by curved beam

The above equation shows the strain to vary hyperbolically across the section. Using the plane stress constitutive relation, Eq. (20) becomes

$$\sigma = \frac{-Ey \Delta\theta}{(R-y)\Delta\phi} \quad (21)$$

Now it is appropriate to derive the formulas for flexural stress. First assume that the portion of the beam is in equilibrium. Following directly one may write the equations of equilibrium for an arbitrary section.

$$\Sigma F_{\text{axial}} = 0$$

$$\int_A \sigma da = 0 \quad (22)$$

Making the appropriate substitutions for the stress Eq. (22) becomes

$$\int_A \frac{-Ey\Delta\theta da}{(R-y)\Delta\phi} = 0 \quad (23)$$

Assuming  $E$ ,  $\Delta\phi$ , and  $\Delta\theta$  to be constants the integral is simplified as shown in Eq. (24).

$$\int_A \frac{y da}{(R-y)} = 0 \quad (24)$$

It is possible to solve Eq. (24) for the radius of curvature and thus locate the neutral surface; however, it will suffice to let Eq. (24) stand as is for now.

Referring to Figure 42 and summing moments about the

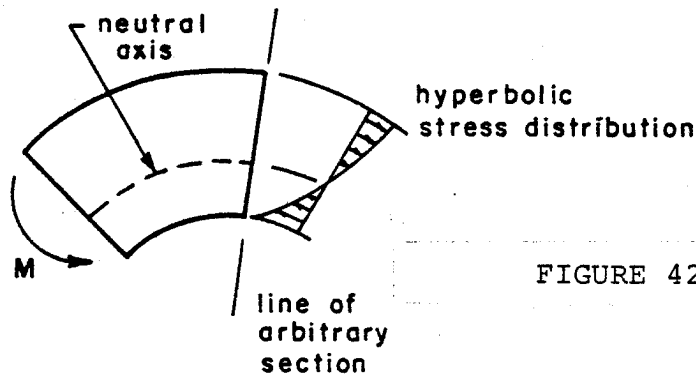


FIGURE 42

neutral axis, one finds that the stress distribution must also satisfy the equation below.

$$M = -\int_A \sigma y da \quad (25)$$

making the appropriate substitutions, Eq. (25) becomes

$$M = -\int_A E \left( \frac{-y \Delta \theta}{(R-y) \Delta \phi} \right) y da \quad (26)$$

$$M = \frac{E \Delta \theta}{\Delta \phi} \int_A \frac{y^2}{(R-y)} da \quad (27)$$

Notice the algebraic relation that permits the substitution of an equivalent expression into Eq. (27).

$$\frac{y^2}{R-y} = \frac{Ry}{R-y} - y \quad (28)$$

Eq. (27) now becomes

$$M = \frac{E \Delta \theta}{\Delta \phi} \left[ \int_A \frac{Ry da}{R-y} - \int_A y da \right] \quad (29)$$

and from the result of Eq. (24)

$$M = \frac{E \Delta \theta}{\Delta \phi} (R(0) - a\bar{u}) \quad (30)$$

where

$a$  = area

$\bar{u}$  = distance between the neutral and centroidal axes

Rearranging Eq. (30) yields

$$\frac{\Delta \theta}{\Delta \phi} = \frac{-M}{E a \bar{u}} \quad (31)$$



Comparing this equation with the well-known deflection equation for straight beams, it is apparent that

$$\frac{d^2y}{dx^2} = \frac{M}{EI} \quad (32)$$

the left hand side of Eq. (31) is not yet suitable. The ultimate goal of such an analysis is to seek an equation that relates the deflection of the neutral axis to the position along the neutral axis.

Consider Figure 43 shown below.

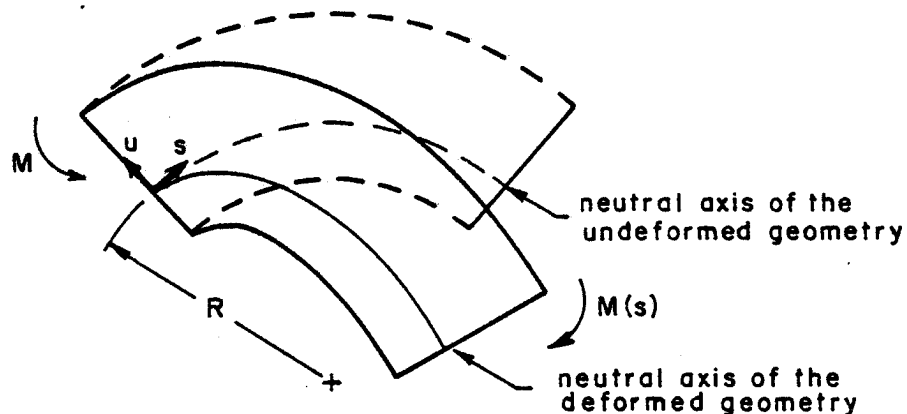


FIGURE 43: CURVED BEAM ELEMENT SUBJECT TO DEFLECTION

The beam is deflected as shown to illustrate the most general case of a non-constant moment. That is, the moment is a function of position. Now the deflection can be measured as the deviation between the undeformed neutral surface and the deformed neutral surface. For convenience just the neutral axis and appropriate parameters are drawn in Figure 44.

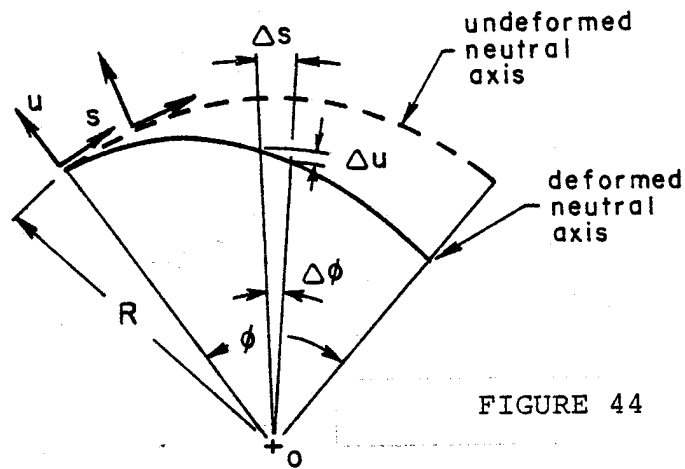


FIGURE 44

A coordinate system  $u, s$  is defined and shown in the figure where  $s$  traverses tangentially to the undeformed neutral axis and  $u$  is defined to be perpendicular to that axis.

Enlarging the area of interest and focusing on the triangle of Figure 45, one finds that

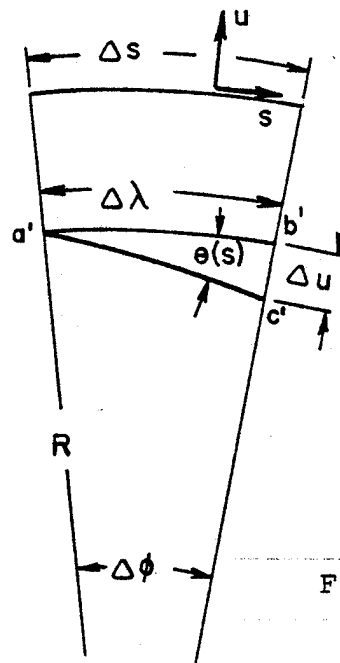


FIGURE 45

$$\theta(s) = \frac{\Delta u}{\Delta \lambda}$$

Realizing that  $\tan \alpha \approx \alpha$  for small  $\alpha$ , it follows that

$$\Delta \lambda = \frac{(R+u)\Delta s}{R}$$

and thus

$$\theta(s) = \frac{R\Delta u}{(R+u)\Delta s}$$

which may be written as

$$\frac{\Delta u}{\Delta s} = \frac{(R+u)\theta(s)}{R} \quad (33)$$

Finally in the limit as  $\Delta s \rightarrow 0$ : Eq. (33) becomes

$$\lim_{\Delta s \rightarrow 0} \frac{\Delta u}{\Delta s} = \frac{(R+u)\theta(s)}{R} = \frac{du}{ds} \quad (34)$$

From Eq. (31), several simplifications can be made with the proper substitutions.

$$\frac{\Delta \theta}{\Delta \phi} = \frac{-M}{Ea\bar{u}}$$

where

$$\Delta \phi = \frac{\Delta s}{R}$$

$$\lim_{\Delta s \rightarrow 0} \frac{\Delta \theta}{\Delta s} = \frac{-M}{REa\bar{u}} = \frac{d\theta}{ds} \quad (35)$$

Differentiating Eq. (34) with respect to  $s$  yields

$$\frac{d^2 u}{ds^2} = \frac{(R+u)}{R} \frac{d\theta}{ds} \quad (36)$$

and substituting Eq. (35) into Eq. (36) yields the final results - a second order differential equation relating deflection to position in terms of the applied moment.

$$\frac{d^2 u}{ds^2} = \frac{(R+u)M}{R^2 E a \bar{u}} \quad (37)$$

## Appendix B

### Beam Bending Model of the "Joggle-Lap" Joint

SEGl may be modeled as a straight beam shown in Figure 46.

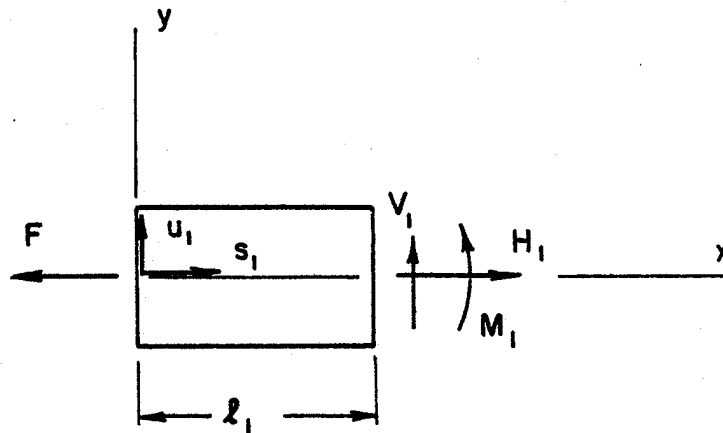


FIGURE 46: SEGl MODELED AS A STRAIGHT BEAM

In general, the moment experienced by any segment originates from two sources: eccentricity from geometry and eccentricity due to deflection. The preceding statement may be written algebraically as follows.

$$M = F(e_{\text{geom}} + e_{\text{defl}}) \quad (38)$$

where

$M$  = moment

$F$  = applied force

$e$  = eccentricity

It is readily seen that  $e_{\text{geom}} = 0$  for SEGl. Writing Eq. (38) in the local coordinate system, the moment experienced by

this segment reduces to

$$M = Fu_1 \quad (39)$$

where

$u_1$  = deflection in the local coordinate system

Substituting Eq. (39) into Eq. (5) yields

$$\frac{d^2 u_1}{ds_1^2} - \frac{Fu_1}{EI} = 0 \quad (40)$$

The corresponding boundary conditions are expressed below

$$u_1(0) = 0$$

$$u_1(l_1) = u_0$$

where  $u_0$  is yet undetermined.

The solution of Eq. (40) is of standard form and known to be

$$u_1 = C_1 \sinh \sqrt{F/EI} \cdot s_1 + C_2 \cosh \sqrt{F/EI} \cdot s_1 \quad (41)$$

Applying the boundary conditions to Eq. (41) determines the constants  $C_1$  and  $C_2$  to be

$$C_2 = 0$$

$$C_1 = u_0 / \sinh \sqrt{F/EI} \cdot l_1$$

and thus

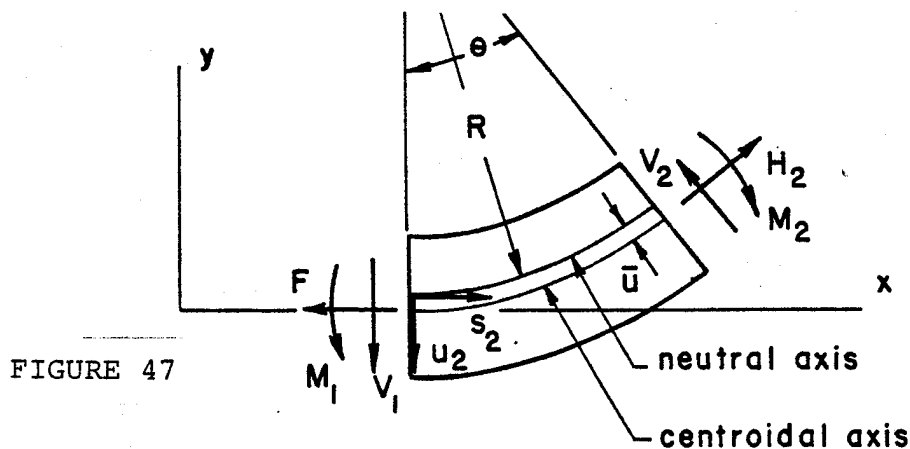
$$u_1 = u_0 \frac{\sinh \sqrt{F/EI} \cdot s_1}{\sinh \sqrt{F/EI} \cdot \ell_1} \quad 0 < s_1 < \ell_1 \quad (42)$$

where  $u_0$  is necessarily negative to correspond with the physical system. In other words, for a given tensile load it is expected that SEG1 will deflect downward. (Figure 6). Also

$$\frac{du_1}{ds_1}(\ell_1) = u_0 \frac{\sqrt{F/EI} \cosh \sqrt{F/EI} \ell_1}{\sinh \sqrt{F/EI} \ell_1}$$

It should be noted that the deflection as given by Eq. (42) is not known explicitly in terms of the given parameters.  $U_0$  is still unknown and it will be shown later how this value may be determined uniquely.

SEG2 is modeled as a curved beam and shown in Figure 47. The local coordinate system is a curvilinear coordinate system with the  $s_2$  axis traversing the neutral axis as shown. Positive deflections are measured normal to the undeformed neutral axis in the direction of  $u_2$ .



From the derivation of the general case for a curved beam in pure bending (see Appendix A), the governing equation for the deflection is

$$\frac{d^2 u_2}{ds_2^2} = \frac{(R + u_2)M}{R^2 E a \bar{u}} \quad (43)$$

where

$s_2$  = arc length

$u_2$  = deflection normal to neutral axis

$M$  = moment

$R$  = radius of curvature

$E$  = modulus of elasticity

$a$  = cross sectional area

$\bar{u}$  = distance between neutral axis and centroidal axis and its value is necessarily negative

The moment may be written as the product of the applied load and the eccentricity, where the eccentricity in this case consists of both geometry and deflection considerations.

At this point, it is appropriate to introduce the notion of extensional effects. It is realized that with the given loading conditions, the "joggle-joint" will undergo deflections parallel to the neutral axis as well. This fact would be of little concern if all beam segments of the joint configuration had their neutral axis aligned with the loading axis. If this were the case, the longitudinal displacement would not affect the eccentricity.



However, it is evident that the extensional strains in the curved beam segments give rise to an added component of eccentricity defined to be  $e_{ext}$ . To calculate the value of  $e_{ext}$ , one merely applies the criterion of force equilibrium to SEG2 (Figure 47) in the local coordinate system.

$$\Sigma F_{u_2} = 0 \quad H_2 \cos \theta + V_2 \sin \theta = F$$

$$\Sigma F_{s_2} = 0 \quad H_2 \sin \theta = V_2 \cos \theta$$

thus  $H_2 = F \cos \theta$

where  $\theta$  = angle subtended by SEG2

Employing the constitutive relationship

$$\sigma = E \epsilon$$

where  $\sigma$  = stress

$$E = \text{modulus of elasticity}$$

$$\epsilon = \text{strain}$$

and considering only the y (global coordinate) component of the extension we thus arrive with the expression for  $e_{ext}$ .

$$e_{ext} = \frac{F s_2 \cos(s_2/R) \sin(s_2/R)}{aE} \quad (44)$$

Eq. (44) must be added to the other terms which comprise the eccentricity due to deflection.

Therefore Eq. (43) becomes

$$\frac{d^2 u_2}{ds_2^2} = \frac{-(R-u_2)F}{R^2 Ea \bar{u}} [e_{\text{geom}} + e_{\text{defl}} + e_{\text{ext}}] \quad (45)$$

where

$$e_{\text{geom}} = R(1 - \cos(\frac{s_2}{R}) + \bar{u})$$

$$e_{\text{defl}} = u_2 \cos(\frac{s_2}{R})$$

$$e_{\text{ext}} = \frac{Fs_2 \cos(s_2/R) \sin(s_2/R)}{aE}$$

Initial conditions for SEG2 are found by matching deflection and slope at the 1-2 interface.

$$u_2(0) = u_0$$

$$\frac{du_2}{ds_2}(0) = u_0 \frac{\sqrt{F/EI} \cosh \sqrt{F/EI} \ell_1}{\sinh \sqrt{F/EI} \ell_1}$$

Using a numerical integration routine to solve Eq. (45) the deflection  $u_2$  may be marched out as a function of arc length  $s_2$ . A Runge-Kutta method based on Verners fifth and sixth order pair of formulas was used. An explanation of the integration routine DVERK may be referenced in Appendix C.

Figure 48 shows SEG3 modeled as a curved beam. From Eq. (37) the governing differential equation for a curved beam in pure bending is

$$\frac{d^2 u_3}{ds_3^2} = \frac{(R+u_3)}{R^2 Ea \bar{u}} M \quad (46)$$

where  $M = F(e_{\text{geom}} + e_{\text{defl}} + e_{\text{ext}})$

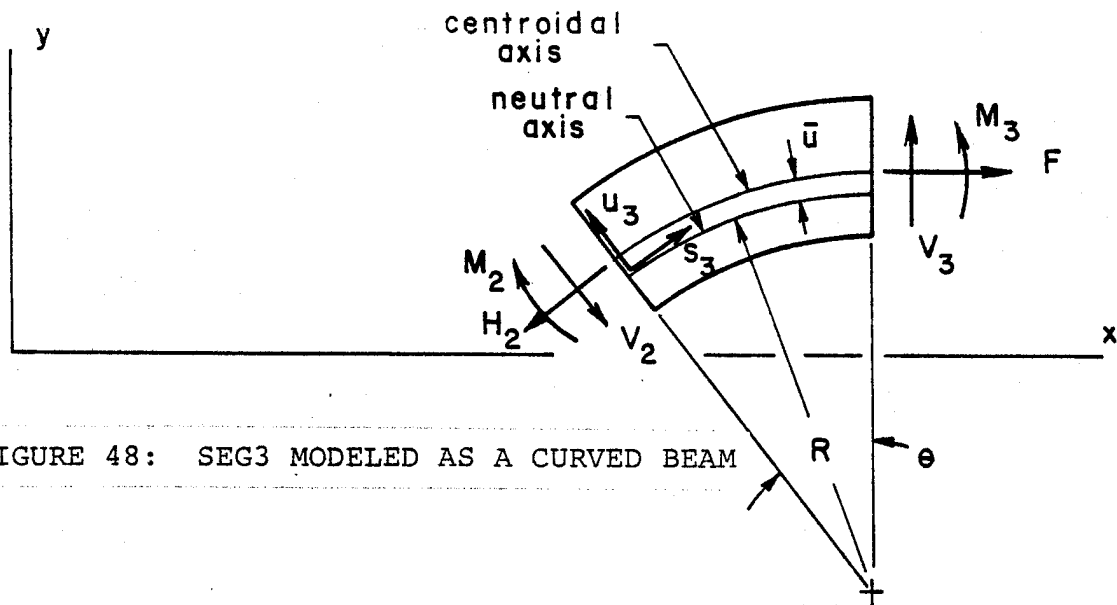


FIGURE 48: SEG3 MODELED AS A CURVED BEAM

Through geometric considerations  $e_{\text{geom}}$  can be shown to be

$$e_{\text{geom}} = \bar{u} + R(1 - \cos\theta) - 2\bar{u}\cos\theta + R\sin(\frac{\pi}{2} - \theta + s_3/R) - \cos\theta \quad (47)$$

where

$\theta$  = angle subtended by SEG3

$\bar{u}$  = distance between centroidal and neutral axes

$R$  = radius of curvature

$s_3$  = arc length along neutral surface of SEG3

Also 
$$e_{\text{defl}} = M \cos(\pi/2 - \theta + s_3/R) \quad (48)$$

From a similar argument developed earlier it may be shown that  $e_{\text{ext}}$  for SEG3 is given by

$$e_{\text{ext}} = \frac{Fs_3 \cos(\theta - s_3/R) \sin(\theta - s_3/R)}{aE} \quad (49)$$

Thus Eq. (46) becomes

$$\frac{d^2 u_3}{ds_3^2} = \frac{-(R+u)}{R^2 E a \bar{y}} F (e_{\text{geom}} + e_{\text{defl}} + e_{\text{ext}}) \quad (50)$$

where  $e_{\text{geom}}$ ,  $e_{\text{defl}}$ , and  $e_{\text{ext}}$ , are given by Eqs. (47), (48), and (49) respectively. Matching boundary conditions at the 2-3 interface provides initial conditions to Eq. (50) which may be integrated numerically as before.

SEG4 is analyzed as a multi-layered beam and shown in Figure 49. Treating this segment to be composed of three linear elastic beam elements, the governing differential equation follows from Eq. (5) with a slight modification.

$$\frac{d^2 u_4}{ds_4^2} = \frac{M}{\sum_{i=1}^3 E_i I_i} \quad (51)$$

where

$I_i$  = moment of inertia of the  $i$ th section about the neutral axis

$E_i$  = modulus of elasticity of the  $i$ th element

$\sum_{i=1}^3 E_i I_i$  is referred to as an effective flexural stiffness

and is merely a constant. The moment is defined in the usual manner as

$$M = F(e_{\text{geom}} + e_{\text{defl}})$$

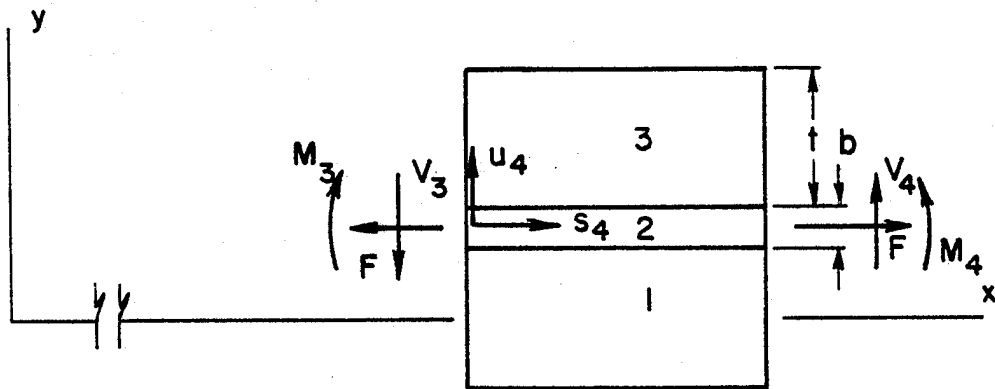


FIGURE 49: SEG4 MODELED AS A LAYERED BEAM

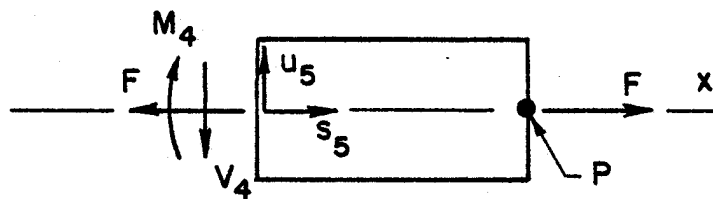


FIGURE 50: SEG5 MODELED AS A STRAIGHT BEAM

where  $e_{\text{geom}} = .5(t+b)$   
 $e_{\text{defl}} = u_4$

Thus Eq. (51) becomes

$$\frac{d^2 u_4}{ds_4^2} = \frac{F (.5(t+b) + u_4)}{3 \sum_{i=1} E_i I_i} \quad (52)$$

Initial conditions are found by equating the deflection and slope at the 3-4 interface. Following in the usual manner, Eq. (52) is integrated to obtain an expression for the deflection of SEG4 as a function of arc length in the local coordinate system.

Finally SEG5 is shown in Figure 50 modeled as a straight beam member. The governing differential equation is the same as Eq. (5)

$$\frac{d^2 u_5}{ds_5^2} = \frac{M}{EI} \quad (53)$$

where  $M = Fu_5$

and the initial conditions are obtained by matching the deflection and slope at the 4-5 interface. Upon integration of Eq. (53) the deflection SEG5 will be a known function of the abscissa  $s_5$  of the local coordinate system. Therefore the deflection and slope at point P of Figure 50 are also known. But it should be apparent that the values of the deflection

and slope at this point must be zero or at least within certain tolerance limits. This in fact is the final boundary condition to the problem that is needed to uniquely determine the value of  $u_0$ , which was previously assumed to be arbitrary. Thus, through an iterative process, a correct value of  $u_0$  may be calculated by assuring that the deflection and slope of point P of SEG5 is sufficiently<sup>3</sup> close to zero. To avoid confusion, it should be noted that by specifying zero deflection at point P we will force the slope to zero by the nature of the deflection function of SEG5. So in fact this is a well-posed problem, whereby we specify only enough boundary conditions as there are unknowns. The process for correctly determining  $u_0$  is shown schematically in Figure 51.

---

<sup>3</sup>it was found that reliable results were obtained by using the tolerance limits listed here.

|deflection (P)| < .00001  
|slope (P)| < .00005

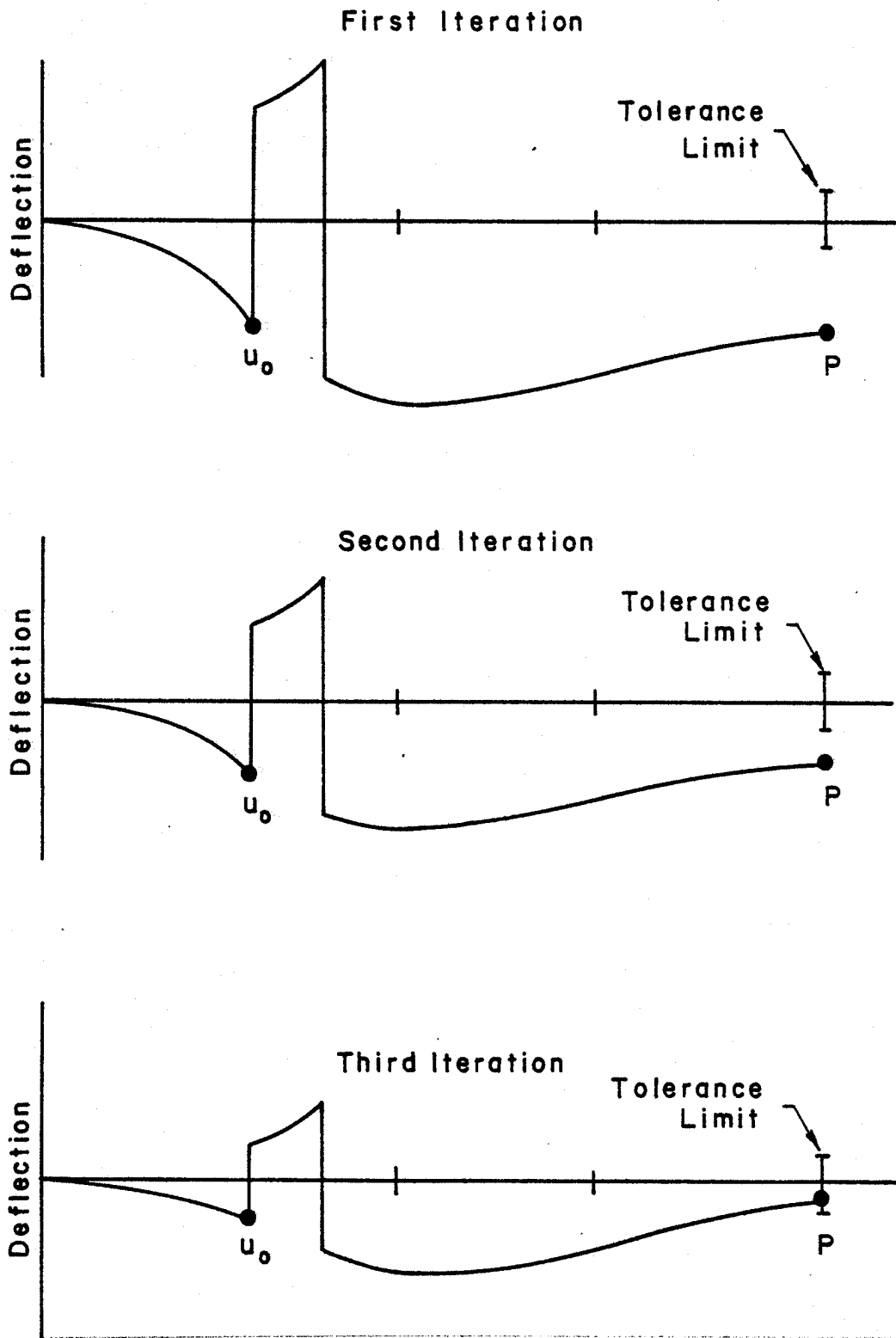


FIGURE 51: ITERATIVE PROCESS FOR DETERMINING  $u_0$



## Appendix C

### Computer Programs

#### a. JOGGLE

To facilitate ease of calculation, a computer routine identified as JOGGLE was developed and may be referenced below. Essentially this program calculates a correct value of  $u_0$  and proceeds to determine a solution for the deflection while calculating stress profiles along the joint configuration. These stress profiles are linear in the straight beam members (SEG1, SEG5) and hyperbolic in the curved beams (SEG2, SEG3).

```

C-          J  00000  GGGGG  GGGGG  L      EEEEE  00000003
C-          J  0  0    G      G      L      E      00000004
C-          J  0  0    G  GG   G  GG   L      EEE    00000005
C-          J  J  0  0    G  G    G  G    L      E      00000006
C-          JJJJJ  00000  GGGGG  GGGGG  LLLLL  EEEEE  00000007
C-                                     00000008
C-                                     00000009
C-                                     00000010
C-                                     00000011
C-                                     00000015
C-                                     00000016
C-          ANALYTICAL BEAM BENDING MODEL  00000020
C-          FOR A JOGGLE LAP JOINT        00000021
C-                                     00000024
C-                                     00000025
C-          DEVELOPED BY: RICHARD C. GIVLER 00000026
C-          UNIVERSITY OF DELAWARE         00000027
C-          SEPT 78 - JAN 79              00000028
C-                                     00000040
C-                                     00000041
C-                                     00000042
C-                                     00000043
C-          $SET AUTOBIND                 00000100
C-          $RESET FREE                   00000110
C-          FILE 6(KIND=REMOTE,MAXRECSIZE=22) 00000120
C-          DIMENSION PROD(3), ERR(1), T(2), EI(3), YPRIME(2) 00000150
C-          COMMON R, PLOAD, ESMC, WIDTH, THICK, YBAR, THETA, EADH, PI 00000175
C-          BOND, J, TORC, TORCS, TRAC, TRACE, SHEAR 00000176
C-                                     00000178
C-                                     00000180
C-          C-----PARAMETERS AND NOMENCLATURE 00000200
C-                                     00000210
C-                                     00000220
C-          C-----MATERIAL THICKNESS          00000300
C-          THICK=.1                        00000400
C-          C-----LONGITUDINAL MODULUS OF ELASTICITY OF SMC IN PSI 00000500
C-          ESMC=2.1E+06                    00000600
C-          C-----MODULUS OF ELASTICITY OF ADHESIVE IN PSI 00000700
C-          EADH=1.0E+05                    00000800
C-          C-----LOAD IN LBS                  00000900
C-          PLOAD=200.                      00001000
C-          C-----INSIDE RADIUS IN INCHES      00001100
C-          RADI=2.5*THICK                  00001200
C-          C-----OUTSIDE RADIUS IN INCHES     00001300
C-          RADO=3.5*THICK                  00001400
C-          C-----BONDING THICKNESS IN INCHES  00001500
C-          BOND=.03                        00001600
C-          C-----CONTACT WIDTH IN INCHES      00001700
C-          CONTA=1.0                       00001800
C-          C-----SPECIMEN WIDTH              00001900
C-          WIDTH=1.0                       00002000
C-          C-----LENGTH OF SEGMENT 1         00002100
C-          SEGA=3.5                        00002200
C-          C-----LENGTH OF SEGMENT 5         00002300
C-          SEGB=4.0                        00002400
C-          C-----LEFT INTERVAL LIMIT FOR ITERATION 00002420
C-          AINT=-.04                       00002430
C-          C-----RIGHT INTERVAL LIMIT FOR ITERATION 00002435
C-          BINT=+.01                       00002440
C-          C-----TOLERANCE LIMIT ON INITIAL DISPLACEMENT 00002445
C-          ERR(1)=.00001                  00002450

```

```

C-----STEP SIZE FOR NUMERICAL INTEGRATION
STEP=50.
PI=3.141592654
C-----TRACING CONSTANTS
TRAC=1.0
TRACE=1.0
C-----
C-----NOTE:DEFLECTIONS ARE MEASURED NORMAL TO THE UNDEFORMED
C-      NEUTRAL AXIS
C-
      YO=(AINT+BINT)/2.
C-
C-----ITERATIVE CALCULATION OF YO TO FORCE ZERO DEFLECTION
C-----AND SLOPE AT END OF SEG5
C-----YO MUST LIE BETWEEN THE PROPOSED LIMITS OF AINT AND BINT
C-
C-*****
C-*****
C-*****
C NUMERICAL INTEGRATION VIA LIBRARY ROUTINES DVERK AND UERTST
C-*****
C-*****
C-*****
C-
101  CONTINUE
      DO 200 X=0,SEGA+.005,SEGA/STEP
      PROD(3)=SQRT(LOAD/(ESMC*(WIDTH*THICK**3./12.)))
      PROD(1)=YO*(.5*(EXP(PROD(3)*X)-EXP(-PROD(3)*X)))
      PROD(2)=.5*(EXP(PROD(3)*SEGA)-EXP(-PROD(3)*SEGA))
      T(1)=PROD(1)/PROD(2)
      T(2)=YO*PROD(3)/PROD(2)*(.5*(EXP(PROD(3)*X)+EXP
      -((-PROD(3)*X)))
200  CONTINUE
      DIMENSION C(24), Y(2), W(2.9)
      EXTERNAL FCN1
C-----CALCULATION OF THE RADIUS OF CURVATURE FOR CURVED MEMBERS
      R=WIDTH*THICK/(ALOG(RADO/RADI))
      NW=2
C-----CALCULATION OF THE ANGLE SUBTENDED BY SEG2 AND SEG3
      THETA=ARCOS((5.*THICK*BOND)/(6.*THICK))
      N=2
C-----CALCULATION OF THE DISTANCE BETWEEN NEUTRAL AXIS AND
C-----CENTROIDAL AXIS OF CURVED MEMBERS
      YBAR=RADI+THICK/2.-R
      X=0.0
      Y(1)=-T(1)
      Y(2)=-T(2)
      TOL=.000001
      IND=1
      DO 300 Z=0.0,R*THETA+.001,R*THETA/STEP
      XEND=FLOAT(Z)
      CALL DVERK(N,FCN1,X,Y,XEND,TOL,IND,C,NW,W,IER)
      IF(IND.LT.0.OR.IER.GT.0) GO TO 20
300  CONTINUE
20  CONTINUE
      RINT=RNEW
      EXTERNAL FCN2
      X=0.0
      Y(1)=-Y(1)
      Y(2)=-Y(2)
      NW=2
      N=2

```

00002451  
00002452  
00002475  
00002500  
00002501  
00002502  
00002600  
00002700  
00002800  
00002900  
00003000  
00003100  
00003200  
00003210  
00003220  
00003400  
00003405  
00003410  
00003420  
00003425  
00003430  
00003435  
00003440  
00003445  
00003450  
00004200  
00004300  
00004400  
00004500  
00004600  
00004700  
00004800  
00005100  
00006000  
00006100  
00006150  
00006200  
00006300  
00006350  
00006400  
00006500  
00006550  
00006552  
00006600  
00006700  
00006800  
00006900  
00007000  
00007100  
00007200  
00007300  
00007400  
00007500  
00007800  
00007900  
00007950  
00008600  
00008700  
00008720  
00008730  
00008800  
00008900

```

IND=1
DO 250 M=1,24
C(M)=0.0
250 CONTINUE
DO 350 Z=0.0,R*THETA+.001,R*THETA/STEP
XEND=FLOAT(Z)
CALL DVERK(N,FCN2,X,Y,XEND,TOL,IND,C,NW,W,IER)
IF(IND.LT.0.OR.IER.GT.0) GO TO 70
350 CONTINUE
70 CONTINUE
EXTERNAL FCN3
X=0.0
NW=2
N=2
IND=1
DO 290 M=1,24
C(M)=0.0
290 CONTINUE
DO 400 Z=0.0,CONTA+.005,CONTA/STEP
XEND=FLOAT(Z)
CALL DVERK(N,FCN3,X,Y,XEND,TOL,IND,C,NW,W,IER)
IF(IND.LT.0.OR.IER.GT.0) GO TO 80
400 CONTINUE
80 CONTINUE
EXTERNAL FCN4
X=0.0
NW=2
N=2
IND=1
DO 291 M=1,24
C(M)=0.0
291 CONTINUE
DO 246 Z=0.0,SEGB+.005,SEGB/STEP
XEND=FLOAT(Z)
CALL DVERK(N,FCN4,X,Y,XEND,TOL,IND,C,NW,W,IER)
IF(IND.LT.0.OR.IER.GT.0) GO TO 81
246 CONTINUE
81 CONTINUE
IF(ABS(Y(1)).LT.ERR(1)) GO TO 88
IF(Y(1).GT.0) GO TO 100
IF(Y(1).LT.0) GO TO 89
100 CONTINUE
BINT=YO
YO=(AINT+BINT)/2.
GO TO 101
89 CONTINUE
AINT=YO
YO=(AINT+BINT)/2.
GO TO 101
88 CONTINUE
C-*****
C-*****
C-*****
C-
C- ---- CALCULATION OF DEFLECTION AND SLOPE AS A FUNCTION
C- OF X FOR SEGMENT 1.
C-
WRITE(6,500) YO
500 FORMAT('//////////,10X,'YO=',F14.11,)
WRITE(6,501)
501 FORMAT('-----')
WRITE(6,502)

```

```

00009000
00009100
00009200
00009300
00009400
00009500
00009600
00009700
00010000
00010100
00011000
00011100
00011200
00011300
00011400
00011500
00011600
00011700
00011800
00011900
00012000
00012100
00012400
00012500
00013400
00013500
00013600
00013700
00013800
00013900
00014000
00014100
00014200
00014300
00014400
00014500
00014800
00014900
00014961
00014962
00014963
00015000
00015075
00015076
00015077
00015080
00015085
00015086
00015087
00015099
00016020
00016030
00016040
00024000
00024100
00024200
00024300
00024400
00024500
00024600
00024700
00024800

```

```

502 FORMAT('-----')
WRITE(6,2)
2 FORMAT('/////.' DEFLECTION AND SLOPE FOR SEGMENT 1'./)
WRITE(6,9)
9 FORMAT(10X,'X DISTANCE'.5X,'DEFLECTION'.7X,'SLOPE'.9X,'STRESS'
-.8X,'MOMENT'./)
JW=0
DO 505 X=0.0,SEGA+.005,SEGA/STEP
PROD(3)=SQRT(PLOAD/(ESMC*(WIDTH*THICK**3./12.)))
PROD(1)=YO*(.5*(EXP(PROD(3)*X)-EXP(-PROD(3)*X)))
PROD(2)=.5*(EXP(PROD(3)*SEGA)-EXP(-PROD(3)*SEGA))
T(1)=PROD(1)/PROD(2)
T(2)=YO*PROD(3)/PROD(2)*(.5*(EXP(PROD(3)*X)+EXP
-(-PROD(3)*X)))
C----CALCULATION OF TOP AND BOTTOM FIBER STRESSES
SIGT=-PLOAD*T(1)*THICK/2./((1./12.*WIDTH*THICK**3)+PLOAD/
-(WIDTH*THICK))
SIGB=PLOAD*T(1)*THICK/2./((1./12.*WIDTH*THICK**3)+PLOAD/
-(WIDTH*THICK))
J=JW+2
IF(INT(J/2).NE.J/2.0) GO TO 199
WRITE(6,10) X, T(1), T(2), SIGT, PLOAD*T(1)
10 FORMAT(10X,5(E11.4,3X))
WRITE(6,11) SIGB
11 FORMAT(52X,E11.4./)
199 JW=JW+1
505 CONTINUE
C-
C----CALCULATION OF DEFLECTION AND SLOPE AS A FUNCTION
C- OF ARC LENGTH FOR SEGMENT 2
C-
WRITE(6,24)
24 FORMAT('/////.' DEFLECTION AND SLOPE FOR SEGMENT 2'./)
WRITE(6,25)
25 FORMAT(10X,'ARC LENGTH'.5X,'DEFLECTION'.7X,'SLOPE'.10X,'STRESS'
-.12X,'MOMENT'.11X,'SHEAR'./)
EXTERNAL FCN1
R=WIDTH*THICK/(ALOG(RADO/RADI))
NW=2
THETA=ARCOS((5.*THICK-BOND)/(6.*THICK))
N=2
YBAR=RADI+THICK/2.-R
X=0.0
Y(1)=-T(1)
Y(2)=-T(2)
TOL=.000001
IND=1
J=0
DO 510 Z=0.0,R*THETA+.001,R*THETA/STEP
XEND=FLOAT(Z)
CALL DVERK(N,FCN1,X,Y,XEND,TOL,IND,C,NW,W,IER)
IF(IND.LT.0.OR.IER.GT.0) GO TO 511
JW=J+10
IF(INT(JW/10).NE.JW/10.0) GO TO 299
WRITE(6,30) X,Y(1),Y(2), TORC, SHEAR
30 FORMAT(10X,3(E11.4,3X),20X,E11.4,5X,E11.4./)
YGLOBAL=-.5*THICK
DO 660 H=-(RADO-R),R-RADI,THICK/10.
C----STRESSES FROM THE MOMENT DISTRIBUTION SUPERIMPOSED
C----ON TENSILE STRESSES AS A FUNCTION OF BEAM THICKNESS
AREA=WIDTH*THICK
BSIGX=TORC*H/((R-H)*WIDTH*THICK*YBAR)+PLOAD*COS(X/R)/AREA

```

```

        WRITE(6.600) YGLOB, BSIGX
600  FORMAT(52X,F4.2,1X,E11.4)
        YGLOB=YGLOB+THICK/10.
660  CONTINUE
299  J=J+1
510  CONTINUE
511  CONTINUE
C-
C-----CALCULATION OF DEFLECTION AND SLOPE FOR SEGMENT 3
C-   AS A FUNCTION OF ARC LENGTH
C-
        WRITE(6.27)
27  FORMAT(/////.' DEFLECTION AND SLOPE FOR SEGMENT 3'.//)
        WRITE(6.26)
26  FORMAT(10X.'ARC LENGTH'.5X.'DEFLECTION'.7X.'SLOPE'.10X.'STRESS'
        .12X.'MOMENT'.11X.'SHEAR'./)
        EXTERNAL FCN2
        X=0.0
        Y(1)=-Y(1)
        Y(2)=-Y(2)
        NW=2
        N=2
        IND=1
        DO 515 M=1,24
        C(M)=0.0
515  CONTINUE
        J=0
        DO 520 Z=0.0,R*THETA+.001 ,R*THETA/STEP
        XEND=FLOAT(Z)
        CALL DVERK(N,FCN2,X,Y,XEND,TOL,IND,C,NW,W,IER)
        IF(IND.LT.0.OR.IER.GT.0) GO TO 525
        JW=J+10
        IF(INT(JW/10).NE.JW/10.0) GO TO 349
        WRITE(6.60) X, Y(1), Y(2), TORCS, SHEAR
60  FORMAT(10X,3(E11.4,3X),20X,E11.4,5X,E11.4,/)
        YGLOB=-.5*THICK
        DO 770 H=-(RADO-R),R-RADI,THICK/10.
C-----STRESSES FROM THE MOMENT DISTRIBUTION SUPERIMPOSED
C-----ON TENSILE STRESSES AS A FUNCTION OF BEAM THICKNESS
        CSIGX=-TORCS*H/((R-H)*WIDTH*THICK*YBAR)+PLOAD*COS(THETA-X/R)/
        -(WIDTH*THICK)
        WRITE(6.700) YGLOB, CSIGX
700  FORMAT(52X,F4.2,1X,E11.4)
        YGLOB=YGLOB+THICK/10.
770  CONTINUE
349  J=J+1
520  CONTINUE
525  CONTINUE
C-
C-----CALCULATION OF DEFLECTION AND SLOPE AS A FUNCTION
C-   OF X FOR SEGMENT 4
C-
        WRITE(6.28)
28  FORMAT(/////.' DEFLECTION AND SLOPE FOR SEGMENT 4'.//)
        WRITE(6.29)
29  FORMAT(10X.'X DISTANCE'.5X.'DEFLECTION'.7X.'SLOPE'./)
        EXTERNAL FCN3
        X=0.0
        NW=2
        N=2
        IND=1
        DO 530 M=1,24

```

03029961  
03029962  
03029966  
03029968  
03030000  
03030100  
03030200  
03030300  
03030400  
03030500  
03030600  
03030700  
03030800  
03030900  
03031000  
03031100  
03031200  
03031300  
03031400  
03031500  
03031700  
03031800  
03031900  
03032000  
03032100  
03032200  
03032300  
03032400  
03032500  
03032600  
03032700  
03032800  
03032900  
03033000  
03033100  
03033140  
03033150  
03033155  
03033157  
03033160  
03033161  
03033162  
03033164  
03033166  
03033168  
03033200  
03033300  
03033400  
03033600  
03033700  
03033800  
03033900  
03034000  
03034100  
03034200  
03034300  
03034400  
03034500  
03034600  
03034700  
03034800  
03034900

```

530 C(M)=0.0
CONTINUE
J=0
DO 535 Z=0.0,CONTA+.005,CONTA/STEP
XEND=FLOAT(Z)
CALL DVERK(N,FCN3,X,Y,XEND,TOL,IND,C,NW,W,IER)
IF(IND.LT.0.OR.IER.GT.0) GO TO 540
JW=J+10
IF(INT(JW/10).NE.JW/10.0) GO TO 399
WRITE(6,62) X, Y(1), Y(2)
62 FORMAT(10X,3(E11.4,3X),/)
399 J=J+1
535 CONTINUE
540 CONTINUE
C-
C-----CALCULATION OF DEFLECTION AND SLOPE AS A FUNCTION OF
C- X FOR SEGMENT 5
C-
WRITE(6,31)
31 FORMAT(//////,' DEFLECTION AND SLOPE FOR SEGMENT 5',/)
WRITE(6,32)
32 FORMAT(10X,'X DISTANCE',5X,'DEFLECTION',7X,'SLOPE',10X,'STRESS',
.12X,'MOMENT',/)
EXTERNAL FCN4
X=0.0
NW=2
N=2
IND=1
DO 545 M=1,24
C(M)=0.0
545 CONTINUE
J=0
DO 550 Z=0.0,SEGB+.005,SEGB/STEP
XEND=FLOAT(Z)
CALL DVERK(N,FCN4,X,Y,XEND,TOL,IND,C,NW,W,IER)
IF(IND.LT.0.OR.IER.GT.0) GO TO 555
JW=J+10
IF(X.EQ..15) GO TO 244
IF(INT(JW/10).NE.JW/10.0) GO TO 245
244 WRITE(6,65) X, Y(1), Y(2), PLOAD*Y(1)
65 FORMAT(10X,3(E11.4,3X),20X,E11.4,/)
DO 880 H=-THICK/2,THICK/2,THICK/10.
C-----STRESSES FROM THE MOMENT DISTRIBUTION SUPERIMPOSED
C-----ON TENSILE STRESSES AS A FUNCTION OF BEAM THICKNESS
ESIGX=-PLOAD*Y(1)*H/(1./12.*WIDTH*THICK**3)+PLOAD/(WIDTH*THICK)
WRITE(6,800) H, ESIGX
800 FORMAT(52X,F4.2,1X,E11.4)
880 CONTINUE
245 J=J+1
550 CONTINUE
555 CONTINUE
STOP
END
C-*****
C-*****
C-*** SUBROUTINES ***
C-*****
C-*****
C-
C-----NUMERICAL INTEGRATION OF SEG2
C-
SUBROUTINE FCN1(N,X,Y,YPRIME)

```

00035000  
00035100  
00035200  
00035300  
00035400  
00035500  
00035600  
00035700  
00035800  
00035900  
00036000  
00036100  
00036200  
00036300  
00036400  
00036500  
00036600  
00036700  
00036800  
00036900  
00037000  
00037100  
00037150  
00037200  
00037300  
00037400  
00037500  
00037600  
00037700  
00037800  
00037900  
00038000  
00038100  
00038200  
00038300  
00038400  
00038500  
00038550  
00038600  
00038700  
00038800  
00038840  
00038850  
00038855  
00038860  
00038880  
00038890  
00038895  
00038900  
00039000  
00039100  
00039300  
00039400  
00039410  
00039420  
00039430  
00039440  
00039450  
00039460  
00039470  
00039480  
00039500

```

COMMON R, PLOAD, ESMC, WIDTH, THICK, YBAR, THETA, EADH, PI
- BOND, J, TORC, TORCS, TRAC, TRACE, SHEAR
DIMENSION Y(2), YPRIME(2)
YPRIME(1)=Y(2)
00039600
00039700
00039800
00039900
00039950
00039955
00039960
C-
C-----ECCENTRICITY DUE ONLY TO EXTENSIONAL EFFECTS
C-
YECC=PLOAD*X*COS(X/R)*SIN(X/R)/(WIDTH*THICK*ESMC)
TORC=PLOAD*(YECC*TRAC+YBAR+R*(1.-COS(X/R))-Y(1)*COS(X/R))
SHEAR=PLOAD*(PLOAD/(WIDTH*THICK*ESMC)*(X/R*COS(X/R)**2
+SIN(X/R)*(X/R*(-SIN(X/R))+COS(X/R)))+SIN(X/R)+Y(1)/R
-SIN(X/R))
00040000
00040100
00040150
00040160
00040170
560 YPRIME(2)=(R+Y(1))*TORC/(R**2.*ESMC*WIDTH*THICK*YBAR)
RETURN
END
00040500
00040600
00040700
C-
C-----NUMERICAL INTEGRATION OF SEG3
C-
SUBROUTINE FCN2(N,X,Y,YPRIME)
COMMON R, PLOAD, ESMC, WIDTH, THICK, YBAR, THETA, EADH, PI
- BOND, J, TORC, TORCS, TRAC, TRACE, SHEAR
DIMENSION Y(2), YPRIME(2)
YPRIME(1)=Y(2)
00040750
00040755
00040760
00040800
00040900
00041000
00041100
00041200
C-
C-----ECCENTRICITY DUE TO GEOMETRY
C-
AEGEO=YBAR+R*(1.-COS(THETA))-2.*YBAR*COS(THETA)
00041250
00041260
00041270
00041300
C-
C-----ECCENTRICITY DUE TO GEOMETRY
C-
BEGEO=R*(SIN(X/R+PI/2.-THETA)-SIN(PI/2.-THETA))
00041350
00041360
00041370
00041400
C-
C-----ECCENTRICITY DUE ONLY TO EXTENSIONAL EFFECTS
C-
EEXT=PLOAD*(SIN(PI/2.-THETA+X/R))*SIN(THETA-X/R)*X/(
-WIDTH*THICK*ESMC)
00041450
00041460
00041470
00041500
C-
C-----ECCENTRICITY DUE TO DEFLECTION
C-
EDEFL=Y(1)*COS(THETA-X/R)
TORCS=PLOAD*(AEGEO+BEGEO+EDEFL+EEXT*TRACE)
SHEAR=PLOAD*(COS(X/R+PI/2.-THETA)-Y(1)/R*SIN(PI/2.
-THETA+X/R)+PLOAD*((SIN(PI/2.-THETA+X/R))*(SIN(THETA-
X/R)/(WIDTH*THICK*ESMC)-X/(WIDTH*THICK*R*ESMC)*COS
-(THETA-X/R))+X/(WIDTH*THICK*ESMC*R)*SIN(THETA-X/R)
-COS(PI/2.-THETA+X/R)))
00041600
00041650
00041660
00041670
00041700
00041800
00041850
00041860
00041870
00041880
00041890
00042000
00042100
00042200
00042250
C-
C-----NUMERICAL INTEGRATION OF SEG4
C-
SUBROUTINE FCN3(N,X,Y,YPRIME)
COMMON R, PLOAD, ESMC, WIDTH, THICK, YBAR, THETA, EADH, PI
- BOND
DIMENSION Y(2), YPRIME(2), EI(3)
EI(1)=ESMC*(1./12.*THICK**3.*WIDTH+WIDTH*THICK*(.5*THICK+BOND
-/2.))**2.)
EI(2)=EADH*1./12.*THICK**3*WIDTH
EI(3)=ESMC*(1./12.*WIDTH*THICK**3+WIDTH*THICK*(.5*THICK+BOND/
-2.))**2.)
YPRIME(1)=Y(2)
00042260
00042270
00042300
00042400
00042500
00042600
00042700
00042800
00042900
00043000
00043100
00043200

```



```
DEN=EI(1)+EI(2)+EI(3)
YPRIME(2)=PLOAD*(.5*THICK+BOND/2.+Y(1))/DEN
RETURN
END
C-
C-----NUMERICAL INTEGRATION OF SEGS
C-
SUBROUTINE FCN4(N,X,Y,YPRIME)
COMMON R, PLOAD, ESMC, WIDTH, THICK, YBAR, THETA, EADH, PI
, BOND
DIMENSION Y(2), YPRIME(2)
YPRIME(1)=Y(2)
YPRIME(2)=PLOAD*(Y(1))/(ESMC*WIDTH*THICK**3./12.)
RETURN
END
```

00043300  
00043400  
00043500  
00043600  
00043650  
00043660  
00043670  
00043700  
00043800  
00043900  
00044000  
00044100  
00044200  
00044300  
00044400

b. CONVERT

The program CONVERT essentially performs the tedious calculations involved in computing the boundary conditions for the finite-element model. Stresses dictated by the beam bending model are converted to equivalent point forces which are then applied to the finely meshed ends of the finite-element structure. In converting the stress distribution from deformed to undeformed geometry the program insures that the model be maintained in equilibrium through the introduction of a correcting moment.

The important parameters utilized in the routine are defined in the nomenclature section of the program. Frequent comment cards are intended to assist the user in the utilization of the program.

```

C-  CCCCC  00000  N  N  V  V  EEEEE  RRRRR  TTTT  00000004
C-  C      0  0  NN  N  V  V  E      R  R  T  00000005
C-  C      0  0  NN  N  V  V  EEE    RRRRR  T  00000006
C-  C      0  0  N  NN  V  V  E      R  R  T  00000007
C-  CCCCC  00000  N  N  V      EEEEE  R  R  T  00000008
C-                                     00000010
C-                                     00000011
C-                                     00000012
C-                                     00000013
C-                                     00000014
C-                                     00000015
C-                                     00000016
C-                                     00000017
C-                                     00000018
C-                                     00000019
C-                                     00000020
C-                                     00000030
C-                                     00000031
C-                                     00000032
C-                                     00000033
C-                                     00000034
C-                                     00000035
C-                                     00000036
C-                                     00000037
C-                                     00000100
SRESET FREE
      DIMENSION ZOM(5), RES(5), PART(4), ZOMX(5), RESB(5)
      -. RESX(5), RESY(5), ZOMA(5), ZOMB(5), BMOM(5), ZOMXB(5)
      -. RESXB(5), RESYB(5)
C-
C-----PARAMETERS AND NOMENCLATURE
C-
C-----MATERIAL THICKNESS
      THICK=.1
C-----MATERIAL WIDTH
      WIDTH=1.
C-----ROTATION OF LEFT HAND FACE FROM UNDEFORMED GEOMETRY (RAD)
      DUDSA=-.01642
C-----ROTATION OF RIGHT HAND FACE FROM UNDEFORMED GEOMETRY (RAD)
      DUDSB=.008420
C-----TOTAL MOMENT ON LEFT HAND FACE (IN. LBS.)
      TOTMOA=10.64
C-----SHEAR ON LEFT HAND FACE
      SHEARA=132.6
C-----TOTAL MOMENT ON RIGHT HAND FACE (IN. LBS.)
      TOTMOB=-1.968
      AREA=WIDTH*THICK
C-----OUTSIDE RADIUS IN INCHES
      RADO=3.5*THICK
C-----INSIDE RADIUS IN INCHES
      RADI=2.5*THICK
C-----RADIUS OF CURVATURE OF CURVED MEMBERS
      R=WIDTH*THICK/(ALOG(RADO/RADI))
C-----DIFFERENCE BETWEEN NEUTRAL AXIS AND CENTROIDAL AXIS (IN.)
      YBAR=RADI+THICK/2.-R
C-----ADHESIVE BOND THICKNESS IN INCHES
      BOND=.03
C-----ANGLE SUBTENDED BY CURVED MEMBERS IN RADIAN
      THETA=ARCOS((5.*THICK-BOND)/(6.*THICK))
C-----TENSILE LOAD
      PLOAD=200.
C-

```

```

00000004
00000005
00000006
00000007
00000008
00000010
00000011
00000012
00000013
00000014
00000015
00000016
00000017
00000018
00000019
00000020
00000030
00000031
00000032
00000033
00000034
00000035
00000036
00000037
00000100
00000200
00000300
00000400
00000420
00000430
00000440
00000470
00000500
00000550
00000600
00000650
00000700
00000750
00000800
00000850
00000900
00000925
00000950
00000975
00001000
00001100
00001150
00001200
00001250
00001300
00001350
00001400
00001450
00001500
00001550
00001600
00001650
00001700
00001750
00001800
00001850

```

```

C-----NOTE: DEFLECTIONS ARE MEASURED NORMAL TO THE NEUTRAL AXIS
C-
C-----DEFLECTION OF LEFT HAND FACE (IN.)
      DEFLA=-.01547
C-----DEFLECTION OF RIGHT HAND FACE (IN.)
      DEFLB=-.007872
C-----
C-----
C-----
C-----RESOLVING STRESS DISTRIBUTION ON LEFT HAND FACE
C-----
C-----
C-----
C-----CALCULATION OF RESULTANT POINT FORCES FROM THE
C-----STRESS DISTRIBUTION
C-----
      H=R-RADI
      DO 100 N=1.5
      PART(1)=TOTMOA/(YBAR*AREA)*(R-H-R*ALOG(R-H))
      +PLOAD/AREA*COS(THETA+DUDSA)*H
      H=H-.02
      PART(2)=TOTMOA/(YBAR*AREA)*(R-H-R*ALOG(R-H))
      +PLOAD/AREA*COS(THETA+DUDSA)*H
      RES(N)=PART(1)-PART(2)
      100 CONTINUE
C-----
C-----CALCULATION OF ACTUAL MOMENTS FROM THE STRESS DISTRIBUTION
C-----
      H=R-RADI
      DO 200 N=1.5
      PART(3)=TOTMOA/(YBAR*AREA)*(-1.)*( .5*(R-H)**2-2.*R*(R-H)+R**2
      -ALOG(R-H))+.5*PLOAD/AREA*COS(THETA+DUDSA)*H**2
      H=H-.02
      PART(4)=TOTMOA/(YBAR*AREA)*(-1.)*( .5*(R-H)**2-2.*R*(R-H)+R**2
      -ALOG(R-H))+.5*PLOAD/AREA*COS(THETA+DUDSA)*H**2
      ZOM(N)=PART(3)-PART(4)
      200 CONTINUE
C-----
C-----CALCULATION OF CORRECTION MOMENT DUE TO THE
C-----REPRESENTATION OF THE STRESS DISTRIBUTION BY POINT
C-----FORCES
C-----
      H=R-RADI-.01
      DO 300 N=1.5
      ZOMX(N)=ZOM(N)-RES(N)*H
      H=H-.02
      300 CONTINUE
C-----
C-----CALCULATION OF MOMENT DUE TO TRANSLATION OF THE STRESS
C-----DISTRIBUTION THROUGH SPACE FROM THE DEFORMED GEOMETRY
C-----TO THE UNDEFORMED GEOMETRY
C-----
C-----
C-----CALCULATION OF MOMX FOR INPUT INTO THE FINITE ELEMENT
C-----MODEL
C-----
      H=R-RADI-.01
      DO 400 N=1.5
      ZOMA(N)=-RES(N)*((H+DEFLA)*COS(DUDSA)-H)
      ZOMX(N)=ZOMX(N)+ZOMA(N)
      H=H-.02

```

```

00001852
00001854
00001870
00001900
00001970
00002000
00002010
00002020
00002100
00002200
00002300
00002320
00002400
00002500
00002600
00002700
00002800
00002900
00003000
00003100
00003200
00003300
00003400
00003500
00003600
00003800
00003900
00004000
00004100
00004200
00004300
00004400
00004600
00004700
00004800
00004900
00005000
00005200
00005300
00005400
00005500
00005600
00005700
00005800
00005900
00006000
00006200
00006300
00006400
00006500
00006600
00006700
00006800
00006900
00007000
00007100
00007200
00007300
00007400
00007500
00007700
00007900

```

```

400 CONTINUE                                00008000
C-----                                00008100
C-----CALCULATION OF FY AND FZ FOR INPUT INTO THE FINITE 00008200
C-----ELEMENT MODEL                                00008300
C-----                                00008400
      WRITE(6,25)                                00008500
25  FORMAT(////////,6X,'BOUNDARY CONDITIONS FOR LEFT HAND SEGMENT',/) 00008600
      WRITE(6,30)                                00008700
30  FORMAT(/,4X,'NODE',6X,'FY',13X,'FZ',12X,'MOMX',/) 00008800
      DO 500 N=1,5                                00008900
        RESX(N)=-RES(N)*COS(THETA+DUDSA)-SHEARA/5.*SIN(THETA) 00009000
        RESY(N)=-RES(N)*SIN(THETA+DUDSA)+SHEARA/5.*COS(THETA) 00009100
        WRITE(6,2) N, RESX(N), RESY(N), -ZOMX(N) 00009200
      2  FORMAT(5X,F2.0,3X,3(E10.4,5X),/) 00009300
500 CONTINUE                                00009400
C-----                                00009500
C-----                                00009600
C-----                                00009700
C-----                                00009800
C-----RESOLVING STRESS DISTRIBUTION ON RIGHT HAND FACE 00009900
C-----                                00010000
C-----                                00010100
C-----                                00010200
C-----                                00010300
C-----                                00010400
C-----CALCULATION OF RESULTANT POINT FORCES FROM THE STRESS 00010500
C-----DISTRIBUTION                                00010600
C-----                                00010700
      H=THICK/2.                                00010800
      DO 1000 N=1,5                                00010900
        PART(1)=-.5*TOTMOB*H**2/(1./12.*WIDTH*THICK**3)+PLOAD/AREA*H 00011000
        H=H-.02                                00011100
        PART(2)=-.5*TOTMOB*H**2/(1./12.*WIDTH*THICK**3)+PLOAD/AREA*H 00011200
        RESB(N)=PART(1)-PART(2) 00011300
1000 CONTINUE                                00011500
C-----                                00011600
C-----CALCULATION OF ACTUAL MOMENTS FROM THE STRESS 00011700
C-----DISTRIBUTION                                00011800
C-----                                00011900
      H=THICK/2.                                00012000
      DO 1100 N=1,5                                00012100
        PART(3)=1./3.*(TOTMOB)*H**3/(1./12.*WIDTH*THICK**3) 00012200
        --.5*PLOAD/AREA*H**2 00012300
        H=H-.02                                00012350
        PART(4)=1./3.*(TOTMOB)*H**3/(1./12.*WIDTH*THICK**3) 00012400
        --.5*PLOAD/AREA*H**2 00012500
        BMOM(N)=PART(3)-PART(4) 00012600
1100 CONTINUE                                00012800
C-----                                00012900
C-----CALCULATION OF CORRECTION MOMENT DUE TO THE 00013000
C-----REPRESENTATION OF THE STRESS DISTRIBUTION BY POINT 00013100
C-----FORCES                                00013200
C-----                                00013300
      H=THICK/2.-.01 00013400
      DO 1200 N=1,5                                00013500
        ZOMXB(N)=BMOM(N)+RESB(N)*H 00013600
        H=H-.02                                00013750
1200 CONTINUE                                00013800
C-----                                00013900
C-----CALCULATION OF THE MOMENT DUE TO TRANSLATING THE STRESS 00014000
C-----DISTRIBUTION FROM DEFORMED TO UNDEFORMED GEOMETRY 00014100
C-----                                00014200

```

C-----	00014300
C-----CALCULATION OF MOMENT MX FOR INPUT INTO THE FINITE	00014400
C-----ELEMENT MODEL	00014500
C-----	00014600
H=THICK/2.-.01	00014700
DO 1300 N=1,5	00014800
ZOMB(N)=RESB(N)*((H-DEFLB)*COS(DUDSB)-H)	00014900
ZOMXB(N)=ZOMXB(N)+ZOMB(N)	00015100
H=H-.02	00015200
1300 CONTINUE	00015300
C-----	00015400
C-----CALCULATION OF FY AND FZ FOR INPUT INTO THE FINITE	00015500
C-----ELEMENT MODEL	00015600
C-----	00015700
WRITE(6,40)	00015800
40 FORMAT(////////.10X,'BONDARY CONDITIONS FOR SEGB',//)	00015900
WRITE(6,45)	00016000
45 FORMAT(/.4X,'NODE'.6X,'FY'.13X,'FZ'.12X,'MOMX',//)	00016100
DO 1400 N=1,5	00016200
RESXB(N)=RESB(N)*COS(DUDSB)	00016300
RESYB(N)=RESB(N)*SIN(DUDSB)	00016400
WRITE(6,20) N, RESXB(N), RESYB(N), ZOMXB(N)	00016500
20 FORMAT(5X,F2.0,3X,3(E10.4,5X),//)	00016600
1400 CONTINUE	00016700
END	00016800

```

C      SUBROUTINE DVERK (N,FCN,X,Y,XEND,TOL,IND,C,NW,W,IER)      DVEK0010
C      C-DVERK-----S-----LIBRARY 3-----DVEK0020
C      C      FUNCTION      - SOLUTION OF A SYSTEM OF FIRST ORDER ORDINARY DVEK0030
C      C      DIFFERENTIAL EQUATIONS OF THE FORM DVEK0040
C      C      DY/DX = F(X,Y) WITH INITIAL CONDITIONS. DVEK0050
C      C      A RUNGE-KUTTA METHOD BASED ON VERNERS FIFTH DVEK0060
C      C      AND SIXTH ORDER PAIR OF FORMULAS IS USED. DVEK0070
C      C      USAGE      - CALL DVERK(N,FCN,X,Y,XEND,TOL,IND,C,NW,W,IER) DVEK0080
C      C      PARAMETERS  N      - NUMBER OF EQUATIONS. (INPUT) DVEK0090
C      C      FCN      - NAME OF SUBROUTINE FOR EVALUATING FUNCTIONS. DVEK0100
C      C      (INPUT) DVEK0110
C      C      THE SUBROUTINE ITSELF MUST ALSO BE PROVIDED DVEK0120
C      C      BY THE USER AND IT SHOULD BE OF THE DVEK0130
C      C      FOLLOWING FORM DVEK0140
C      C      SUBROUTINE FCN(N,X,Y,YPRIME) DVEK0150
C      C      DIMENSION Y(N),YPRIME(N) DVEK0160
C      C      : DVEK0170
C      C      : DVEK0180
C      C      : DVEK0190
C      C      : DVEK0200
C      C      : DVEK0210
C      C      FCN SHOULD EVALUATE YPRIME(1),....YPRIME(N) DVEK0220
C      C      GIVEN N,X, AND Y(1),....Y(N). YPRIME(I) DVEK0230
C      C      IS THE FIRST DERIVATIVE OF Y(I) WITH DVEK0240
C      C      RESPECT TO X. DVEK0250
C      C      FCN MUST APPEAR IN AN EXTERNAL STATEMENT IN DVEK0260
C      C      THE CALLING PROGRAM AND N,X,Y(1),....Y(N) DVEK0270
C      C      MUST NOT BE ALTERED BY FCN. DVEK0280
C      C      X      - INDEPENDENT VARIABLE. (INPUT AND OUTPUT) DVEK0290
C      C      ON INPUT, X SUPPLIES THE INITIAL VALUE. DVEK0300
C      C      ON OUTPUT, X IS REPLACED WITH XEND UNLESS DVEK0310
C      C      ERROR CONDITIONS ARISE. SEE THE DES- DVEK0320
C      C      cription OF PARAMETER IND. DVEK0330
C      C      Y      - DEPENDENT VARIABLES. VECTOR OF LENGTH N. DVEK0340
C      C      (INPUT AND OUTPUT) DVEK0350
C      C      ON INPUT, Y(1),....Y(N) SUPPLY INITIAL DVEK0360
C      C      VALUES. DVEK0370
C      C      ON OUTPUT, Y(1),....Y(N) ARE REPLACED WITH DVEK0380
C      C      AN APPROXIMATE SOLUTION AT XEND UNLESS DVEK0390
C      C      ERROR CONDITIONS ARISE. SEE THE DES- DVEK0400
C      C      cription OF PARAMETER IND. DVEK0410
C      C      XEND      - VALUE OF X AT WHICH SOLUTION IS DESIRED. DVEK0420
C      C      (INPUT) DVEK0430
C      C      XEND MAY BE LESS THAN THE INITIAL VALUE OF DVEK0440
C      C      X. DVEK0450
C      C      TOL      - TOLERANCE FOR ERROR CONTROL. (INPUT) DVEK0460
C      C      THE SUBROUTINE ATTEMPTS TO CONTROL A NORM DVEK0470
C      C      OF THE LOCAL ERROR IN SUCH A WAY THAT THE DVEK0480
C      C      GLOBAL ERROR IS PROPORTIONAL TO TOL. DVEK0490
C      C      MAKING TOL SMALLER IMPROVES ACCURACY AND DVEK0500
C      C      MORE THAN ONE RUN. WITH DIFFERENT VALUES DVEK0510
C      C      OF TOL, CAN BE USED IN AN ATTEMPT TO DVEK0520
C      C      ESTIMATE THE GLOBAL ERROR. DVEK0530
C      C      IN THE DEFAULT CASE (IND=1), THE GLOBAL DVEK0540
C      C      ERROR IS DVEK0550
C      C      MAX(ABS(E(1)),....ABS(E(N))) DVEK0560
C      C      WHERE E(K)=(Y(K)-YT(K))/MAX(1,ABS(Y(K))) DVEK0570
C      C      YT(K) IS THE TRUE SOLUTION, AND DVEK0580
C      C      Y(K) IS THE COMPUTED SOLUTION AT XEND. DVEK0590
C      C      FOR K=1,2,....N. DVEK0600
C      C      OTHER ERROR CONTROL OPTIONS ARE AVAILABLE. DVEK0610

```

SEE THE DESCRIPTION OF PARAMETERS IND AND C BELOW. D/EK0620  
 IND - INDICATOR. (INPUT AND OUTPUT) D/EK0630  
 ON INITIAL ENTRY IND MUST BE SET EQUAL TO D/EK0640  
 EITHER 1 OR 2. D/EK0650  
 IND = 1 CAUSES ALL DEFAULT OPTIONS TO BE D/EK0660  
 USED AND ELIMINATES THE NEED TO SET D/EK0670  
 SPECIFIC VALUES IN THE COMMUNICATIONS D/EK0680  
 VECTOR C. D/EK0690  
 IND = 2 ALLOWS OPTIONS TO BE SELECTED. IN D/EK0700  
 THIS CASE, THE FIRST 9 COMPONENTS OF C D/EK0710  
 MUST BE INITIALIZED TO SELECT OPTIONS AS D/EK0720  
 DESCRIBED BELOW. D/EK0730  
 THE SUBROUTINE WILL NORMALLY RETURN WITH D/EK0740  
 IND = 3, HAVING REPLACED THE INITIAL VALUES D/EK0750  
 OF X AND Y WITH, RESPECTIVELY, THE VALUE D/EK0760  
 XEND AND AN APPROXIMATION TO Y AT XEND. D/EK0770  
 THE SUBROUTINE CAN BE CALLED REPEATEDLY WITH D/EK0780  
 NEW VALUES OF XEND WITHOUT CHANGING ANY D/EK0790  
 OF THE OTHER PARAMETERS. D/EK0800  
 THREE ERROR RETURNS ARE ALSO POSSIBLE. IN D/EK0810  
 WHICH CASE X AND Y WILL BE THE MOST D/EK0820  
 RECENTLY ACCEPTED VALUES. D/EK0830  
 IND = -3 INDICATES THAT THE SUBROUTINE WAS D/EK0840  
 UNABLE TO SATISFY THE ERROR REQUIREMENT. D/EK0850  
 THIS MAY MEAN THAT TOL IS TOO SMALL. D/EK0860  
 IND = -2 INDICATES THAT THE VALUE OF HMIN D/EK0870  
 (MINIMUM STEP-SIZE) IS GREATER THAN HMAX D/EK0880  
 (MAXIMUM STEP-SIZE). WHICH PROBABLY MEANS D/EK0890  
 THAT THE REQUESTED TOL (WHICH IS USED IN D/EK0900  
 THE CALCULATION OF HMIN) IS TOO SMALL. D/EK0910  
 IND = -1 INDICATES THAT THE ALLOWED MAXIMUM D/EK0920  
 NUMBER OF FCN EVALUATIONS HAS BEEN D/EK0930  
 EXCEEDED. THIS CAN ONLY OCCUR IF OPTION D/EK0940  
 C(7), AS DESCRIBED BELOW, HAS BEEN USED. D/EK0950  
 C - COMMUNICATIONS VECTOR OF LENGTH 24. (INPUT IF D/EK0960  
 IND.NE.1, AND OUTPUT). D/EK0970  
 C IS USED TO SELECT OPTIONS AND TO RETAIN D/EK0980  
 INFORMATION BETWEEN CALLS. THE USER NEED D/EK0990  
 NOT BE CONCERNED WITH THE FOLLOWING D/EK1000  
 DESCRIPTION OF THE ELEMENTS OF C WHEN D/EK1010  
 DEFAULT OPTIONS ARE USED (IND=1). D/EK1020  
 HOWEVER, WHEN IT IS DESIRED TO USE IND=2 D/EK1030  
 AND SELECT OPTIONS, A BASIC UNDERSTANDING D/EK1040  
 OF DVERK IS REQUIRED. THE FOLLOWING D/EK1050  
 PARAGRAPH DESCRIBES, BRIEFLY, THE BASIC D/EK1060  
 TERMS. FOR MORE DETAILS, SEE THE D/EK1070  
 REFERENCE. D/EK1080  
 DVERK ADVANCES THE INDEPENDENT VARIABLE D/EK1090  
 X ONE STEP AT A TIME UNTIL XEND IS D/EK1100  
 REACHED. THE SOLUTION IS COMPUTED AT D/EK1110  
 XTRIAL = X+HTRIAL ALONG WITH AN ERROR D/EK1120  
 ESTIMATE EST. IF EST IS LESS THAN OR D/EK1130  
 EQUAL TO TOL (SUCCESSFUL STEP), THE STEP D/EK1140  
 IS ACCEPTED AND X IS ADVANCED TO XTRIAL. D/EK1150  
 IF EST IS GREATER THAN TOL (FAILURE) D/EK1160  
 HTRIAL IS ADJUSTED AND THE SOLUTION IS D/EK1170  
 RECOMPUTED. HMAG = ABS(HTRIAL) IS NEVER D/EK1180  
 ALLOWED TO EXCEED HMAX NOR IS IT ALLOWED D/EK1190  
 TO BECOME SMALLER THAN HMIN. THE FIRST D/EK1200  
 TRIAL STEP IS HSTART. DURING THE D/EK1210  
 COMPUTATION, A COUNTER (C(23)) IS D/EK1220  
 D/EK1230



INCREMENTED EACH TIME A TRIAL STEP FAILS DVEK1240  
 TO PROVIDE A SOLUTION SATISFYING THE ERROR DVEK1250  
 TOLERANCE. ANOTHER COUNTER (C(22)) IS DVEK1260  
 USED TO RECORD THE NUMBER OF SUCCESSFUL DVEK1270  
 STEPS. AFTER A SUCCESSFUL STEP, C(23) IS DVEK1280  
 SET TO ZERO. DVEK1290  
 OPTIONS. IF THE SUBROUTINE IS ENTERED WITH DVEK1300  
 IND=2, THE FIRST 9 COMPONENTS OF THE DVEK1310  
 COMMUNICATIONS VECTOR MUST BE INITIALIZED DVEK1320  
 BY THE USER. NORMALLY THIS IS DONE BY DVEK1330  
 FIRST SETTING THEM ALL TO ZERO, AND THEN DVEK1340  
 THOSE CORRESPONDING TO PARTICULAR OPTIONS DVEK1350  
 ARE MADE NON-ZERO. DVEK1360  
 C(1) - ERROR CONTROL INDICATOR. DVEK1370  
 THE SUBROUTINE ATTEMPTS TO CONTROL A NORM DVEK1380  
 OF THE LOCAL ERROR IN SUCH A WAY THAT THE DVEK1390  
 GLOBAL ERROR IS PROPORTIONAL TO TOL. DVEK1400  
 THE DEFINITION OF GLOBAL ERROR FOR THE DVEK1410  
 DEFAULT CASE (IND=1) IS GIVEN IN THE DVEK1420  
 DESCRIPTION OF PARAMETER TOL. THE DEFAULT DVEK1430  
 WEIGHTS ARE  $1/\text{MAX}(1, \text{ABS}(Y(K)))$ . WHEN IND=2 DVEK1440  
 IS USED, THE WEIGHTS ARE DETERMINED DVEK1450  
 ACCORDING TO THE VALUE OF C(1). DVEK1460  
 IF C(1)=1 THE WEIGHTS ARE 1 DVEK1470  
 (ABSOLUTE ERROR CONTROL) DVEK1480  
 IF C(1)=2 THE WEIGHTS ARE  $1/\text{ABS}(Y(K))$  DVEK1490  
 FOR K=1,2,...,N. DVEK1500  
 (RELATIVE ERROR CONTROL) DVEK1510  
 IF C(1)=3 THE WEIGHTS ARE DVEK1520  
 $1/\text{MAX}(\text{ABS}(C(2)), \text{ABS}(Y(K)))$  DVEK1530  
 FOR K=1,2,...,N. DVEK1540  
 (RELATIVE ERROR CONTROL, UNLESS DVEK1550  
 $\text{ABS}(Y(K))$  IS LESS THAN THE FLOOR DVEK1560  
 VALUE,  $\text{ABS}(C(2))$ ) DVEK1570  
 IF C(1)=4 THE WEIGHTS ARE DVEK1580  
 $1/\text{MAX}(\text{ABS}(C(K+30)), \text{ABS}(Y(K)))$  DVEK1590  
 FOR K=1,2,...,N. DVEK1600  
 (HERE INDIVIDUAL FLOOR VALUES DVEK1610  
 ARE USED) DVEK1620  
 IN THIS CASE, THE DIMENSION OF C DVEK1630  
 MUST BE GREATER THAN OR EQUAL TO DVEK1640  
 N+30 AND C(31), C(32),...,C(N+30) DVEK1650  
 MUST BE INITIALIZED BY THE USER. DVEK1660  
 IF C(1)=5 THE WEIGHTS ARE  $1/\text{ABS}(C(K+30))$  DVEK1670  
 FOR K=1,2,...,N. DVEK1680  
 IN THIS CASE, THE DIMENSION OF C DVEK1690  
 MUST BE GREATER THAN OR EQUAL TO DVEK1700  
 N+30 AND C(31), C(32),...,C(N+30) DVEK1710  
 MUST BE INITIALIZED BY THE USER. DVEK1720  
 FOR ALL OTHER VALUES OF C(1), INCLUDING DVEK1730  
 C(1)=0 THE DEFAULT VALUES OF DVEK1740  
 THE WEIGHTS ARE TAKEN TO BE DVEK1750  
 $1/\text{MAX}(1, \text{ABS}(Y(K)))$  DVEK1760  
 FOR K=1,2,...,N. DVEK1770  
 C(2) - FLOOR VALUE. USED WHEN THE INDICATOR C(1) DVEK1780  
 HAS THE VALUE 3. DVEK1790  
 C(3) - HMIN SPECIFICATION. IF NOT ZERO, THE SUB- DVEK1800  
 ROUTINE CHOOSES HMIN TO BE  $\text{ABS}(C(3))$ . DVEK1810  
 OTHERWISE IT USES THE DEFAULT VALUE DVEK1820  
 $10 \times \text{MAX}(\text{DWARF}, \text{RREB} \times \text{MAX}(\text{NORM}(Y)/\text{TOL}, \text{ABS}(X)))$  DVEK1830  
 WHERE DWARF IS A VERY SMALL POSITIVE MACHINEDVEK1840  
 NUMBER AND RREB IS THE RELATIVE ROUNDOFF DVEK1850

ERROR BOUND. DVEK1860

C(4) - HSTART SPECIFICATION. IF NOT ZERO, THE SUB- DVEK1870  
ROUTINE WILL USE AN INITIAL HMAG EQUAL TO DVEK1880  
ABS(C(4)). EXCEPT OF COURSE FOR THE RE- DVEK1890  
STRICTIONS IMPOSED BY HMIN AND HMAX. DVEK1900  
OTHERWISE IT USES THE DEFAULT VALUE DVEK1910  
HMAX\*(TOL)\*\*(1/6). DVEK1920

C(5) - SCALE SPECIFICATION. THIS IS INTENDED TO BE DVEK1930  
A MEASURE OF THE SCALE OF THE PROBLEM. DVEK1940  
LARGER VALUES OF SCALE TEND TO MAKE THE DVEK1950  
METHOD MORE RELIABLE. FIRST BY POSSIBLY RE- DVEK1960  
STRICTING HMAX (AS DESCRIBED BELOW) AND DVEK1970  
SECOND, BY TIGHTENING THE ACCEPTANCE DVEK1980  
REQUIREMENT. IF C(5) IS ZERO, A DEFAULT DVEK1990  
VALUE OF 1 IS USED. FOR LINEAR HOMOGENEOUS DVEK2000  
PROBLEMS WITH CONSTANT COEFFICIENTS, AN DVEK2010  
APPROPRIATE VALUE FOR SCALE IS A NORM OF DVEK2020  
THE ASSOCIATED MATRIX. FOR OTHER PROBLEMS, DVEK2030  
AN APPROXIMATION TO AN AVERAGE VALUE OF A DVEK2040  
NORM OF THE JACOBIAN ALONG THE TRAJECTORY DVEK2050  
MAY BE APPROPRIATE. DVEK2060

C(6) - HMAX SPECIFICATION. FOUR CASES ARE POSSIBLE. DVEK2070  
IF C(6).NE.0 AND C(5).NE.0, HMAX IS TAKEN DVEK2080  
TO BE MIN(ABS(C(6)),2/ABS(C(5))). DVEK2090  
IF C(6).NE.0 AND C(5).EQ.0, HMAX IS TAKEN DVEK2100  
TO BE ABS(C(6)). DVEK2110  
IF C(6).EQ.0 AND C(5).NE.0, HMAX IS TAKEN DVEK2120  
TO BE 2/ABS(C(5)). DVEK2130  
IF C(6).EQ.0 AND C(5).EQ.0, HMAX IS GIVEN DVEK2140  
A DEFAULT VALUE OF 2. DVEK2150

C(7) - MAXIMUM NUMBER OF FUNCTION EVALUATIONS. IF DVEK2160  
NOT ZERO, AN ERROR RETURN WITH IND = -1 DVEK2170  
WILL BE CAUSED WHEN THE NUMBER OF FUNCTION DVEK2180  
EVALUATIONS EXCEEDS ABS(C(7)). DVEK2190

C(8) - INTERRUPT NUMBER 1. IF NOT ZERO, THE SUB- DVEK2200  
ROUTINE WILL INTERRUPT THE CALCULATIONS DVEK2210  
AFTER IT HAS CHOSEN ITS PRELIMINARY VALUE DVEK2220  
OF HMAG, AND JUST BEFORE CHOOSING HTRIAL DVEK2230  
AND XTRIAL IN PREPARATION FOR TAKING A STEP DVEK2240  
(HTRIAL MAY DIFFER FROM HMAG IN SIGN, AND DVEK2250  
MAY REQUIRE ADJUSTMENT IF XEND IS NEAR). DVEK2260  
THE SUBROUTINE RETURNS WITH IND = 4, AND DVEK2270  
WILL RESUME CALCULATION AT THE POINT OF DVEK2280  
INTERRUPTION IF RE-ENTERED WITH IND = 4. DVEK2290

C(9) - INTERRUPT NUMBER 2. IF NOT ZERO, THE SUB- DVEK2300  
ROUTINE WILL INTERRUPT THE CALCULATIONS DVEK2310  
IMMEDIATELY AFTER IT HAS DECIDED WHETHER OR DVEK2320  
NOT TO ACCEPT THE RESULT OF THE MOST RECENT DVEK2330  
TRIAL STEP, WITH IND = 5 IF IT PLANS TO DVEK2340  
ACCEPT, OR IND = 6 IF IT PLANS TO REJECT. DVEK2350  
Y(\*) IS THE PREVIOUSLY ACCEPTED RESULT. DVEK2360  
WHILE W(\*,9) IS THE NEWLY COMPUTED TRIAL DVEK2370  
VALUE, AND W(\*,2) IS THE UNWEIGHTED ERROR DVEK2380  
ESTIMATE VECTOR. THE SUBROUTINE WILL RESUME DVEK2390  
CALCULATIONS AT THE POINT OF INTERRUPTION DVEK2400  
ON RE-ENTRY WITH IND = 5 OR 6. DVEK2410  
IND MAY BE CHANGED BY THE USER IN ORDER TO DVEK2420  
FORCE ACCEPTANCE OF A STEP (BY CHANGING IND DVEK2430  
FROM 6 TO 5) THAT WOULD OTHERWISE BE DVEK2440  
REJECTED, OR VICE VERSA. DVEK2450

NW - THE FIRST DIMENSION OF W AS IT APPEARS IN THE DVEK2460  
CALLING PROGRAM. (INPUT) DVEK2470

C		NW MUST BE GREATER THAN OR EQUAL TO N.	D/EK2480
C	W	- WORKSPACE MATRIX.	D/EK2490
C		THE FIRST DIMENSION OF W MUST BE NW AND THE	D/EK2500
C		SECOND MUST BE GREATER THAN OR EQUAL TO 9.	D/EK2510
C	IER	- ERROR PARAMETER. (OUTPUT)	D/EK2520
C		TERMINAL ERRORS	D/EK2530
C		IER = 129. NW IS LESS THAN N OR TOL IS LESS	D/EK2540
C		THAN OR EQUAL TO ZERO.	D/EK2550
C		IER = 130. IND IS NOT IN THE RANGE 1 TO 6.	D/EK2560
C		IER = 131. XEND HAS NOT BEEN CHANGED FROM	D/EK2570
C		PREVIOUS CALL OR X IS NOT SET TO	D/EK2580
C		THE PREVIOUS XEND VALUE.	D/EK2590
C		IER = 132. THE RELATIVE ERROR CONTROL	D/EK2600
C		OPTION (C(1)=2) WAS SELECTED AND	D/EK2610
C		ONE OF THE SOLUTION COMPONENTS	D/EK2620
C		IS ZERO.	D/EK2630
C	PRECISION	- SINGLE	D/EK2640
C	REQD. IMSL ROUTINES	- UERTST	D/EK2650
C	LANGUAGE	- FORTRAN	D/EK2660
C			D/EK2670
C	LATEST REVISION	- DECEMBER 15, 1976	D/EK2680
C		BGH	D/EK2690
	INTEGER	N,IND,NW,K	D/EK2700
	INTEGER	IER	D/EK2710
	REAL	X,Y(N),XEND,TOL,C(1),W(NW,9),TEMP	D/EK2720
	REAL	ZERO,ONE,TWO,THREE,FOUR,FIVE,SEVEN,TEN,HALF,P9	D/EK2730
	1	C4D15,C2D3,C5D6,C1D6,C1D15,C2D96	D/EK2740
	REAL	RK(39),REPS,RTOL	D/EK2750
	DATA	ZERO/0.0/,ONE/1.0/,TWO/2.0/,THREE/3.0/	D/EK2760
	DATA	FOUR/4.0/,FIVE/5.0/,SEVEN/7.0/	D/EK2770
	DATA	TEN/10.0/,HALF/0.5/,P9/0.9/	D/EK2780
	DATA	C4D15/.26666666667/	D/EK2790
	DATA	C2D3/.66666666667/	D/EK2800
	DATA	C5D6/.83333333333/	D/EK2810
	DATA	C1D6/.16666666667/	D/EK2820
	DATA	C1D15/.66666666667E-1/	D/EK2830
	DATA	C2D96/120.42729108/	D/EK2840
	DATA	REPS/013010000000000000/	D/EK2850
	DATA	RTOL/016310000000000000/	D/EK2860
	DATA	RK( 1)/.16666666667E+00/	D/EK2870
	DATA	RK( 2)/.53333333333E-01/	D/EK2880
	DATA	RK( 3)/.21333333333E+00/	D/EK2890
	DATA	RK( 4)/.83333333333E+00/	D/EK2900
	DATA	RK( 5)/.26666666667E+01/	D/EK2910
	DATA	RK( 6)/.25000000000E+01/	D/EK2920
	DATA	RK( 7)/.25781250000E+01/	D/EK2930
	DATA	RK( 8)/.91666666667E+01/	D/EK2940
	DATA	RK( 9)/.66406250000E+01/	D/EK2950
	DATA	RK(10)/.88541666667E+00/	D/EK2960
	DATA	RK(11)/.24000000000E+01/	D/EK2970
	DATA	RK(12)/.80000000000E+01/	D/EK2980
	DATA	RK(13)/.65604575163E+01/	D/EK2990
	DATA	RK(14)/.30555555556E+00/	D/EK3000
	DATA	RK(15)/.34509803922E+00/	D/EK3010
	DATA	RK(16)/.55086666667E+00/	D/EK3020
	DATA	RK(17)/.16533333333E+01/	D/EK3030
	DATA	RK(18)/.94558823529E+00/	D/EK3040
	DATA	RK(19)/.32400000000E+00/	D/EK3050
	DATA	RK(20)/.23378823529E+00/	D/EK3060
	DATA	RK(21)/.20354651163E+01/	D/EK3070
	DATA	RK(22)/.69767441860E+01/	D/EK3080
	DATA	RK(23)/.56481798146E+01/	D/EK3090

DATA	RK(24)/.13738156761E+00/	DVEK3100
DATA	RK(25)/.28630226610E+00/	DVEK3110
DATA	RK(26)/.14417855672E+00/	DVEK3120
DATA	RK(27)/.75000000000E-01/	DVEK3130
DATA	RK(28)/.38992869875E+00/	DVEK3140
DATA	RK(29)/.31944444444E+00/	DVEK3150
DATA	RK(30)/.13503836317E+00/	DVEK3160
DATA	RK(31)/.10783298827E-01/	DVEK3170
DATA	RK(32)/.69805194805E-01/	DVEK3180
DATA	RK(33)/.62500000000E-02/	DVEK3190
DATA	RK(34)/.69630124777E-02/	DVEK3200
DATA	RK(35)/.69444444444E-02/	DVEK3210
DATA	RK(36)/.61381074169E-02/	DVEK3220
DATA	RK(37)/.68181818182E-01/	DVEK3230
DATA	RK(38)/.10783298827E-01/	DVEK3240
DATA	RK(39)/.69805194805E-01/	DVEK3250
C		DVEK3260
C	BEGIN INITIALIZATION. PARAMETER	DVEK3270
C	CHECKING. INTERRUPT RE-ENTRIES	DVEK3280
C	IER = 0	DVEK3290
C	ABORT IF IND OUT OF RANGE 1 TO 6	DVEK3300
C	IF (IND.LT.1.OR.IND.GT.6) GO TO 290	DVEK3310
C	CASES - INITIAL ENTRY, NORMAL	DVEK3320
C	RE-ENTRY, INTERRUPT RE-ENTRIES	DVEK3330
C	GO TO (5,5,40,145,265,265), IND	DVEK3340
C	CASE 1 - INITIAL ENTRY (IND.EQ. 1	DVEK3350
C	OR 2) ABORT IF N.GT.NW OR TOL.LE.0	DVEK3360
C		DVEK3370
C	5 IF (N.GT.NW.OR.TOL.LE.ZERO) GO TO 295	DVEK3380
C	IF (IND.EQ.2) GO TO 15	DVEK3390
C	INITIAL ENTRY WITHOUT OPTIONS (IND	DVEK3400
C	.EQ. 1) SET C(1) TO C(9) EQUAL TO	DVEK3410
C	0	DVEK3420
C		DVEK3430
C	DO 10 K=1,9	DVEK3440
C	C(K) = ZERO	DVEK3450
C	10 CONTINUE	DVEK3460
C	GO TO 30	DVEK3470
C	SUMMARY OF THE COMPONENTS OF THE	DVEK3480
C	COMMUNICATIONS VECTOR	DVEK3490
C	PRESCRIBED AT THE OPTION	DVEK3500
C	OF THE USER	DVEK3510
C	C(1) ERROR CONTROL INDICATOR	DVEK3520
C	C(2) FLOOR VALUE	DVEK3530
C	C(3) HMIN SPECIFICATION	DVEK3540
C	C(4) HSTART SPECIFICATION	DVEK3550
C	C(5) SCALE SPECIFICATION	DVEK3560
C	C(6) HMAX SPECIFICATION	DVEK3570
C	C(7) MAX NO OF FCN EVALS	DVEK3580
C	C(8) INTERRUPT NO 1	DVEK3590
C	C(9) INTERRUPT NO 2	DVEK3600
C		DVEK3610
C	DETERMINED BY THE PROGRAM	DVEK3620
C		DVEK3630
C	C(10) RREB(REL ROUNDOFF ERROR BND)	DVEK3640
C	C(11) DWARF (VERY SMALL MACH NO)	DVEK3650
C	C(12) WEIGHTED NORM Y	DVEK3660
C	C(13) HMIN	DVEK3670
C	C(14) HMAG	DVEK3680
C	C(15) SCALE	DVEK3690
C	C(16) HMAX	DVEK3700
C	C(17) XTRIAL	DVEK3710

15 CONTINUE

INITIAL ENTRY WITH OPTIONS (IND .EQ. DVEK3820

## Appendix D

### Material Property Data

It was necessary to perform a series of elastic modulus determination tests to characterize this adherent material. Slight variations in material properties can be evident in molding compounds even manufactured by the same supplier. In a separate, extensive study concerning material property data, Taggart reported the elastic modulus of SMC-25 to be  $2.1 \times 10^6$  psi and the results shown in Table 4 are in close agreement.

Table 4

Specimen #	Modulus (PSI)
SPEC1	$2.21 \times 10^6$
SPEC2	$2.26 \times 10^6$
SPEC3	$2.18 \times 10^6$

Plate 6 shows a typical test specimen used for modulus determination. The data for these tests may be found on the following pages.

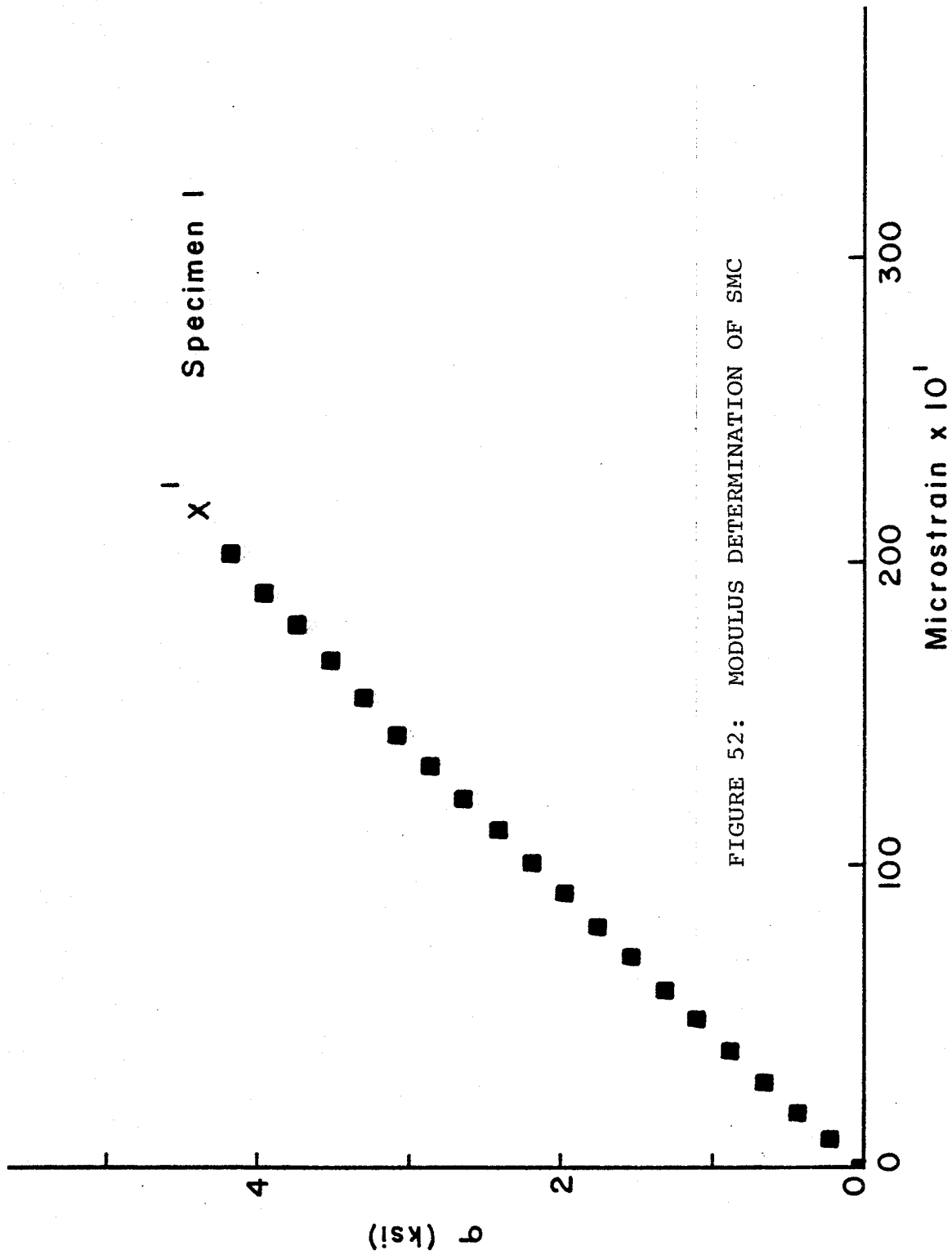


FIGURE 52: MODULUS DETERMINATION OF SMC

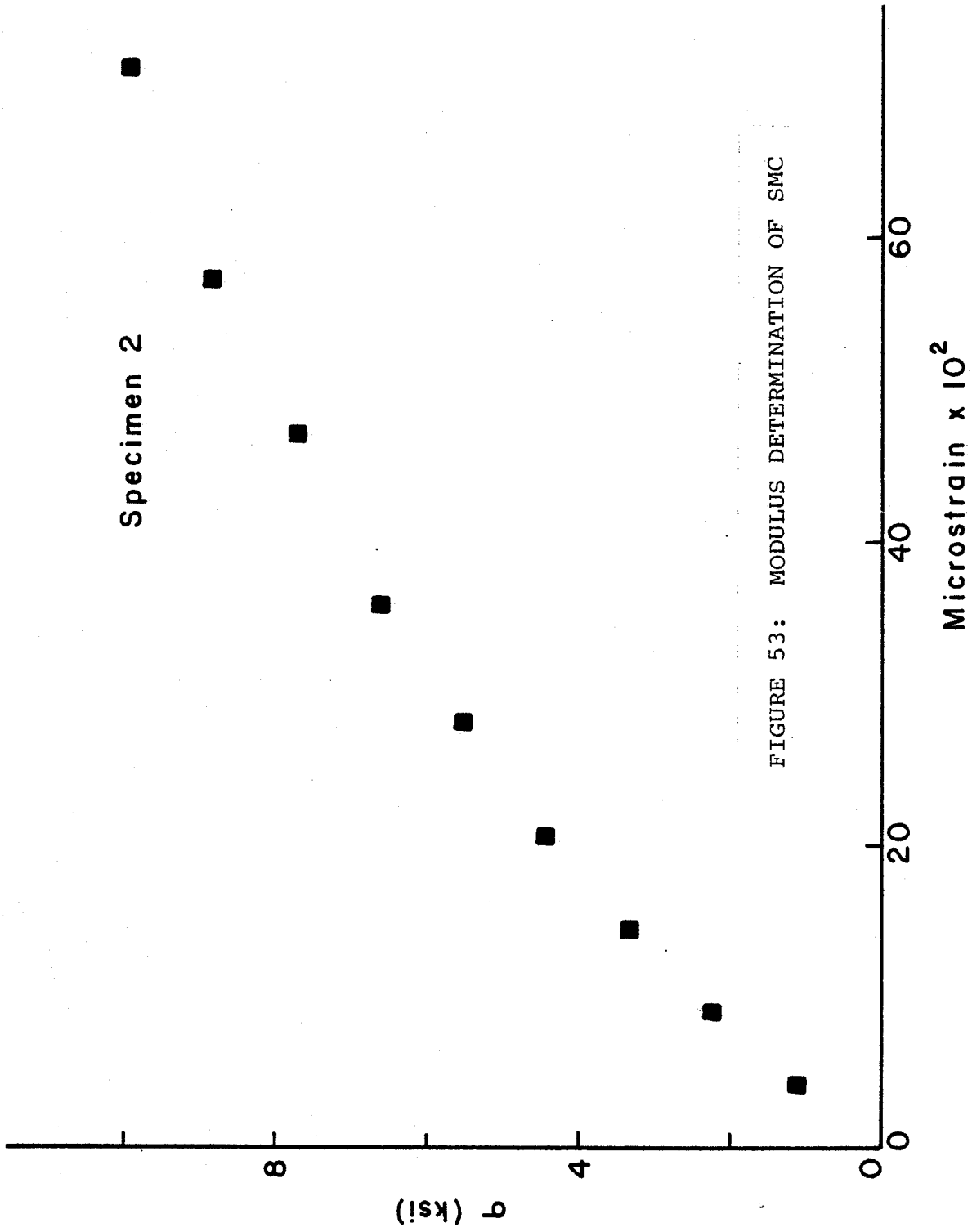


FIGURE 53: MODULUS DETERMINATION OF SMC



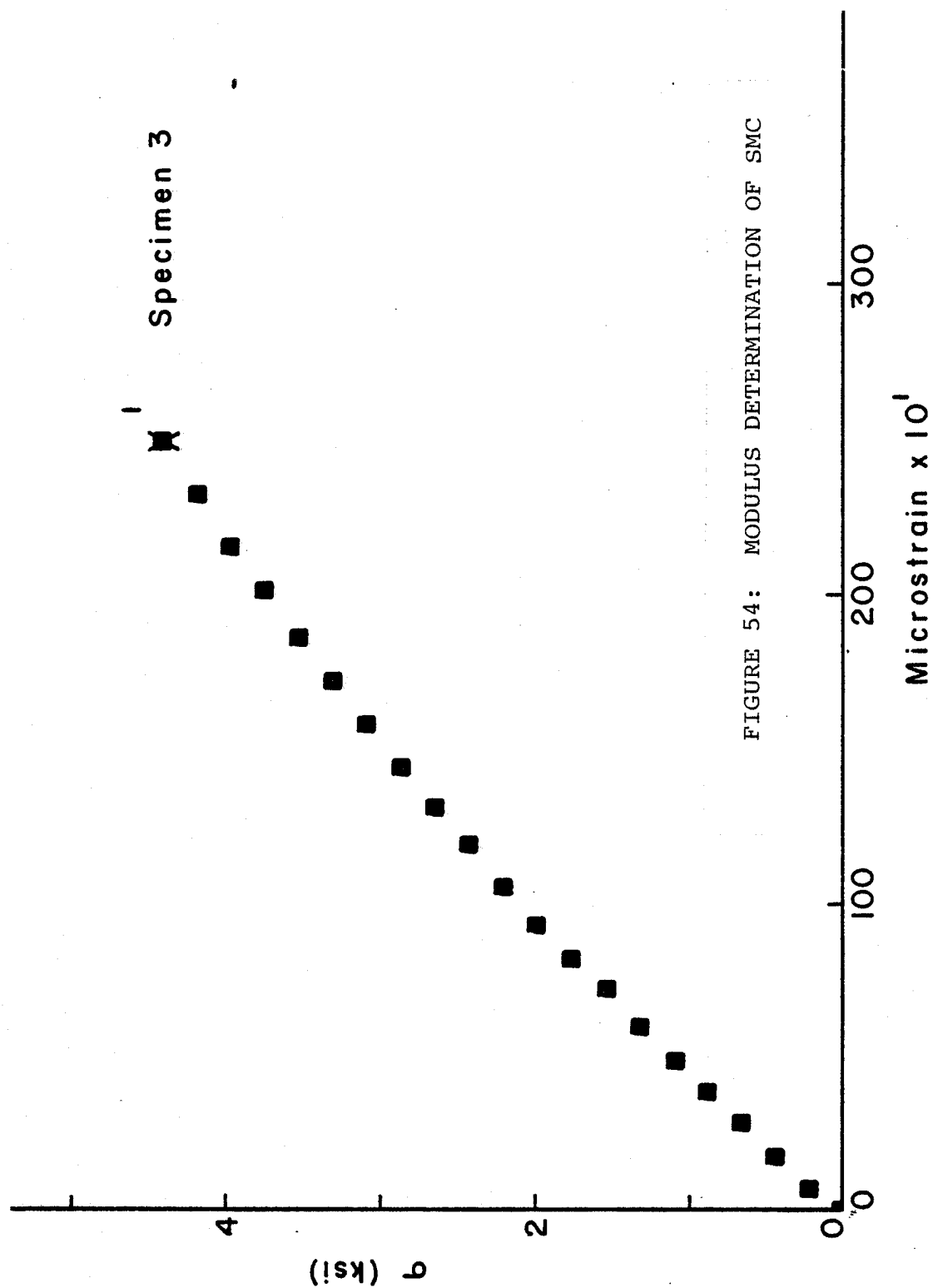


FIGURE 54: MODULUS DETERMINATION OF SMC

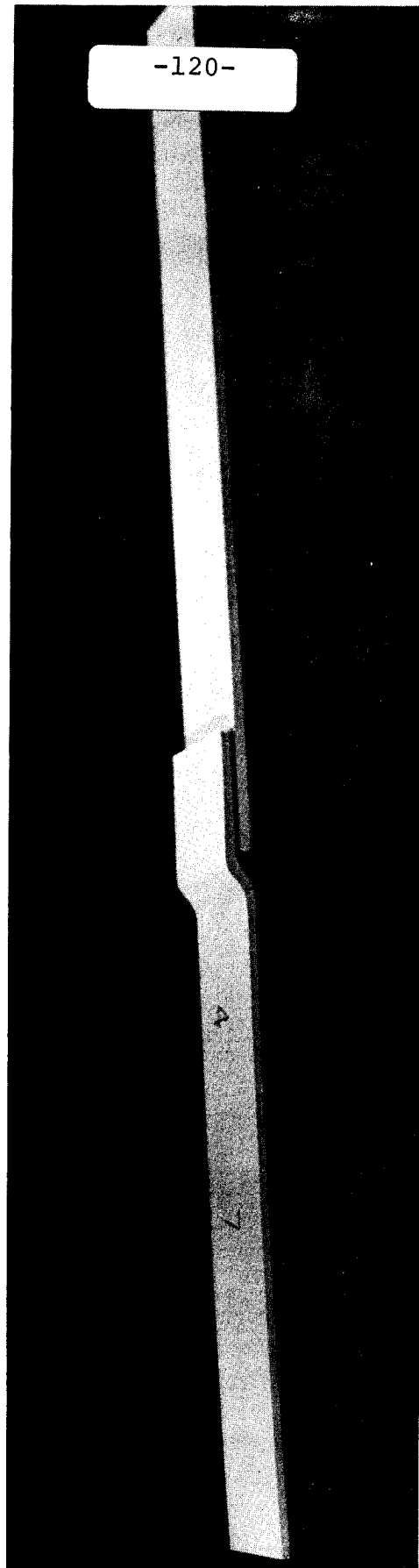


PLATE 1: Typical Test Specimen

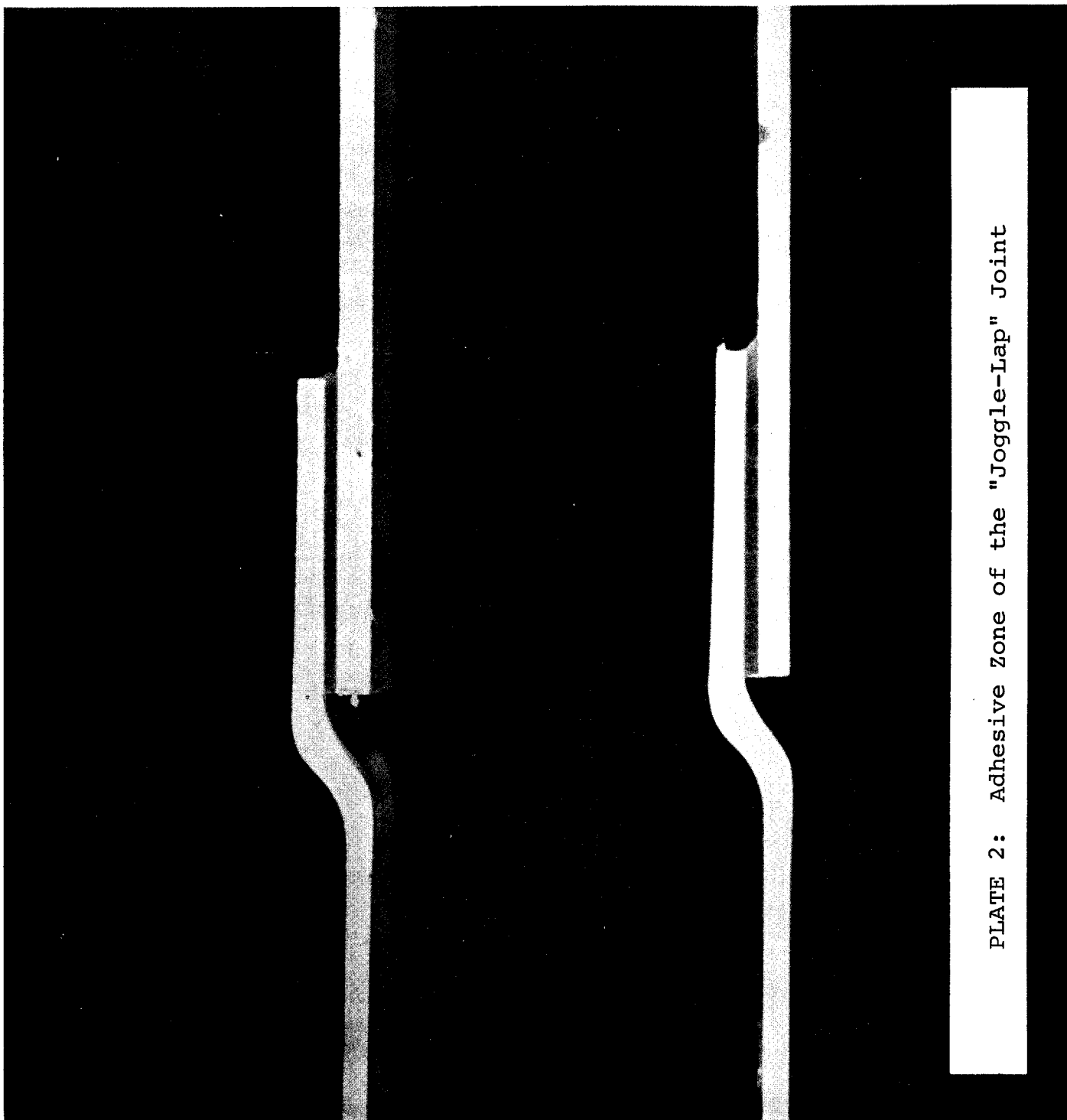
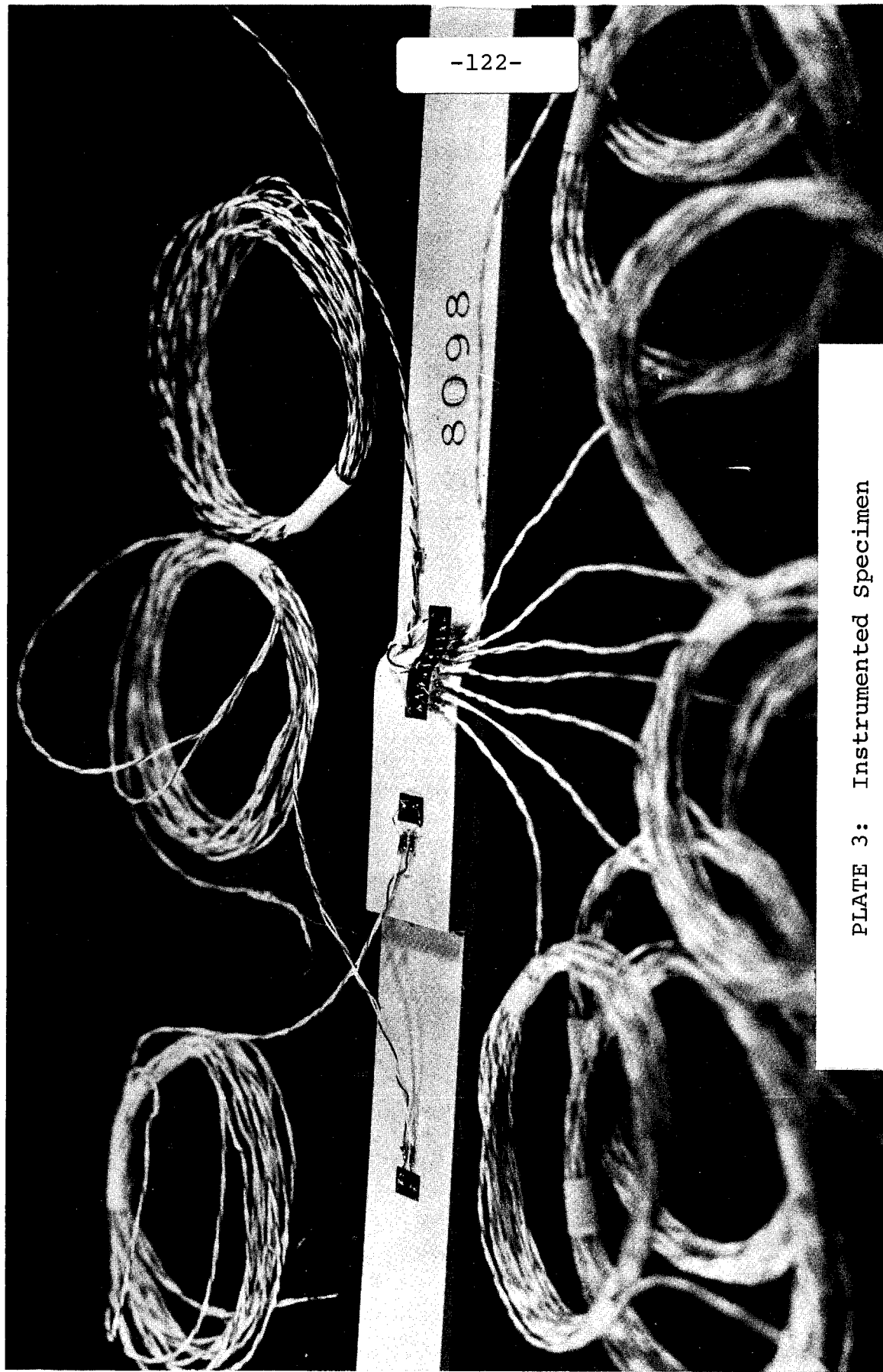


PLATE 2: Adhesive Zone of the "Joggle-Lap" Joint

-122-

8098

PLATE 3: Instrumented Specimen



-123-

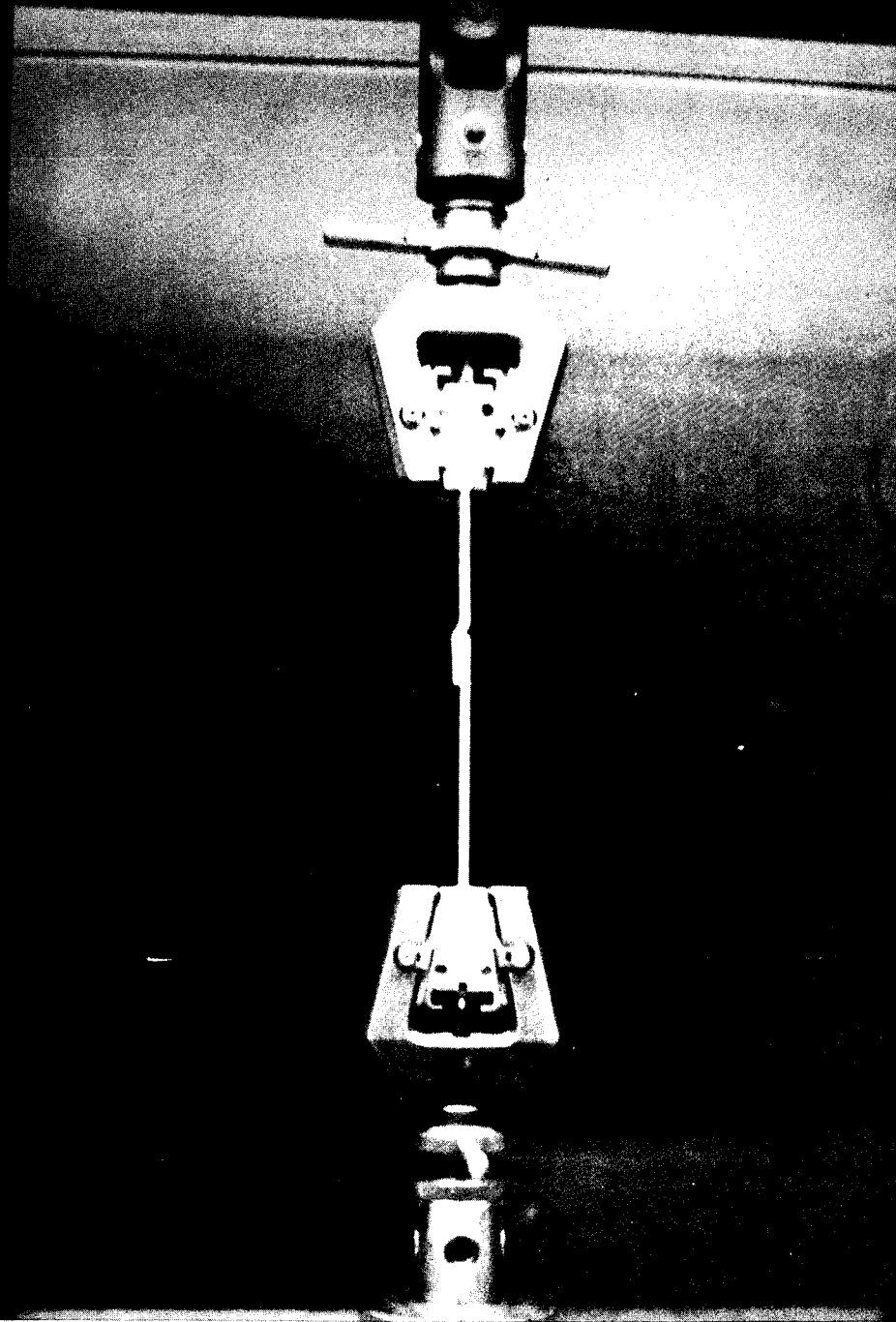


PLATE 4: "Joggle-Lap" Joint Subject to Tension

-124-

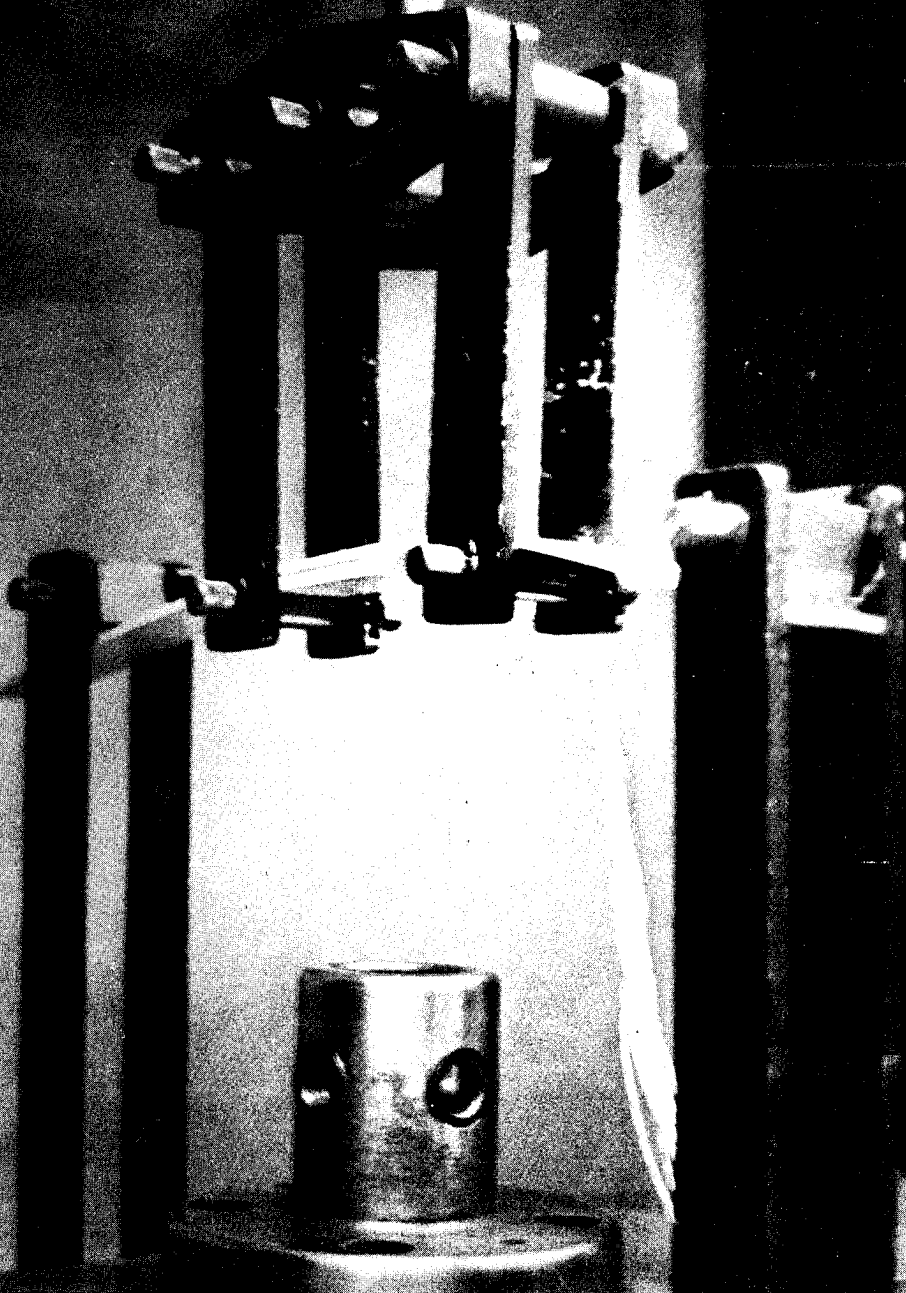


PLATE 5: "Joggle-Lap" Joint Subject to Bending

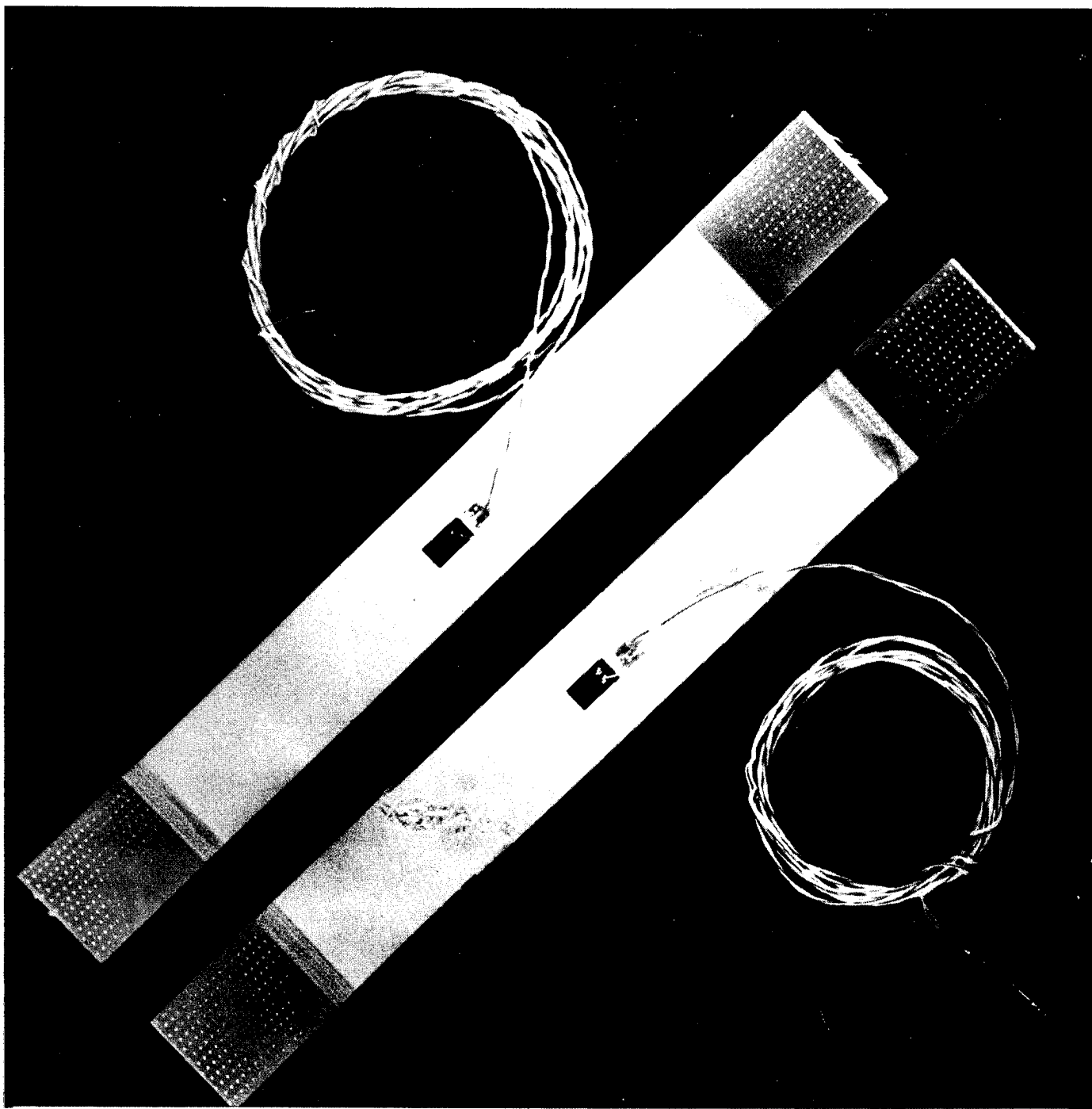
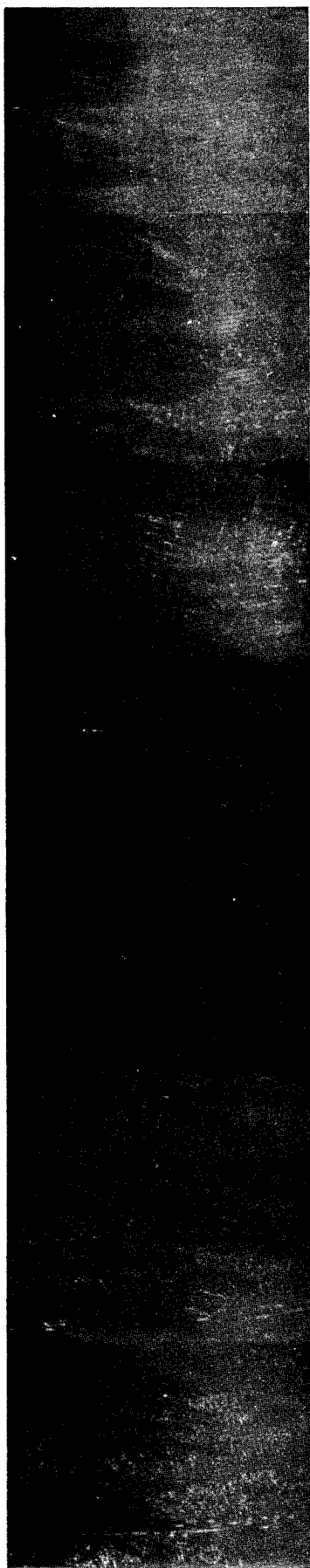


PLATE 6: Tensile Coupons for Modulus Determination



-126-

Curved Section (SEG3)



PLATE 7: Photomicrographs Showing Relative Fiber Content